

Spring 2017

CHARACTERIZATION OF GRANITE AND SUBSEQUENT GROUND CONTROL MANAGEMENT PLAN AT ORPHAN BOY MINE – BUTTE, MONTANA

Emily Rose
Montana Tech

Follow this and additional works at: http://digitalcommons.mtech.edu/grad_rsch



Part of the [Geology Commons](#), and the [Mining Engineering Commons](#)

Recommended Citation

Rose, Emily, "CHARACTERIZATION OF GRANITE AND SUBSEQUENT GROUND CONTROL MANAGEMENT PLAN AT ORPHAN BOY MINE – BUTTE, MONTANA" (2017). *Graduate Theses & Non-Theses*. 122.
http://digitalcommons.mtech.edu/grad_rsch/122

This Thesis is brought to you for free and open access by the Student Scholarship at Digital Commons @ Montana Tech. It has been accepted for inclusion in Graduate Theses & Non-Theses by an authorized administrator of Digital Commons @ Montana Tech. For more information, please contact sjuskiewicz@mtech.edu.

CHARACTERIZATION OF GRANITE AND SUBSEQUENT GROUND
CONTROL MANAGEMENT PLAN AT ORPHAN BOY MINE – BUTTE,
MONTANA

by
Emily Rose

A thesis submitted in partial fulfillment of the
requirements for the degree of

Master of Science in Mining Engineering

Montana Tech

2017



Abstract

The Underground Mine Education Center (UMEC) and World Museum of Mining facilities began as shallow underground mines in the 1880's during the mining boom that populated Butte, Montana. The UMEC is a multi-disciplinary facility that provides an on-campus underground laboratory environment and a place for students to learn and practice practical underground mining techniques; therefore, the longevity of the facility is important to Montana Tech. The goal of this project is to develop a Ground Control Management Plan (GCMP) for the UMEC and World Museum of Mining facilities.

The World Museum of Mining (Orphan Girl) and UMEC (Orphan Boy) facilities are unique due to the shallow depth of underground mining activities that resumed in 2005 and in 2012, respectively. The Orphan Boy and Orphan Girl mines are connected at the 100-level. Ground support methods in these facilities consist of historic timber square sets in older workings, rock bolts with mesh, and some shotcreted areas in current workings. The GCMP contains a schedule for routine observational checks of the support systems to inspect for mesh tension, wire breakage, rock bolt plate bending, bolt head deformation, and shotcrete cracking (Carlisle, 2015). The GCMP defines a list of minimum geotechnical standards to uphold while developing new headings in these facilities. To construct the GCMP, geologic and geotechnical profiles for each mine were developed to aid in identifying areas of weakness due to rock alteration and/or adverse jointing caused by faulting or seismic activity. Locations in the UMEC that are believed stable regions will become permanent control survey regions to allow accurate measurements to monitor weaker areas for movement. A scanline survey (SLS) was conducted to determine the general direction joints in the granite occur. A joint surface map was created using Maptek Vulcan software. Rock support assessments based on the joint surfaces were completed using Rocscience DIPS software.

Keywords: Ground control, underground mine, granite, GCMP, SLS, UMEC, joint surface map

Acknowledgements

I would like to thank Montana Tech for offering a Graduate Teaching Assistantship that gave me the opportunity to obtain my Master's Degree. Thank you Sonya Rosenthal for reading through my first draft and providing many comments to help improve my writing prior to sending it to my committee. Thank you to my graduate committee members: Scott Carlisle, P.E., Dr. Jeffery Johnson, and Dr. Mary MacLaughlin for your edits and helpful suggestions during the thesis process.

Thank you Chris Roos for providing assistance when working with Vulcan software. Thank you Braxy Baxter, Lucas McQuinn, Jordan Artis for helping me gather all of my rock samples underground and move them to the lab for testing. Thank you to the Practical Underground Mining Class for aiding me in the characterization of the granite while I was conducting my Scanline Survey. Additionally, thank you Dr. Christopher Gammons for providing assistance with the understanding of the geochemistry of the Butte District.

Last, but certainly not least, thank you Scott Rosenthal, committee chair and thesis advisor, for your guidance and ability to keep me on track with this project. I would not have such an amazing thesis topic without your support. Thank you for putting up with my madness, loudness, and confusion for the duration of this project.

Table of Contents

| | |
|---|------------|
| ABSTRACT | II |
| ACKNOWLEDGEMENTS | III |
| LIST OF TABLES | VII |
| LIST OF FIGURES..... | IX |
| LIST OF EQUATIONS | XVI |
| | |
| 1. INTRODUCTION | 1 |
| 2. GEOLOGIC SETTING | 2 |
| 2.1. <i>Boulder Batholith</i> | 2 |
| 2.2. <i>Butte Granite</i> | 4 |
| 2.2.1. Butte Quartz-Monzonite | 4 |
| 2.2.2. Aplite Dikes..... | 5 |
| 2.2.3. Quartz-Porphyry Dikes | 5 |
| 2.3. <i>Rhyolite Complex</i> | 5 |
| 3. PREVIOUS MINING ACTIVITIES..... | 7 |
| 3.1. <i>Nomenclature</i> | 9 |
| 3.2. <i>Orphan Boy and Orphan Girl Mine Development</i> | 9 |
| 4. SITE LOCATION | 10 |
| 4.1. <i>Underground Mine Education Center (UMEC)</i> | 10 |
| 4.2. <i>Granitic Features at UMEC</i> | 11 |
| 5. CHARACTERIZATION OF GRANITE | 12 |
| 5.1. <i>Weathering Grade Classification</i> | 12 |
| 5.1.1. Weathering Grade Mapping..... | 13 |
| 5.2. <i>Field Characterization</i> | 14 |
| 5.3. <i>Laboratory Characterization</i> | 15 |

| | | |
|----------|--|----|
| 5.3.1. | Sample Preparation | 15 |
| 5.3.2. | Ultrasonic Velocity Test (ULT) | 16 |
| 5.3.2.1. | Ultrasonic Velocity Test Results | 16 |
| 5.3.3. | Unconfined Compressive Strength Test | 18 |
| 5.3.3.1. | UCS Test Results..... | 18 |
| 5.3.4. | Triaxial Compressive Strength Test | 21 |
| 5.3.4.1. | Triaxial Compressive Strength Test Results..... | 23 |
| 5.3.5. | Mohr-Coulomb failure Envelope | 24 |
| 5.3.5.1. | Consideration of the Generalized Hoek-Brown Method..... | 26 |
| 5.3.6. | Brazilian Test | 27 |
| 5.3.6.1. | Brazilian Test Results..... | 27 |
| 5.3.7. | Point Load Test (PLT)..... | 28 |
| 5.3.7.1. | PLT Results | 29 |
| 5.3.8. | Strength Based Weathering Grade Classification..... | 30 |
| 5.4. | <i>Software Analysis</i> | 30 |
| 5.4.1. | RocScience DIPS | 31 |
| 5.4.2. | RocScience Unwedge | 32 |
| 5.4.2.1. | Consideration of Numerical Model Development | 36 |
| 5.4.3. | MapTek Vulcan..... | 36 |
| 6. | UMEC ROCK CLASSIFICATIONS | 38 |
| 6.1. | <i>Rock Quality Designation for UMEC Granite</i> | 38 |
| 6.1.1. | Palmström’s RQD | 38 |
| 6.1.2. | Priest and Hudson’s RQD..... | 39 |
| 6.1.3. | Differences in methodology | 39 |
| 6.2. | <i>Rock Mass Rating for UMEC Granite</i> | 39 |
| 6.3. | <i>Q-System Classification for UMEC Granite</i> | 40 |
| 6.4. | <i>Applications of the Rock Structure Rating (RSR)</i> | 43 |
| 7. | DEVELOPMENT OF GROUND CONTROL MANAGEMENT PLAN..... | 45 |
| 8. | CONCLUSIONS..... | 46 |

| | |
|---|-----|
| 9. RECOMMENDATIONS..... | 48 |
| 10. REFERENCES CITED..... | 49 |
| APPENDIX A: WEATHERING GRADES OBSERVED AT UMEC..... | 52 |
| APPENDIX B: ADDITIONAL MAPS | 55 |
| APPENDIX C: CUMULATIVE CORE DATA..... | 58 |
| APPENDIX D: GCTS ULT-100 TESTING RESULTS..... | 61 |
| APPENDIX E: UCS TEST CORE SAMPLE RESULTS | 68 |
| APPENDIX F: TRIAXIAL TEST CORE SAMPLE RESULTS | 75 |
| APPENDIX G: BRAZILIAN TEST AND POINT LOAD TEST CORE SAMPLE RESULTS..... | 82 |
| APPENDIX H: SUPPLEMENTAL SOFTWARE FIGURES..... | 86 |
| APPENDIX I: ADDITIONAL CALCULATIONS..... | 100 |
| APPENDIX J: GROUND CONTROL MANAGEMENT PLAN..... | 108 |

List of Tables

| | |
|---|----|
| Table I: ISRM classification system (Modified from Barton, 1978)..... | 13 |
| Table II: SLS data collected in the field. | 14 |
| Table III: Core sample subdivision..... | 15 |
| Table IV: UCS Test Results..... | 18 |
| Table V: Young’s Modulus values derived from the slope of the stress-strain curves. | 19 |
| Table VI: Triaxial Test Results..... | 23 |
| Table VII: Young’s Modulus values derived from the slope of the stress-strain curves...24 | |
| Table VIII: Brazilian test results..... | 28 |
| Table IX: PLT results..... | 29 |
| Table X: UCS values compared to ISRM published values (Modified from Barton, 1978).30 | |
| Table XI: Average strike and dip measurements selected in DIPS. | 32 |
| Table XII: Unwedge input data parameters | 33 |
| Table XIII: Unwedge output..... | 34 |
| Table XIV: Unwedge input data parameters. | 35 |
| Table XV: RMR parameters (Modified from Bieniawski, 1989)..... | 39 |
| Table XVI: RMR parameters and determined ratings. | 40 |
| Table XVII: Q-System input parameters (Modified from Hoek, 2007). | 41 |
| Table XVIII: Q-System input parameters..... | 41 |
| Table XIX: RSR selection summary..... | 43 |
| Table XX: Core sample parameters..... | 58 |
| Table XXI: ULT Testing Results. Values that are not listed were unable to be obtained during testing..... | 58 |

| | |
|--|-----|
| Table XXII: UCS Test and Triaxial Test results. | 59 |
| Table XXIII: Brazilian test results. | 59 |
| Table XXIV: Brazilian test results continued. | 60 |
| Table XXV: Point Load Test results. | 60 |
| Table XXVI: Point Load Test results continued. | 60 |
| Table XXVII: Cumulative Mohr Circle failure envelope results. | 60 |
| Table XXVIII: Interpretation summary. | 107 |

List of Figures

| | |
|---|----|
| Figure 1: Butte, Montana location in relation to the Boulder Batholith. Butte identified with red star (Modified from Foster et al., 2010)..... | 3 |
| Figure 2: Orphan Girl headframe sunk on the footwall side of the ore vein (Chaleen et al., 1981). | 7 |
| Figure 3: Cross sectional and profile view of the square-set timber alignment used in Butte mines. (Modified from Dunshee, 1913)..... | 8 |
| Figure 4: Geologic Map of the Butte District. Orphan Girl mine indicated with OG. Site location indicated with black star (Modified from Houston and Dilles, 2013). | 10 |
| Figure 5: UMEC in relationship to surface topography..... | 11 |
| Figure 6: Ultrasonic velocity test results for P-wave..... | 17 |
| Figure 7: Ultrasonic velocity test results for S-wave..... | 17 |
| Figure 8: Plot of the Axial Force versus Strain curves produced using the TerraTek software for the UCS tests..... | 19 |
| Figure 9: Plot of Axial Force versus Axial Strain curves produced using the TerraTek software for the UCS tests. | 21 |
| Figure 10: Axial Force versus axial strain test results obtained during triaxial testing. 500 psi confining pressure indicated with solid line. 150 psi confining pressure indicated with dashed line. | 23 |
| Figure 11: Mohr-Coulomb failure envelope for Grade I granite developed from laboratory testing. Cohesion and friction angle values are 362 psi and 63°, respectively. | 25 |
| Figure 12: Mohr-Coulomb failure envelope for Grade II granite developed from laboratory testing. Cohesion and friction angle values are 402 psi and 54°, respectively. | 25 |

Figure 13: Mohr-Coulomb failure envelope for Grade III granite developed from laboratory testing. Cohesion and friction angle values are 396 psi and 47°, respectively.26

Figure 14: DIPS stereonet projection with density contour and primary joint sets. A larger view of the stereonet is available in Appendix F.....32

Figure 15: Unwedge predicted wedge failures.34

Figure 16: Unwedge predicted wedge failures with added bolt support. Additional views are available in Appendix H.35

Figure 17: Zoomed in section of UMEC showing strike and dip projection planes. Full scale figure available in Appendix B.37

Figure 18: UMEC Q and Q_{wall} . Extrapolated values indicated with dashed red line. Q and Q_{wall} range are indicated by red shaded area.42

Figure 19: RSR value for the UMEC. Red line indicates the type of bolt used.44

Figure 20: Weathering Grade I observed at UMEC.52

Figure 21: Weathering Grade II observed at UMEC.52

Figure 22: Weathering Grade III observed at UMEC.53

Figure 23: Weathering Grade IV observed at UMEC.53

Figure 24: Weathering Grade V observed at UMEC.54

Figure 25: Weathering Grade VI observed at UMEC.54

Figure 26: UMEC map with sample locations indicated by red star.55

Figure 27: UMEC weathering grade map.56

Figure 28: UMEC with strike and dip planes.57

Figure 29: P-Wave response for Sample A at 1,590 meters per second.61

Figure 30: S-Wave response for Sample G is unresponsive.61

| | |
|---|----|
| Figure 31: P-Wave response for Sample J at 1,222 meters per second. | 61 |
| Figure 32: S-Wave response for Sample J is unresponsive. | 62 |
| Figure 33: P-Wave response for Sample K at 1,047 meters per second. | 62 |
| Figure 34: S-Wave response for Sample K is unresponsive. | 62 |
| Figure 35: P-Wave response for Sample L1 at 2,992 meters per second. | 62 |
| Figure 36: S-Wave response for Sample L1 at 1,345 meters per second. | 63 |
| Figure 37: P-Wave response for Sample A at 1,590 meters per second. | 63 |
| Figure 38: S-Wave response for Sample A at 1,138 meters per second. | 63 |
| Figure 39: P-Wave response for Sample B at 1,553 meters per second. | 64 |
| Figure 40: S-Wave response for Sample B at 1,057 meters per second. | 64 |
| Figure 41: P-Wave response for Sample D at 1,769 meters per second. | 64 |
| Figure 42: S-Wave response for Sample D at 1,293 meters per second. | 64 |
| Figure 43: P-Wave response for Sample E at 1,296 meters per second. | 65 |
| Figure 44: S-Wave response for Sample E at 946 meters per second. | 65 |
| Figure 45: P-Wave response for Sample F at 1,570 meters per second. | 65 |
| Figure 46: S-Wave response for Sample F at 1,202 meters per second. | 65 |
| Figure 47: P-Wave response for Sample P2 at 2,471 meters per second. | 66 |
| Figure 48: S-Wave response for Sample P2 at 1,425 meters per second. | 66 |
| Figure 49: P-Wave response for Sample P4 at 3,207 meters per second. | 66 |
| Figure 50: S-Wave response for Sample P4 at 1,985 meters per second. | 67 |
| Figure 51: P-Wave response for Sample Q1 at 2,790 meters per second. | 67 |
| Figure 52: S-Wave response for Sample Q1 at 1,647 meters per second. | 67 |

| | |
|---|----|
| Figure 53: Plot of the Stress versus Strain curves produced using the TerraTek software for the UCS tests..... | 68 |
| Figure 54: Sample G prior to axial load. No distinct cracks present in core. | 68 |
| Figure 55: Sample G after axial load. Sample continuously compressed, causing force to undulate until nonviolent shear failure occurred. | 69 |
| Figure 56: Sample J prior to axial load. No distinct cracks present in core. | 69 |
| Figure 57: Sample J after axial load. Sample compressed until nonviolent failure occurred. Failure crack indicated with pencil. | 69 |
| Figure 58: Sample K prior to axial load. No distinct cracks present in core. | 70 |
| Figure 59: Sample K after axial load. Sample compressed until nonviolent failure occurred. Failure crack indicated with pencil. | 70 |
| Figure 60: Plot of the Stress versus Strain curves produced using the TerraTek software for the UCS tests..... | 71 |
| Figure 61: Sample A prior to axial load. No distinct cracks present in core. | 71 |
| Figure 62: Sample A after axial load. Sample compressed until nonviolent failure occurred. Failure crack indicated with pencil. | 71 |
| Figure 63: Sample B prior to axial load. No distinct cracks present in core. | 71 |
| Figure 64: Sample B after axial load. Sample compressed until nonviolent failure occurred. Failure crack indicated with pencil. | 72 |
| Figure 65: Sample E after axial load. No photograph was taken prior to axial load. Sample compressed until nonviolent failure occurred. Multiple axial splits developed while under load. Failure crack indicated with pencil. | 72 |

| | |
|---|----|
| Figure 66: Plot of the Stress versus Strain curves produced using the TerraTek software for the UCS tests..... | 73 |
| Figure 67: Sample P1 prior to axial load. Large crack approximately 30° from vertical. . | 73 |
| Figure 68: Sample P1 after axial load. Sample compressed until brittle failure occurred along major discontinuity. | 74 |
| Figure 69: Sample P2 prior to axial load. Small fracture indicated with pencil..... | 74 |
| Figure 70: Sample P2 after axial load. Sample compressed until first brittle cracking occurred along major discontinuity, causing sharp drop in axial pressure. Failure occurred shortly after, causing additional cracking to form throughout the core sample..... | 74 |
| Figure 71: Plot of the Stress versus Strain curves produced using the TerraTek software for the triaxial tests at 500 psi confining pressure..... | 75 |
| Figure 72: Sample D prior to triaxial load. No distinct cracks present in core..... | 75 |
| Figure 73: Sample D after triaxial load. Sample failed nonviolently, no distinct shear planes present. | 76 |
| Figure 74: Sample L1 prior to triaxial load. No distinct cracks present in core. Small cracks patched with bolt anchor sulfaset yellow: high speed expansive anchoring compound. | 76 |
| Figure 75: Sample L1 after triaxial load. Sample failed nonviolently, no distinct shear planes present. | 76 |
| Figure 76: Sample P4 prior to triaxial load. No distinct cracks present in core. | 77 |
| Figure 77: Sample P4 after triaxial load. Sample failed nonviolently. Small shear fracture indicated with pencil. | 77 |

| | |
|---|----|
| Figure 78: Plot of the Stress versus Strain curves produced using the TerraTek software for the triaxial tests at 150 psi confining pressure. | 78 |
| Figure 79: Sample F prior to triaxial load. No distinct cracks present in core. | 78 |
| Figure 80: Sample F after triaxial load. Sample failed nonviolently. Small shear fracture indicated with pencil. | 79 |
| Figure 81: Sample O prior to triaxial load. No distinct vertical cracks present in core. Small cracks patched with bolt anchor sulfaset yellow: high speed expansive anchoring compound. | 79 |
| Figure 82: Sample O after triaxial load. Sample failed nonviolently. Small shear fracture indicated with pencil. | 80 |
| Figure 83: Sample Q1 prior to triaxial load. No distinct cracks present in core. | 80 |
| Figure 84: Sample Q1 after triaxial load. Sample failed nonviolently. No shear fracture planes are visible. | 81 |
| Figure 85: Brazilian test results. | 83 |
| Figure 86: Brazilian test results. | 84 |
| Figure 87: Point load test results. | 85 |
| Figure 88: Difference in equal angle and equal area stereonet projection methods (Modified from RocScience, 2017). | 86 |
| Figure 89: DIPS stereonet projection with density contour and primary joint sets. | 87 |
| Figure 90: Unwedge model with different views. | 88 |
| Figure 91: Unwedge model with added bolt support. | 89 |
| Figure 92: Cross section view of Unwedge model with bolt supports. | 90 |
| Figure 93: 45° Unwedge model with different views. | 91 |

| | |
|---|-----|
| Figure 94: 45° Unwedge model with added bolt support. Bolt pattern indicated in blue, spot bolts indicated in green. | 92 |
| Figure 95: 45° Unwedge model with added bolt support with different views. | 93 |
| Figure 96: 90° Unwedge model with different views. | 94 |
| Figure 97: 90° Unwedge model with added bolt support. Bolt pattern indicated in blue, no spot bolts are necessary in this direction. | 95 |
| Figure 98: 90° Unwedge model with added bolt support with different views. | 96 |
| Figure 99: 135° Unwedge model with different views. | 97 |
| Figure 100: 135° Unwedge model with added bolt support. Bolt pattern indicated in blue, spot bolts indicated in green. | 98 |
| Figure 101: 135° Unwedge model with added bolt support with different views. | 99 |
| Figure 102: Q-system selections (Modified from Palmström, 2015). | 102 |
| Figure 103: Q-system selections (Modified from Palmström, 2015). | 104 |
| Figure 104: RMR selections (Modified from Bieniawski, 1989). | 105 |
| Figure 105: RSR selections (Modified from Hoek, 2007). | 106 |

List of Equations

(1).....18
(2).....22
(3).....27
(4).....29
(5).....29
(6).....29
(7).....38
(8).....39
(9).....41
(10).....42
(11).....43
(12).....100
(13).....100
(14).....100
(15).....100

Glossary of Terms¹

| Term | Definition |
|----------------------|--|
| Aureole | Zone surrounding an igneous intrusion in which contact metamorphism of the country rock has taken place. |
| Batholith | A large, generally discordant plutonic mass that has more than 40 square miles of surface exposure and no known floor. Its formation is believed by most investigators to involve magmatic processes. |
| Cut and Fill stoping | A stoping method in which the ore is excavated by successive flat or inclined slices, working upward from the level, as in shrinkage stoping. However, after each slice is blasted down all broken ore is removed, and the stope is filled up to within a few feet of the back before the next slice is taken out, just enough room being left between the top of the waste pile and the back of the stope to provide working space. The term cut-and-fill stoping implies a definite and characteristic sequence of operations: (1) breaking a slice of ore from the back; (2) removing the broken ore; and (3) introducing fill. |
| Dike | Tabular body of igneous rock that cuts across the structure of adjacent rocks or cuts massive rocks |
| Dip | The angle that a stratum or any planar feature makes with the horizontal, measured perpendicular to the strike and in the vertical plane. |
| Drift | A horizontal passage underground that follows the vein, as distinguished from a crosscut, which intersects it, or a level or gallery which may do either. |
| Epigenetic Deposit | Said of a mineral deposit of origin later than that of the enclosing rocks. Examples of deposits include veins, lenses, stocks and pipes that cut through the host rock. Most are hydrothermal or metasomatic in origin. |
| Footwall | The mass of rock beneath a fault, orebody, or mine working; especially the wall rock beneath an inclined vein or fault. |
| Hanging Wall | The overlaying side of an orebody, fault, or mine working; especially the wall rock above an inclined vein or fault. |
| Heading | A smaller excavation driven in advance of the full-size section; it may also be driven laterally, and it is then called a cross heading or side drift. A heading is driven at the top or the bottom of the full-size face; it is then a top or a bottom heading as the case may be. |

¹ All geologic and mining related definitions have been gathered from Bates and Jackson (1984) and Thrush et al. (1968), respectively.

| | |
|--------------------|--|
| Hydrothermal | Of or pertaining to hot water, to the action of hot water, or to the products of this action, such as a mineral deposit precipitated from a hot aqueous solution. |
| Metasomatic | Pertaining to the process of metasomatism which is defined as the process of practically simultaneous capillary solution and deposition by which a new mineral may grow in the body of an old mineral or mineral aggregate. |
| Mohr Coulomb | Failure criterion for soils and rock. Relates normal effective stresses and tangential stresses acting on any plane of the soil at the time of failure. |
| Overhand mining | Overhand cut-and-fill: two level drives are first connected, the lower and upper one by a raise, from the bottom of which mining is begun. The work proceeds upwards, filling the mined-out room, but in the filling, chutes are left through which broken ore falls. In inclined seams the chutes, also inclined, have to be timbered. The lower-level drive is protected either by timbering or vaulting, or by fairly strong pillar of vein fillings. Stopping in the different cuts always proceeds upwards, but as a whole it proceeds between the two level drives in a horizontal direction. |
| Saprolite | A soft, earthy, clay-rich thoroughly decomposed rock formed in place by chemical weathering of igneous or metamorphic rocks, especially in humid or tropical or subtropical climates. The color is commonly red or brown. Saprolite is characterized by preservation of structures that were present in the unweathered rock. |
| Shaft | An excavation of limited area compared with its depth, made for finding or mining ore, raising water, ore, and rock, hoisting and lowering men and material, or ventilating underground workings. The term is often specifically applied to vertical shafts, as distinguished from an incline or inclined shaft. |
| Sill | The floor of a gallery or passage in a mine. |
| Square-set stoping | A method of stoping in which the walls and back of the excavation are supported by regular framed timbers forming a skeleton enclosing a series of connected, hollow, rectangular prisms in the space formerly occupied by the excavated ore and providing continuous lines of support in three directions at right angles to each other. The ore is excavated in small, rectangular blocks just large enough to provide room for standing a set of timber. The essential timbers comprising a standard square set are respectively termed posts, caps, and girts. The posts are the upright members, and the caps and girts are the horizontal members. The ends of the members are framed to give each a bearing against the other two at the corners of the sets where they join together. The stopes usually are mined out in floors or horizontal panels, and the sets of each successive floor are framed into the sets of the preceding floor; however, sometimes the sets are mined out in a series of vertical, or inclined panels. |

| | |
|-----------------------|--|
| Squeezing | The slow increase in weight on pillars or solid material eventually resulting in such things as crushing of material, heaving of the bottom and the driving of pillars into soft floor or top. |
| Stockwork Vein System | Three-dimensional zone laced with closely spaced irregular veinlets that are mineralized. The system generally contains planar and irregular veinlets that are close enough to be mined. |
| Stope | An underground excavation formed by the extraction of ore. |
| Strike | The direction taken by a structural surface as it intersects the horizontal. |
| Supergroup | In stratigraphy, an assemblage of related groups, or of formations and groups, having significant lithologic features in common. |
| Vein | An epigenetic mineral filling of a fault or other fracture, in tabular or sheetlike form, often with associated replacement of the host rock; a mineral deposit of this form and origin |
| Vent | The opening at the Earth's surface through volcanic materials are extruded; also, the channel or conduit through which they pass. |
| Zenith | The point on the celestial sphere that is directly above the observer and directly opposite the nadir; assuming the nadir is the point on the celestial sphere that is directly beneath the observer and directly opposite the zenith. |

1. Introduction

The Underground Mine Education Center (UMEC) and World Museum of Mining facilities began as shallow underground mines in the 1880's during the mining boom that populated Butte, Montana. The primary commodities extracted from the UMEC (Orphan Boy Mine) and World Museum of Mining (Orphan Girl Mine) facilities were lead, zinc, and silver; atypical of Butte's large copper operations. These anomalous commodities formed in a granitic host rock containing mineralized zones of rhodochrosite and aplite with localized zones of clay alteration due to shear zones.

The UMEC and World Museum of Mining facilities are unique due to the shallow depth of underground mining that recommenced beginning in 2005, driving from the 65² level to the 100-level at the Orphan Girl and in 2012 when the Orphan Boy decline was begun (Rosenthal, 2015). The Orphan Boy and Orphan Girl mines are connected at the 100-level.

Ground support methods in these facilities consist of historic timber square sets in older workings (for display purposes only), rock bolts with mesh, and some shotcreted areas in current workings. The timber-supported areas are challenging to inspect as it is difficult to determine if the timber sets are properly blocked, if void spaces exist above the set, or if ground conditions around the set are deteriorating. The goal of this project was to develop an active Ground Control Management Plan (GCMP) for the UMEC and World Museum of Mining facilities, outlining proper protocols for inspection of ground supports, characterization of granite, granitic grade mapping, and proper ground support installation. Granitic characterization included field and laboratory characterization of the granite at the UMEC; specifically weathering grade classification, and sample collection for laboratory analyses involving strength testing.

² The 65-level and 100-level indicate the depth below the surface elevation, not relative to sea level.

2. Geologic Setting

The occurrence of the epigenetic deposits found in the Butte district is extensive. Due to the complex nature of the rock in the district, only formations pertinent to the research are discussed in this section. The primary mineralization found in the Butte district is described as a Cordilleran Vein Deposit; referring to the fault-fissure controlled, lead-zinc-copper mineralized vein districts (Guilbert and Park, 1986). Cordilleran type deposits generally contain the same suite of elements and ore minerals as porphyry coppers within their distinct zonation from tin-tungsten, wolframite-molybdenum through copper-zinc to zinc-lead-manganese-silver (Guilbert and Park, 1986). Copper-zinc zonation progresses to zinc-lead-manganese-silver zonation moving west through the Butte district.

2.1. Boulder Batholith

Butte is situated near the western border of the Late Cretaceous age Boulder Batholith (Sales, 1913). The Batholith is primarily composed of granite, with varying intrusions throughout (Figure 1). The Proterozoic Belt Supergroup hosts the Boulder Batholith (Houston and Dilles, 2013).

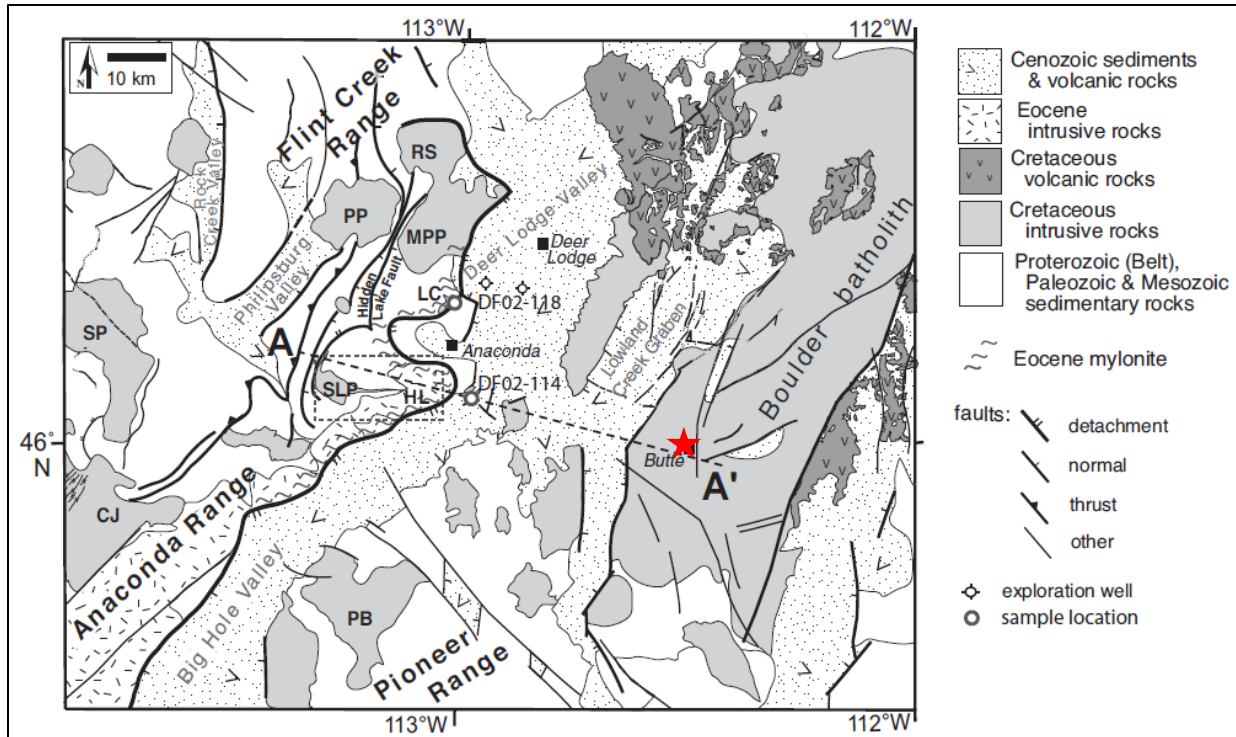


Figure 1: Butte, Montana location in relation to the Boulder Batholith. Butte identified with red star (Modified from Foster et al., 2010).

The Boulder Batholith is an oblong shape with an irregular width that averages 20 miles long. The Batholith was emplaced into the Laramide fold-and-thrust orogenic belt in southwestern Montana. Primary copper ore formation occurred during several geologic events spanning three to four million years. Ore formation is associated with quartz-porphry dike emplacement, rather than the formation of the Boulder Batholith. Early fracturing and faulting is associated with the porphyry copper-molybdenum deposits and additional copper veins in the Laramide period (Houston and Dilles, 2013).

Chemical composition of the granite remains uniform throughout the Boulder Batholith. Localized textural differences, developed due to uneven cooling rates, create physical differences and were documented throughout the Batholith (Sales, 1913). The irregular cooling rate of the granite caused segregation of aplite in the form of dikes or large masses. Aplite dike formation occurred during cooling stages and influenced other occurrences of ore deposits in the Batholith.

Sales (1913) observed the aplite dikes are most prominent around Butte. Continued uplift and unroofing exposed mineralized rocks buried by the Eocene Lowland Creek Volcanic Formation. The Lowland Creek Volcanics and Butte Quartz-Monzonite host a series of rhyolitic dikes exposed during the uplift of the Formation (Houston and Dilles, 2013).

Associated mineralization in Butte is considered a Cordilleran Vein Deposit because the mineralization is characterized by hydrothermally transported ore components deposited in epigenetic stages from solutions in fractures and fault veins (Sawkins, 1972). Deposits are structurally controlled and display well-developed bilaterally symmetrical wall-rock alteration. Sericite is the most abundant alteration mineral in these deposits with presence of siderite, rhodochrosite and ankerite in the vein system (Guilbert and Park, 1986).

2.2. Butte Granite

The Butte Granite and associated aplite dikes constitute approximately 75 percent of the area of the Boulder Batholith. The granite consists of plagioclase, orthoclase, quartz, biotite, hornblende, magnetite, ilmenite, and apatite (Houston and Dilles, 2013). The granite exhibits a well-defined joint system, independent from the well-defined fissure system present in the rock. Aplite dikes are present in the northwestern portion of the Butte district. A series of parallel quartz-porphyry dikes extending in an east-west direction intruded the copper belt in the Butte District. According to Sales (1913), fissures are well documented in the Butte district and are classified based on age.

2.2.1. Butte Quartz-Monzonite

The granitic body that hosts mineralization in the Boulder Batholith was referred to as Butte Quartz-Monzonite (BQM) until Lund and colleagues (2002) determined that the host rock

possessed the geochemical composition of granite rather than a true quartz-monzonite. This discovery has formally renamed the BQM as a granite³.

2.2.2. Aplite Dikes

Aplite dikes are cogenetic with the Butte Granite; emplaced during the latter stages of crystallization (Houston and Dilles, 2013). Aplite dikes are abundant in the northwestern portion of the Butte District and are gently dipping, making up sheeted planar sets (Sales, 1913; Houston and Dilles, 2013). The main copper belt contains little to no aplite dikes (Sales, 1913).

2.2.3. Quartz-Porphyry Dikes

A series of parallel quartz-porphyry dikes intruded the Butte Granite in the central portion of the Butte District in an eastern-striking, southern-dipping fashion (Sales, 1913; Houston and Dilles, 2013). The dikes are relatively narrow and follow closely with the general trend of the earliest system of copper veins, indicating a close genetic relation between the oldest copper vein system and the quartz porphyry dikes (Sales, 1913). Geochemical studies conducted by Houston and Dilles (2013) determined that two pre-Main stage porphyry copper-molybdenum mineralization and alteration locales formed simultaneously with the intrusion of the quartz porphyry dikes.

2.3. Rhyolite Complex

Intrusive and extrusive rhyolite occurs in the west and northwest of the Butte District. Intrusive rhyolite forms the main body of Big Butte⁴. Numerous rhyolitic dikes offshoot in a general north-south direction from the main body (Sales, 1913). Rhyolitic dikes exposed at Big

³ Due to the name change, the BQM will be referred to as Butte Granite in subsequent sections.

⁴ Big Butte is informally known as “The M” in present day terms.

Butte form a rhyolitic vent complex that is part of the Lowland Creek Volcanics. The vent cross cuts older Butte Granite and postdates Main Stage veins (Houston and Dilles, 2013). Extrusive rhyolite extends northwest from Big Butte, covering a large area, remnant of a much larger rhyolite flow that previously covered the western half of the Boulder Batholith (Sales, 1913).

3. Previous Mining Activities

Butte originated as a placer mining camp, as gold was discovered in Silver Bow Creek in 1864 (Daly et al., 1925). After the discovery of immense subsurface copper deposits, the Butte district mine openings consisted almost entirely of vertical shafts, cut and fill, or square set mining. The shafts were sunk on the footwall side of the steeply dipping vein deposits (Figure 2). Stations were cut at intervals of 100 to 200 feet; crosscuts were driven to intersect the veins. Drifts extended along the strike of the veins. Sills were opened up based on the characteristics of the vein and the vein width. Typically, working out of sills on large veins consisted of removing all the ore on the sill between the hanging wall and the footwall, square-setting and filling, leaving the drift open on the footwall side.

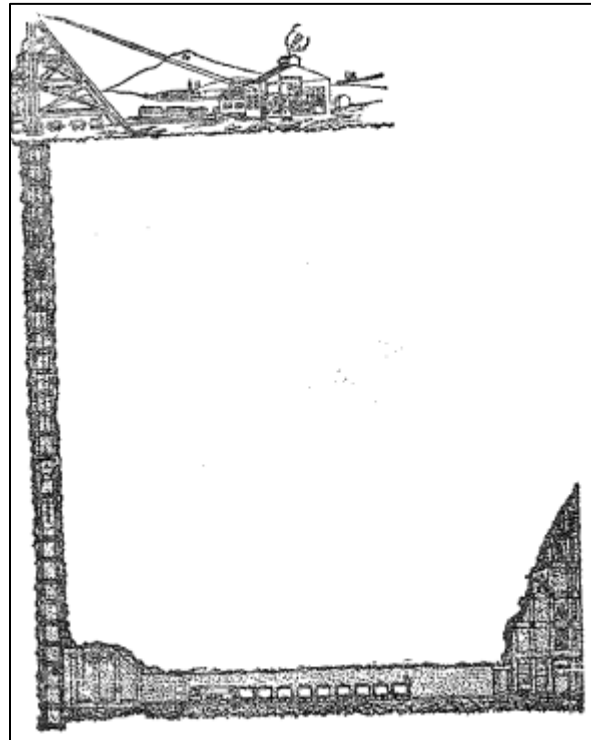


Figure 2: Orphan Girl headframe sunk on the footwall side of the ore vein (Chaleen et al., 1981).

The primary mining method used in the Butte district was overhand cut and fill with square-set framing for support. Approximately two-thirds of the Butte mining district uses the timber square-set framing design for stabilization of overhand cut and fill activities (Tunnell, 1922). The square-set framing solved the problem of large ore-bodies that were stoped and the timbers held the ground to prevent caving without any filling (Dunshee, 1913). Square-sets are used to timber the active mining level along the sill floor in order to stabilize the level (Tunnell, 1922). Figure 3 depicts the standard configuration used when developing headings on different levels.

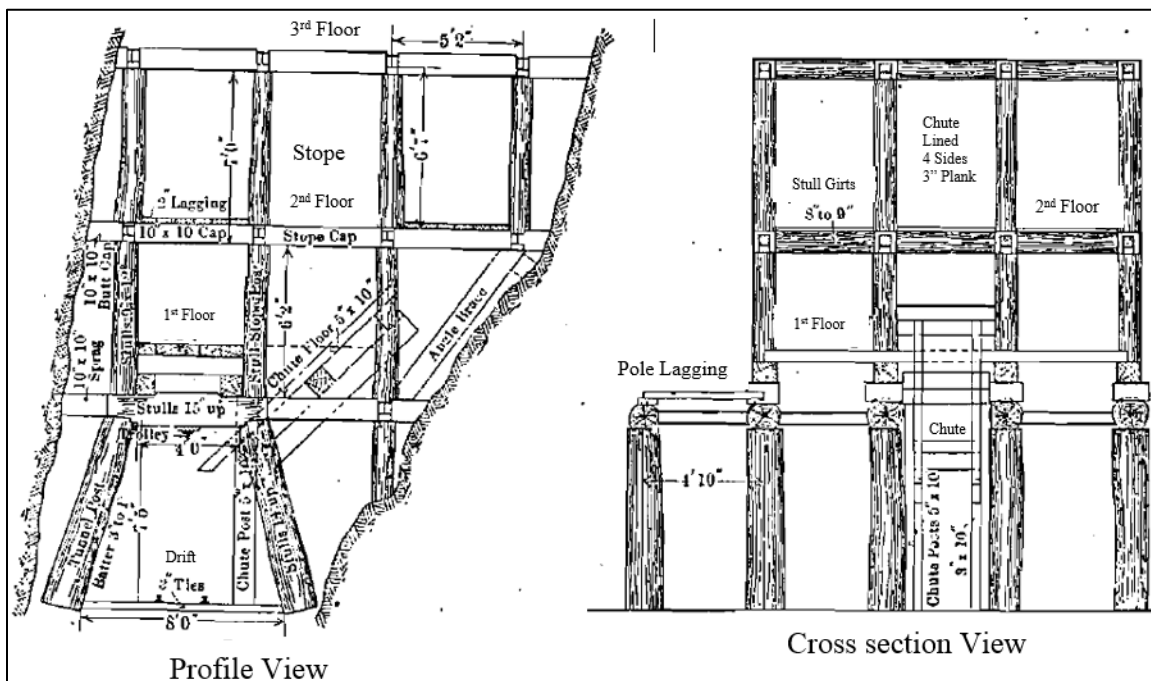


Figure 3: Cross sectional and profile view of the square-set timber alignment used in Butte mines. (Modified from Dunshee, 1913).

Using overhand stoping, the ore is blasted from a series of ascending drifts. In heavier ground, practices were modified to open the sill with a drift one set wide, leaving the remainder of the ore to be extracted on the level below. The opening above allowed for pressure relief as the mine progressed downwards. Due to the increasing depth of the mines, stopes were backfilled with waste in order to prevent collapse.

3.1. Nomenclature

It is speculated that the Orphan Boy and Orphan Girl lode claims were named based on the unique nature of the deposit. Since Butte is host to a massive porphyry copper deposit, it was unusual, at the time, to have discovered a zinc-lead-manganese-silver deposit that contained little copper. The Orphan Boy Lode and Orphan Girl Lode are aptly named since the deposits have no similarities to no previous lodes (Rosenthal, 2016).

3.2. Orphan Boy and Orphan Girl Mine Development

Marcus Daly discovered the Orphan Girl Lode claim in 1875 and patented the claim in 1895. Production of the Orphan Girl began in 1925 (Chaleen et al., 1988). The Orphan Girl Mine reopened for underground tours May 2, 2005 as part of the World Museum of Mining facility (Rosenthal, 2016).

William A. Clark patented the Orphan Boy Lode claim in 1895. In 2012, Montana Tech began development at the Orphan Boy Mine as the Underground Mine Education Center (UMEC) (Rosenthal, 2016). The UMEC is a student operated mine, as students enrolled in the mining engineering department are required to take the Practical Underground Mining course. The course focuses on teaching students mining techniques used in operating underground mines today. Students are responsible for the drilling, blasting, loading, and hauling of the material in their assigned heading.

4. Site Location

The UMEC site lies slightly northwest of a rhyolitic dike that intruded the Butte Granite in the Butte District (Figure 4).

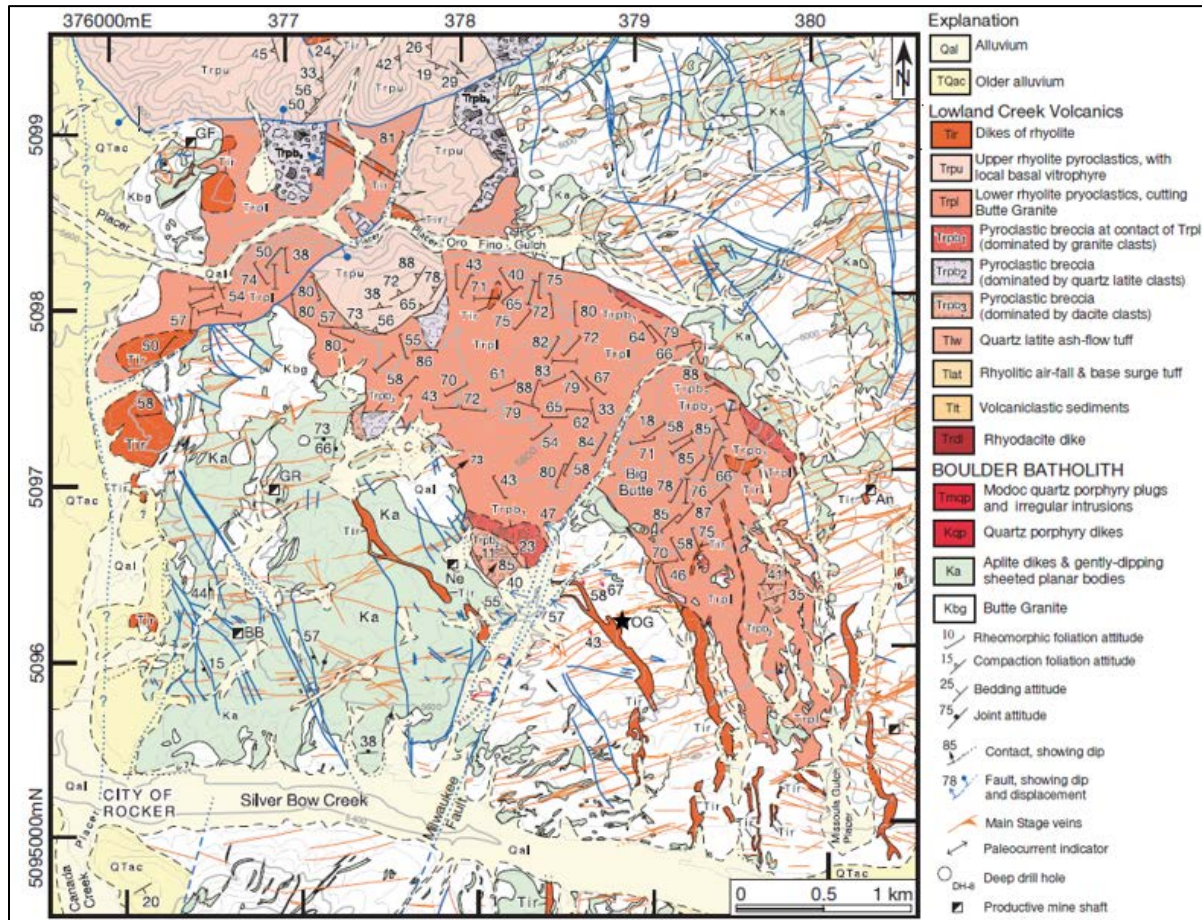


Figure 4: Geologic Map of the Butte District. Orphan Girl mine indicated with OG. Site location indicated with black star (Modified from Houston and Dilles, 2013).

4.1. Underground Mine Education Center (UMEC)

The UMEC is located on the Montana Tech campus (Figure 5). Montana Tech began development of the UMEC in 2012. The UMEC serves as an interactive learning and research facility for students in the Mining Engineering and Geological Engineering Departments at Montana Tech. The Geophysical Engineering Department and Safety, Health and Industrial Hygiene Department have also used the UMEC to conduct field research.



Figure 5: UMEC in relationship to surface topography.

4.2. Granitic Features at UMEC

Granite found on site was emplaced by the Boulder Batholith. Granite in the UMEC and World Museum of Mining facilities is blocky in nature and has varying degrees of weathering. Degree of weathering on site is dependent on latter geologic events (namely the quartz-porphyry dike system and the rhyolitic vent) that caused quartz vein intrusions and sericite alteration. Granitic features in the UMEC consist of fissures, fractures, quartz and calcite filled veins, and heavily jointed masses.

5. Characterization of Granite

Field data and laboratory data are required for the qualitative and quantitative characterization of granite at the UMEC. Field data collection occurred every Wednesday in conjunction with the Practical Underground Mining class. Laboratory data and testing occurred during the Fall 2016 and Spring 2017 semesters. Granitic characterization for the UMEC involved the following phases:

- Field characterization of the granite to determine degree of weathering on site,
- Laboratory characterization of the granite to determine the strength properties,
- Digitization of the field characterization and laboratory results in order to preserve the results of the analysis, and
- Calculations to determine the Rock Quality Designation (RQD), Q-System Classification, and Rock Mass Rating (RMR) of the granite on site.

5.1. Weathering Grade Classification

Several methods of granitic rock characterization have been developed to identify distinct features within the material that affect engineering properties of the rock. The International Society of Rock Mechanics (ISRM) standardized field and laboratory test methods for the quantitative description of discontinuities in rock masses and modeled the standardized format after Deere and Patton (1971). Deere and Patton (1971) outlined properties of residual soils and saprolites in Brazil.

ISRM used Deere and Patton's (1971) model to standardize the field data collection of wall strength. Barton (1978) states that there are two main results of weathering dominated by mechanical disintegration and chemical decomposition. Mechanical weathering results in the opening of discontinuities whereas chemical weathering results in the discoloration of the rock

mass (Barton, 1978). The ISRM divides the character of rock into three stages of weathering based on visual identification: fresh discolored, decomposed, and disintegrated. Alternatively, Barton (1978) identified a six-category classification system, providing an accurate description of weathered states of rock. Table I depicts a simplified version of the ISRM classification scheme using physical weathering properties and easily identifiable chemical weathering indicators, such as crystal decomposition.

Table I: ISRM classification system (Modified from Barton, 1978)

| Zone | Term | Description |
|-------------|----------------------|---|
| I | Fresh | Fully intact, no fractures present. |
| II | Slightly Weathered | Discolored and stained; weathered micas are present; small fractures are present. |
| III | Moderately Weathered | More rock than soil; Potassium feldspar and plagioclase feldspar crystals have begun to weather. Material must still be broken with tools, cannot break with hand. |
| IV | Highly Weathered | Essentially soil; potassium feldspar and plagioclase feldspar crystals are decomposed. Material is highly fissured but will not disintegrate in water. |
| V | Completely Weathered | Similar to saprolite. Completely weathered into soil with relict rock structure intact because material has not been disturbed. Can break without the use of tools. Will disintegrate in water. |
| VI | Residual Soil | Original crystal structure is not present. Disintegrated into soil with no relict rock structure present. |

The six-category classification scheme was used for the purpose of this research because the visual identification scheme developed by ISRM is too generic for granitic classification at the UMEC. Appendix A contains photographs of the weathering grades observed in the UMEC.

5.1.1. Weathering Grade Mapping

Mapping of the Orphan Boy and Orphan Girl mines occurred over the course of several weeks, beginning in January 2016. Mapping consisted of the following activities:

- Assigning the ribs of the Orphan Boy and Orphan Girl weathering zone based on the properties outlined in Table I,
- Performing a Scanline Survey (SLS) of distinct joint sets found on the ribs of the mine, and

- Collecting samples from the locations identified on the map in Appendix B.

5.2. Field Characterization

Field characterization was accomplished using a scanline survey (SLS) to collect fracture information along a line in the rock face (Kermy et al., 2002). A SLS provides detailed information on individual joints and joint sets used to determine an overall joint set trend. Table II outlines the criteria obtained in the field.

Table II: SLS data collected in the field.

| Criteria | Description |
|--------------------------|---|
| Fracture Number | Arbitrary value assigned in order that fractures were obtained. |
| Location | Location along measuring tape. The tape was always placed near a survey point in the mine. |
| Length | Length of the vein or joint. |
| Strike | Measured using the right hand rule when using a Brunton Compass. |
| Dip/Dip Direction | Measured perpendicular to the strike. |
| Roughness | Coefficient assigned based on the rock-wall contact. Assigned 0-4; 0 being very smooth; 4 being discontinuous. Used in determination of the joint roughness number for Q-system of rock classification. |
| Alteration | Contact between joint walls. Coefficient assigned 0-4 based on the material infill. Used in determination of the joint alteration number for the Q-system of rock classification. |
| Filling | Assumed vein material. |
| Reduction | Wetness of joints. Coefficient assigned 0->10 based on the wetness of the joints. Used in determination of the joint water reduction number for the Q-System of rock classification. |
| Aperture | Width of the fracture (if there is filing or if fracture is open). |

Strike and dip measurements were obtained using the “right hand rule” convention. The right hand rule states that if the right hand is placed on the surface of the feature and the hand is rotated such that the fingers point in the downwards direction, the thumb points to the strike (RocScience, 2017). Survey points, predefined by the Mining Engineering department, helped georeference the location of the SLS. SLS measurements were obtained near the survey point, distances from the survey point was noted in order to properly georeference the strike and dip measurements in a Maptek Vulcan database later.

5.3. Laboratory Characterization

Laboratory tests including the Ultrasonic Velocity Test, Uniaxial Compressive Strength (UCS) Test, Triaxial Compression Test, Brazilian Tests, and Point Load Tests were performed on field samples to determine the elastic and strength properties for UMEC granite. The objective of laboratory analyses were to determine the material properties of the UMEC granite and if the results derived from the Ultrasonic Velocity Test, Unconfined Compressive Strength (UCS) Test, Brazilian Test, and Point Load Test are similar.

5.3.1. Sample Preparation

Boulders collected from the sample sites identified in Section 5.1.1 were used to create core samples. Samples were prepped based on ASTM Standard D7012 – 10, 8.1 and 8.2. A full list of the core samples made and the core sample properties are in Appendix C. Core samples were subdivided into three suites based on granitic appearance (Table III). Suite 1 matched Grade III descriptions, Suite 2 matched Grade II descriptions, and Suite 3 matched Grade I descriptions.

Table III: Core sample subdivision

| Suite 1 | Suite 2 | Suite 3 |
|---------|---------|---------|
| G | A | P2 |
| J | B | P4 |
| K | D | Q1 |
| L1 | E | P1 |
| O | F | |

Prior to laboratory testing, the following assumptions were made:

- Samples in Suite 1 would produce strength results consistent with granite Weathering Grade III,
- Samples in Suite 2 would produce strength results consistent with Weathering Grade II, and

- Samples in Suite 3 would produce strength results consistent with granite Weathering Grade I.

Samples that were not of sufficient length for UCS or triaxial testing were set aside for Brazilian tests and Point Load tests. Sample P1 and Sample O were added prior to triaxial testing on February 3, 2017; therefore, the samples were not prepped in time for the ultrasonic velocity testing conducted on January 25, 2017.

5.3.2. Ultrasonic Velocity Test (ULT)

Ultrasonic Velocity (ULT) tests were performed using the GCTS ULT-100 Testing System. Laboratory ULT measurements were used to determine the elastic behavior of the UMEC granite. Testing provides compression (P-wave) and shear (S-wave) velocities that are used to determine dynamic Poisson's Ratio (μ) and dynamic Young's Modulus (E) (GCTS Testing Systems, 2016). ULT testing was conducted on the samples prepared for UCS and triaxial tests. To improve velocity measurement estimates, the coupling quality between the testing platen and the core sample was increased by spreading honey on the core sample. The first break from linear in the wave signal for both the P- and S-wave was manually selected to increase accuracy, and reduce the effect of noise on the results.

5.3.2.1. Ultrasonic Velocity Test Results

The results of the ULT-100 velocity tests showed that the P-wave velocity averages 1,900 meters per second, and the S-wave averages 1,300 meters per second. Higher density core samples produced a greater velocity P- and S-wave (Figures 6 and 7). Raw data exported from the GCTS Testing system is located in Appendix D.

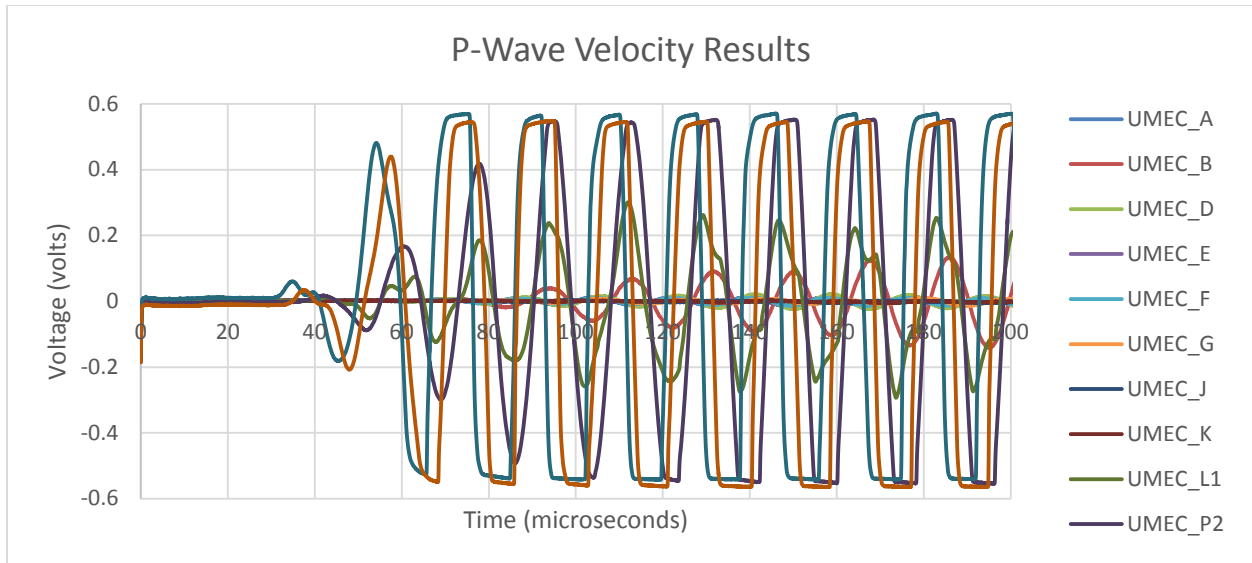


Figure 6: Ultrasonic velocity test results for P-wave.

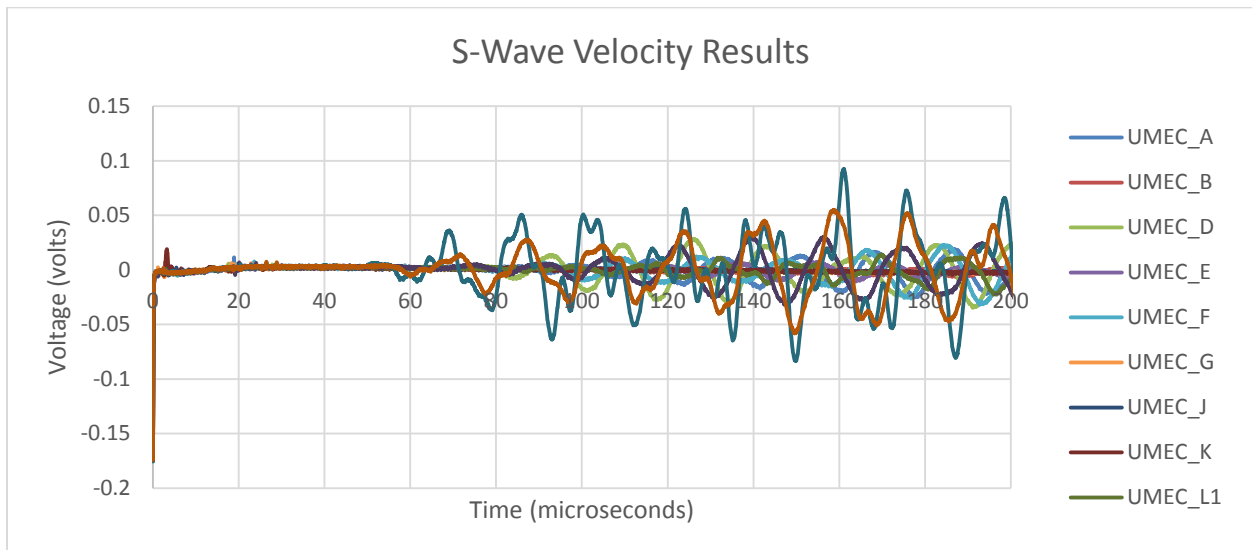


Figure 7: Ultrasonic velocity test results for S-wave.

Average dynamic Poisson's Ratio for the UMEC granite core is 0.22. Average dynamic Young's Modulus for the granite is 5.24×10^6 pounds per square inch (psi). Lower density samples in Suite 1 did not produce a reading for S-wave velocity. There are two reasons speculated for the lack of S-wave response:

1. An internal fracture network that is not visible on the outer surface of the core sample, or

2. The sample is so brittle at the ends of the core that the S-wave cannot complete a full cycle through the granite.

5.3.3. Unconfined Compressive Strength Test

UCS tests were performed using the TerraTek Load frame machine. ASTM Standard D7012 – 10.6 was followed during testing. Uniaxial Compressive Strength (UCS) defined as:

$$\sigma_c = \frac{P}{A} = \frac{4P}{\pi D^2} \quad (1)$$

where P is the load that causes failure, D is the diameter, and A is the cross sectional area of the specimen (Read and Stacey, 2009). Test specimens must maintain a length-to-width ratio of 2 to 2.5 times the diameter in order to perform a proper UCS test. Samples from each suite were selected for UCS and tested using the same parameters. The TerraTek load frame machine was calibrated to obtain Poisson's Ratio when testing Sample A, Sample J, and Sample P1.

5.3.3.1. UCS Test Results

Typical peak strength values for granite range from 20,500 psi to 32,800 psi (Goodman, 1989). Table IV displays the Peak load and UCS values for the tested samples.

Table IV: UCS Test Results

| Sample | Diameter (in) | Peak Force (lbf) | UCS (psi) |
|-----------|---------------|------------------|-----------|
| A | 1.726 | 7,324 | 3,130 |
| B | 1.725 | 4,091 | 1,750 |
| E | 1.725 | 4,776 | 1,900 |
| G | 1.722 | 3,584 | 1,500 |
| J | 1.722 | 5,204 | 2,200 |
| K | 1.724 | 3,018 | 1,300 |
| P1 | 1.723 | 2,482 | 1,000 |
| P2 | 1.729 | 8,541 | 3,640 |

UMEC granite is more weathered than typical granitic core and yields a peak stress value significantly lower than the range outlined by Goodman (1989). Figure 8 shows the plotted UCS test results from the TerraTek software. Segregated stress-strain curves for each suite, along with photos of the core samples pre/post UCS test are located in Appendix E.

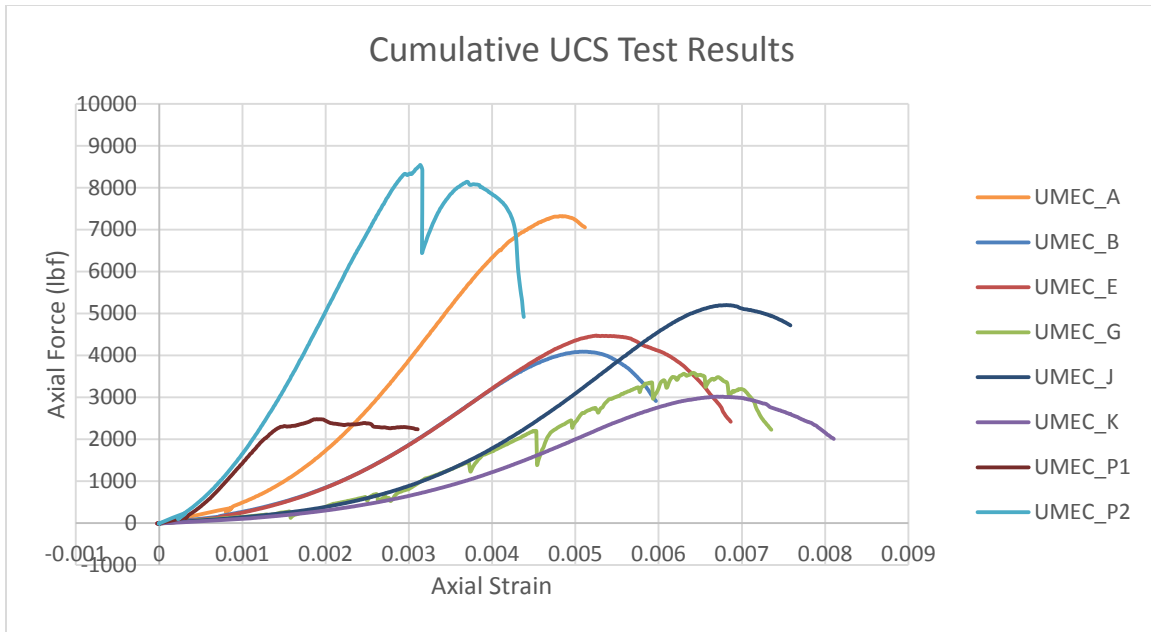


Figure 8: Plot of the Axial Force versus Strain curves produced using the TerraTek software for the UCS tests.

Young's Modulus (E), also known as the modulus of elasticity, and Poisson's Ratio defines the elastic behavior of rock. The brittle or ductile behavior of rock is dependent on the intrinsic properties of the rock and the condition at which stress is applied (González de Vallejo & Ferrer, 2011). The slope of the line was used to determine Young's Modulus, as it is derived from the relationship of axial stress over lateral strain (Table V). The tangent method was used for slope selections along the straight line of the curve. Appendix E contains slope selections segregated by suite.

Table V: Young's Modulus values derived from the slope of the stress-strain curves.

| Sample | Diameter (in) | UCS (psi) | Young's Modulus ($\times 10^6$ psi) |
|--------|---------------|-----------|--------------------------------------|
| A | 1.726 | 3,130 | 2.44 |
| B | 1.725 | 1,750 | 1.31 |
| E | 1.725 | 1,915 | 1.29 |
| G | 1.722 | 1,539 | 0.99 |
| J | 1.722 | 2,234 | 1.47 |
| K | 1.724 | 1,293 | 0.82 |
| P1 | 1.723 | 1,064 | 2.18 |
| P2 | 1.729 | 3,638 | 3.75 |

Static Young's Modulus values selected from the slope of the UCS curve are less than the dynamic values determined during ULT testing. Sample P2 from Suite 3 possessed the highest

Young's Modulus value. Salman and Al-Amawee (2006) determined that the dynamic modulus of elasticity is generally 20, 30, and 40 percent higher than the static modulus of elasticity in high, moderate, and low strength concrete, respectively. Since the UMEC is relatively weak when compared to igneous rocks, the same assumptions are applied. There is a 47 percent difference when comparing the ratio of the static Young's Modulus (2.47×10^6 psi) to the dynamic Young's Modulus (5.25×10^6 psi); indicating that UMEC granite falls within the low strength spectrum outlined by Salman and Al-Amawee (2006).

Static Poisson's ratio was obtained by plotting the lateral strain versus the vertical strain and selecting the slope of the line (Figure 9). In order to maintain consistency with the vertical axis, the lateral strain is multiplied by 100,000.

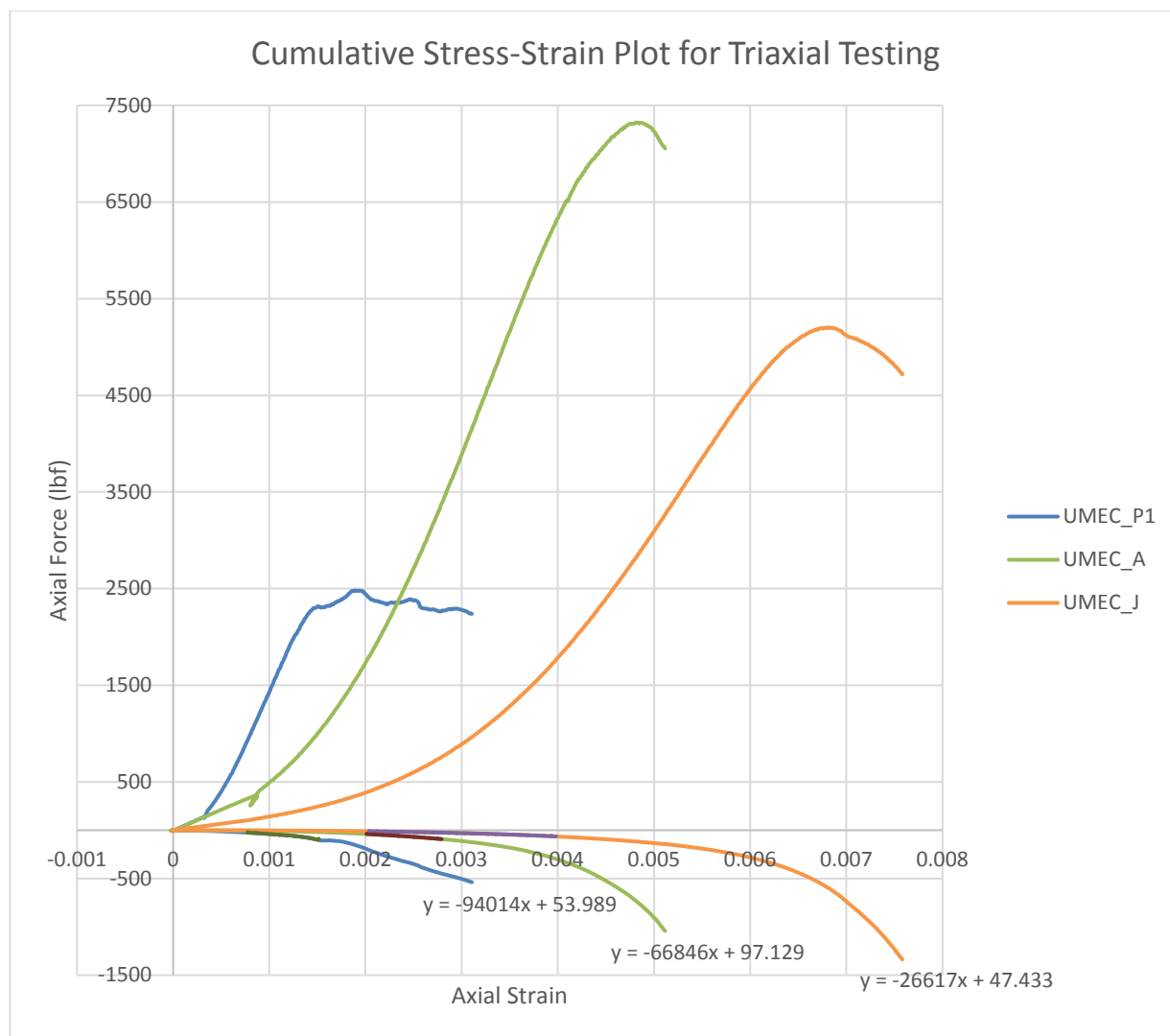


Figure 9: Plot of Axial Force versus Axial Strain curves produced using the TerraTek software for the UCS tests.

The slope of the line (Figure 9) values are divided by -100,000 to obtain Poisson's Ratio for the core sample. Sample J possessed a Poisson's Ratio of 0.26 while the results for Sample A and P1 are inconclusive due to the shallow slope of the line produced (Figure 9).

5.3.4. Triaxial Compressive Strength Test

Triaxial Compressive Strength Tests were performed using the TerraTek Load Frame machine. ASTM Standard D7012 – 10.6 was followed when conducting triaxial tests. A Triaxial compression test is a laboratory experiment that fails a sample by a vertical load that is

experiencing a measured confining pressure (Goodman, 1989). Goodman (1989) justifies the use of the confining pressure in testing since most rock strength increases with confinement, producing differing peak stress values than a typical UCS test. The wider strength characterizations allow for the option of modeling in-situ confining stress conditions and resulting strength properties (Goodman, 1989).

In addition to the UCS tests, two confining pressures were chosen for the triaxial testing to develop the failure envelope. In-situ confining pressures were assumed negligible since the UMEC is roughly 100 feet below the surface, producing approximately 106 psi of vertical pressure. Hoek (2007) states that the horizontal stresses acting on a rock at depth is generally harder to estimate than the vertical stresses; however, the relationship is generally defined by the following equation:

$$\sigma_h = k\sigma_v \quad (2)$$

where k is defined as the relationship of Poisson's Ratio (ν) to one minus ν , and σ_v is the vertical stress. Using Equation 2, where gravity is applied to the rock mass under lateral restraint, the horizontal stress is estimated at 30 psi. This horizontal pressure is not significant enough to have an impact on the selection for confining pressures for triaxial testing does not produce the types of strength values pertinent to this analysis. Three tests applied 500 psi of confining pressure, and three tests applied 150 psi of confining pressure. The criterion of failure is created using the varying peak stress values created by manipulating the confining pressure of the rock (Goodman, 1989). The use of a polyurethane jacket around the sample prevented the confining pressure medium (refined mineral oil) from penetrating samples and creating variable pore pressures. The TerraTek frame was loaded using an induced unit strain per unit time method to produce a continuing strength characterization after the peak stress had been reached by the sample.

5.3.4.1. Triaxial Compressive Strength Test Results

The addition of the confining pressure significantly increased the strength of the rock. This indicates that when using proper ground control methods, Grade III granite has the capability of performing similar to a Grade I granite. Results from triaxial testing are shown in Table VI.

Table VI: Triaxial Test Results

| Sample | Diameter (in) | Confining Pressure (psi) | Peak Load (lbs) | Axial stress at failure (psi) |
|-----------|---------------|--------------------------|-----------------|-------------------------------|
| D | 1.723 | 500 | 16,075 | 6,900 |
| L1 | 1.722 | 500 | 11,101 | 4,770 |
| P4 | 1.725 | 500 | 25,959 | 11,110 |
| F | 1.725 | 150 | 11,057 | 4,730 |
| O | 1.723 | 150 | 9,872 | 4,230 |
| Q1 | 1.723 | 150 | 16,678 | 7,150 |

Triaxial test results obtained from the TerraTek load frame software were plotted in Microsoft Excel. Figure 10 depicts the axial stress versus axial strain graphs obtained during triaxial testing for confining pressures at 500 psi and 150 psi. Photographs of core samples before and after the triaxial loading are available in Appendix F.

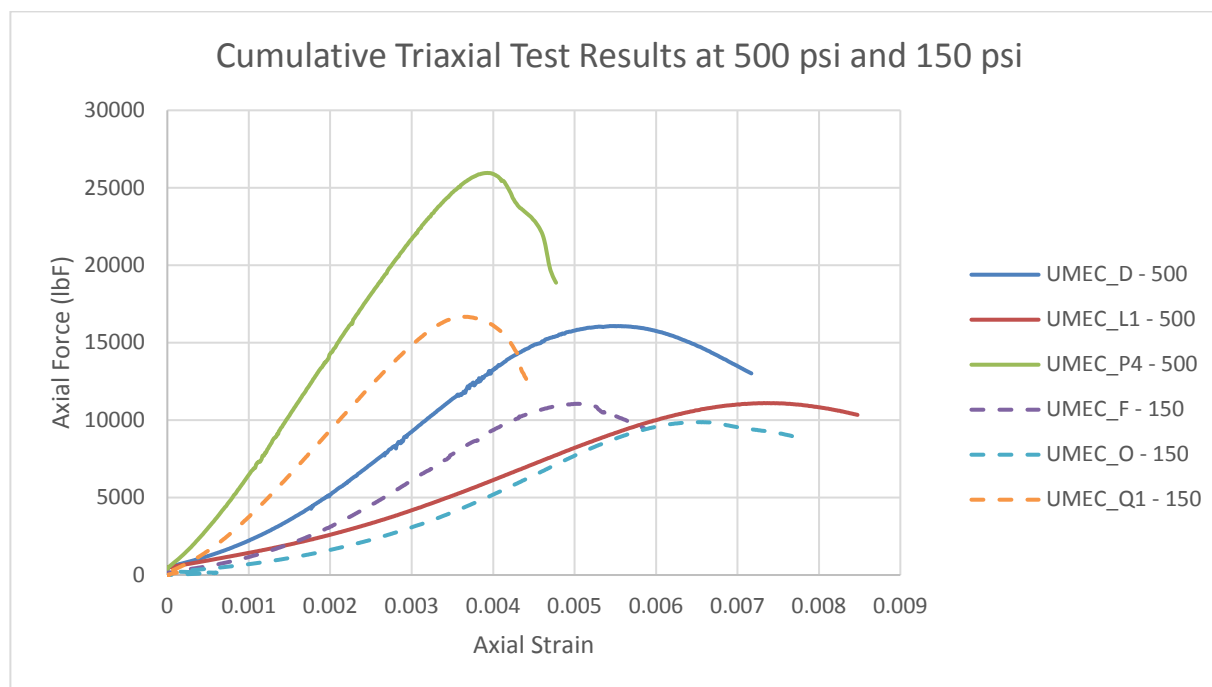


Figure 10: Axial Force versus axial strain test results obtained during triaxial testing. 500 psi confining pressure indicated with solid line. 150 psi confining pressure indicated with dashed line.

The addition of the confining pressure significantly increased the strength of the rock, indicating that the addition of a confining force underground will stabilize the excavation and increase the strength of the roof and ribs of the UMEC.

Young's Modulus values were selected following the same procedures used when selecting the slope for the UCS Young's Modulus (Table VII). Triaxial test graphs with straight line slope selections are available in Appendix F.

Table VII: Young's Modulus values derived from the slope of the stress-strain curves.

| Sample | Diameter (in) | Peak Load (lbs) | Young's Modulus ($\times 10^6$ psi) |
|--------|---------------|-----------------|--------------------------------------|
| D | 1.723 | 16,075 | 4.14 |
| L1 | 1.722 | 11,101 | 1.98 |
| P4 | 1.725 | 25,959 | 7.78 |
| F | 1.725 | 11,057 | 2.96 |
| O | 1.723 | 9,872 | 2.28 |
| Q1 | 1.723 | 16,678 | 5.73 |

Increasing the confining pressure increases Young's Modulus. Average Young's Modulus increases 51 percent when 150 psi of confining pressure is applied and increases 62 percent when 500 psi of confining pressure is applied to the samples.

5.3.5. Mohr-Coulomb failure Envelope

Results from the UCS tests and triaxial tests were plotted to determine the Mohr-Coulomb failure envelope. A series of stress circles were plotted using the confining pressure (σ_3) and peak stress (σ_1) for each test result. A tangential line is drawn across the circles, the slope angle representing internal angle of friction, and the intersection along the y-axis representing the intact strength (cohesion) of the material (Goodman, 1989). Circles were generated using RocScience RocData software. Three failure envelopes were plotted, one for each weathering grade. Figures 11-13 depict the Mohr-Coulomb failure envelope plots from the triaxial test and UCS test results.

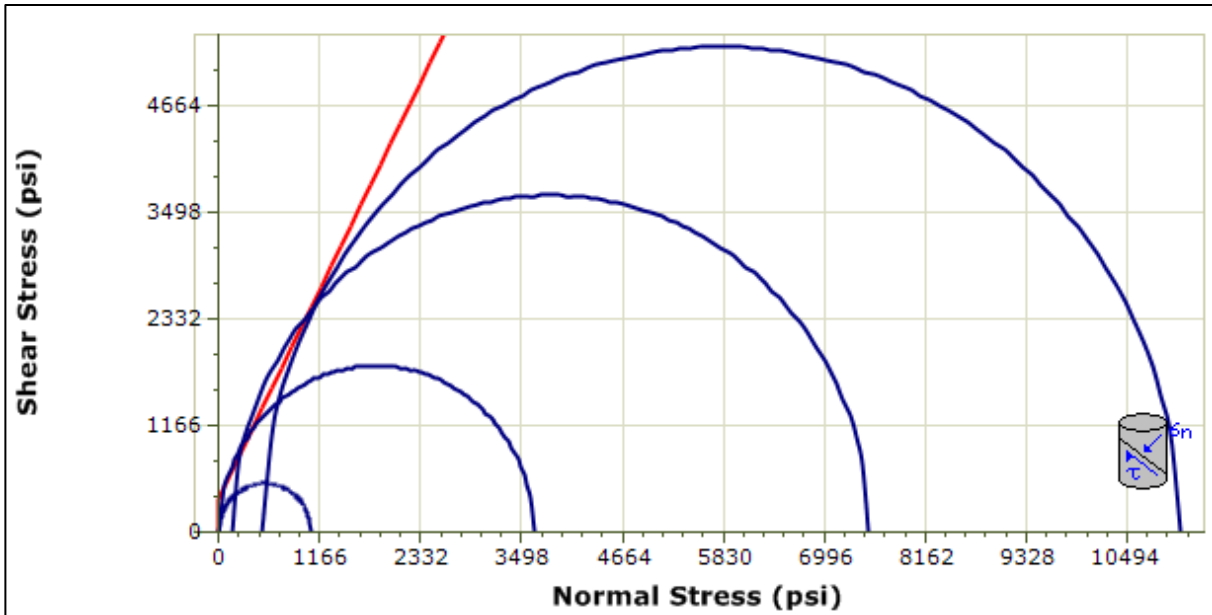


Figure 11: Mohr-Coulomb failure envelope for Grade I granite developed from laboratory testing. Cohesion and friction angle values are 362 psi and 63° , respectively.

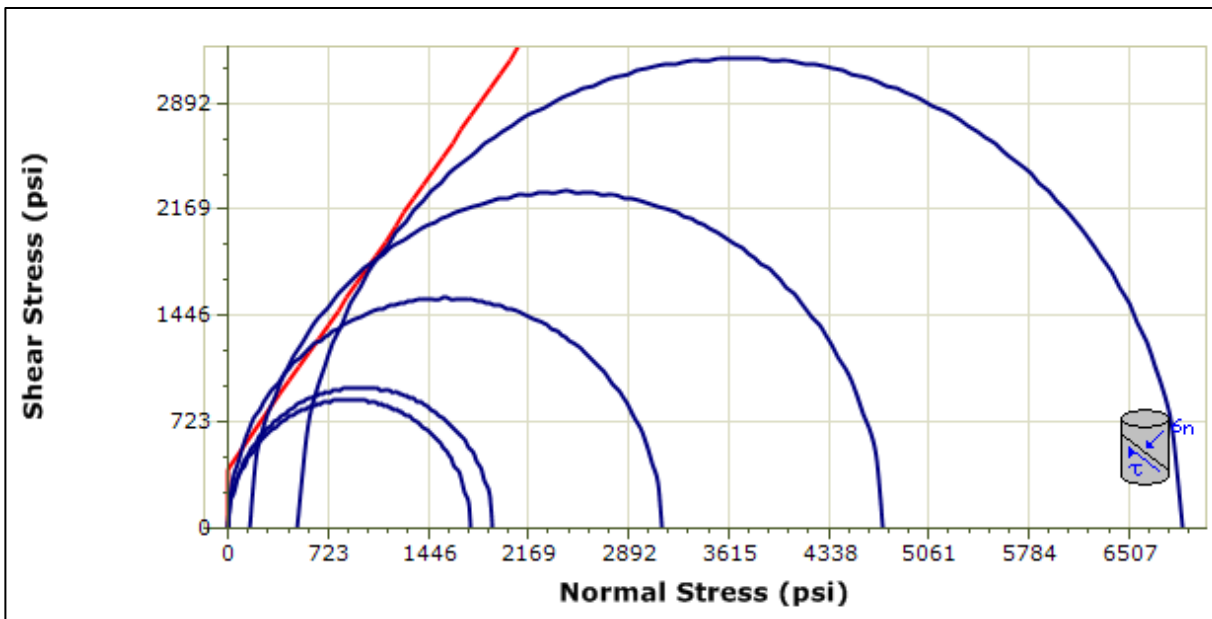


Figure 12: Mohr-Coulomb failure envelope for Grade II granite developed from laboratory testing. Cohesion and friction angle values are 402 psi and 54° , respectively.

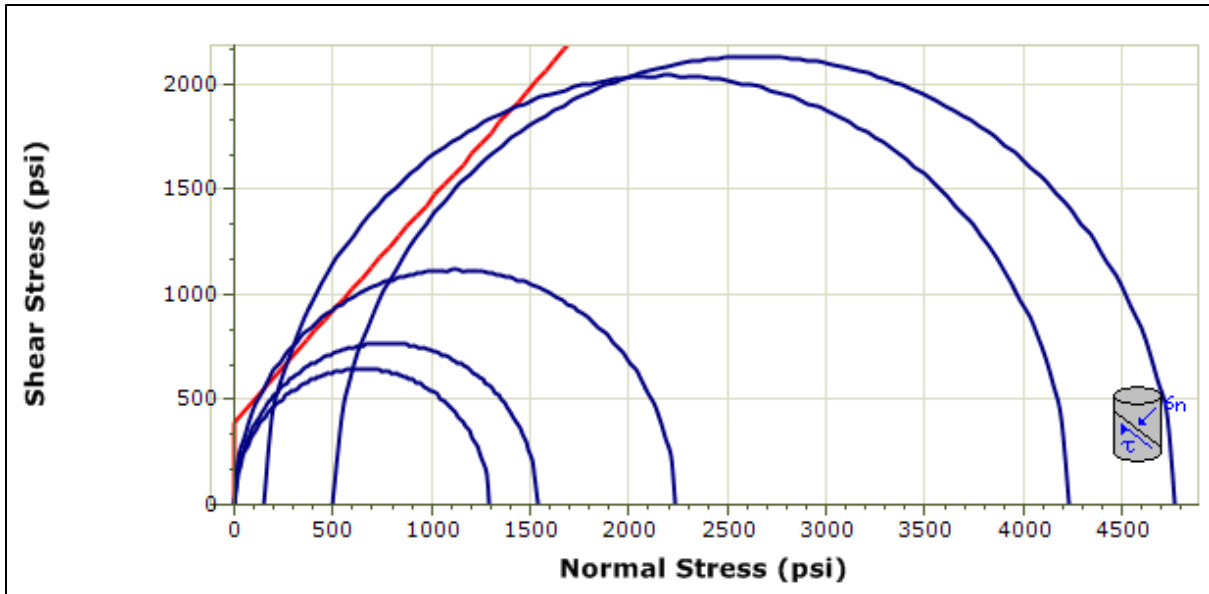


Figure 13: Mohr-Coulomb failure envelope for Grade III granite developed from laboratory testing. Cohesion and friction angle values are 396 psi and 47°, respectively.

Results from the Mohr circle plots indicate that as the weathering grade increases, the friction angle of the material decreases. Cohesion values of the material do not seem to follow a distinct trend; however, it is possible that Sample P1 shearing at 1,060 psi at a joint surface visible in the core skewed Mohr circle for the Grade I granite. Appendix C contains cumulative failure envelope results.

5.3.5.1. Consideration of the Generalized Hoek-Brown Method

The Generalized Hoek-Brown method for determining failure criterion of the UMEC granite was considered as an alternative to the standard Mohr-Coulomb method because the Generalized Hoek-Brown method establishes a non-linear failure envelope based on the results of laboratory testing. The non-linear failure envelope can provide a better fit for failure criterion; however, the generated criterion from the Generalized Hoek-Brown method for the lab results were inconclusive.

5.3.6. Brazilian Test

The Brazilian Test is a testing method for estimating the tensile strength of rock (Goodman, 1989). In order for the Brazilian Test to be considered valid, the specimen must fracture parallel to the platens, therefore; any atypical fractures will cause invalid test results. Samples were prepared to ASTM Standard D7012 – 10, 8.1 and 8.2; however, sample ends can be irregular in Brazilian testing. Samples used in Brazilian testing were fractured off of the samples during preparation for UCS and triaxial testing. According to ASTM D7012 – 10, Brazilian test samples must be measured on either side of the diametric line, or the line that is loaded between the platens in the load frame. Goodman (1989) derived tensile strength from Brazilian Test results using the following equation:

$$\sigma_{tB} = \frac{2P}{\pi Dt} \quad (3)$$

where P is the compression load (lbf) from the load, D is the diameter in inches, and t is the average thickness of the specimen in inches.

5.3.6.1. Brazilian Test Results

The Brazilian tests conducted produced results that assisted in additional characterization of the UMEC granite. Table VIII contains the test results for the valid Brazilian test samples. All results for the Brazilian Test are in Appendix C. Thickness values were obtained by measuring to the right and left of the diametric thickness line and averaging the two values.

Table VIII: Brazilian test results.

| Sample ID | Suite | Diameter (in) | Thickness (in) | Force (lbf) | Tensile Strength (psi) |
|-----------|----------|---------------|----------------|-------------|------------------------|
| A | 2 (GII) | 1.720 | 1.068 | 767 | 270 |
| E | | 1.722 | 1.136 | 1,108 | 360 |
| F1 | 1 (GIII) | 1.725 | 0.966 | 762 | 290 |
| G2 | | 1.721 | 0.700 | 456 | 240 |
| G3 | | 1.720 | 0.778 | 564 | 270 |
| J | | 1.717 | 1.204 | 447 | 140 |
| M | | 1.717 | 0.739 | 1,583 | 790 |
| P1 | 3 (GI) | 1.717 | 0.723 | 1,733 | 890 |
| P2 | | 1.719 | 0.765 | 778 | 380 |
| P3 | | 1.719 | 0.689 | 1,167 | 630 |
| Q1 | | 1.721 | 0.909 | 1,151 | 470 |
| Q2 | | 1.719 | 0.709 | 1,090 | 570 |

Tensile strength values collected from the Brazilian testing are consistent with the compressive strength values obtained from the UCS tests. Pariseau (2012) reports that the tensile strength of a material should be 10 to 20 times less than the compressive strength of the material, with the generally accepted rule of thumb being a factor of 10. The compressive strength is five times the tensile strength when calculating the ratio of the average compressive strength (2,050 psi) to the average tensile strength (440 psi) lying outside the range outlined by Pariseau (2012). When comparing the median of the compressive strength (1,840 psi) to the median tensile strength (370 psi) the results indicate that the median compressive strength remains five times the median tensile strength. Appendix G contains photographs of the test samples after loading in the Brazilian test load frame.

5.3.7. Point Load Test (PLT)

Point Load Testing (PLT) is a less expensive, less accurate alternative to UCS testing and has been used in geotechnical engineering for over 30 years (Rusnak and Mark, 2000). The PLT involves compressing a rock sample between two steel platens until failure occurs in tension and allows for the determination of the uncorrected point load strength index (I_s):

$$I_s = \frac{P}{D^2} \quad (4)$$

where P equals the failure load and D is the core diameter (Rusnak and Mark, 2000). PLT accuracy is dependent on the ratio between the UCS and tensile strength. In order to determine the uncorrected point load strength index, I_s should be corrected to the standard equivalent diameter:

$$I_{s50} = \left(\frac{D}{50}\right)^{0.45} * I_s \quad (5)$$

Bieniawski (1975) determined that UCS can be obtained from PLT from the following relationship:

$$UCS = 24 * I_{s50} \quad (6)$$

where 24 is a standard conversion factor determined by Bieniawski (1975).

5.3.7.1. PLT Results

PLT results are presented in Table IX. Full PLT results including force reported in kilonewtons (kN), and the values for I_s are in Appendix C.

Table IX: PLT results.

| Sample ID | Diameter (in) | Length (in) | Pressure (lbf) | I_{s50} | UCS |
|-----------|---------------|-------------|----------------|-----------|-------|
| C | 1.721 | 3.526 | 962 | 71.3 | 1,712 |
| F5 | 1.728 | 3.513 | 1,419 | 104.5 | 2,507 |
| H | 1.726 | 3.454 | 112 | 8.3 | 199 |
| I | 1.722 | 3.592 | 124 | 9.2 | 220 |
| M | 1.728 | 3.526 | 695 | 51.2 | 1,229 |

Several UCS values from PLT are significantly smaller than the values determined in UCS testing. The discrepancy in UCS values could be due to the core breaking along an internal fracture network near the point load platens. Results from the PLT are not consistent with the results from the UCS testing. Photographs from the PLT fractures are located in Appendix G.

5.3.8. Strength Based Weathering Grade Classification

The peak strength values in the UCS and triaxial testing are lower than Goodman's (1989) published UCS values; however, Barton (1978) provides a range of UCS values per weathering grade. Table X compares Barton's (1978) values with the UCS values obtained in testing.

Table X: UCS values compared to ISRM published values (Modified from Barton, 1978).

| Suite | Sample | UCS (psi) | UCS (MPa) | Barton's Range (MPa) |
|----------|--------|-----------|-----------|----------------------|
| 1 (GIII) | G | 1,539 | 10.6 | 5 – 25 |
| | J | 2,234 | 15.4 | |
| | K | 1,293 | 8.9 | |
| 2 (GII) | A | 3,130 | 21.6 | 25 – 50 |
| | B | 1,750 | 12.1 | |
| | E | 1,915 | 13.2 | |
| 3 (GI) | P1 | 1,064 | 7.3 | 100 – 250 |
| | P2 | 3,638 | 25.1 | |

Suite 1 granite falls within the acceptable range for Weathering Grade III. Suite 2 samples lie between Weathering Grade I and Weathering Grade II. Suite 3 granite samples lie between Weathering Grade I and Weathering Grade II⁵. Since the weathering grade samples do not fall between published values, formal weathering grade identification may not be properly obtained through visual identification of weathering grade.

5.4. Software Analysis

Interpretation of the field results and the laboratory results was performed using a variety of software packages. Strike and dip data obtained during the SLS were processed using RocScience DIPS to assess structure (joint orientations). Weathering grade data and laboratory characterization of the granite were used to create a geotechnical database in Maptek Vulcan.

⁵ Sample P1 failed early during UCS testing due to prevalent fracture network visible on the surface of the core sample.

RocScience Unwedge software was used to gain an understanding of how the joint set orientation may affect stability of the excavated opening for the UMEC.

5.4.1. RocScience DIPS

DIPS is a software program designed for interactive analysis based on geological data; allowing for easy development of stereographic projections and resulting analyses of the projection (RocScience, 2017). Strike and dip data collected in the UMEC were imported into DIPS using the strike (right) and dip notation. The strike (right) and dip notation was selected because field data were collected using the “right hand rule” convention; therefore, no additional calculations were required when using this notation. Strike and dip measurements are displayed as a pole on an equal area, lower hemisphere stereonet projection. The equal area projection was selected because the equal angle projection can distort resultant projections (RocScience, 2017). Appendix H contains a graphic indicating the differences in projection methods.

The DIPS interpretation for the UMEC is shown in Figure 14. A density concentration map is projected over the stereonet. Using the “Add Set” tool in DIPS, high density point clouds were selected to determine the average strike and dip for the high concentration of poles.

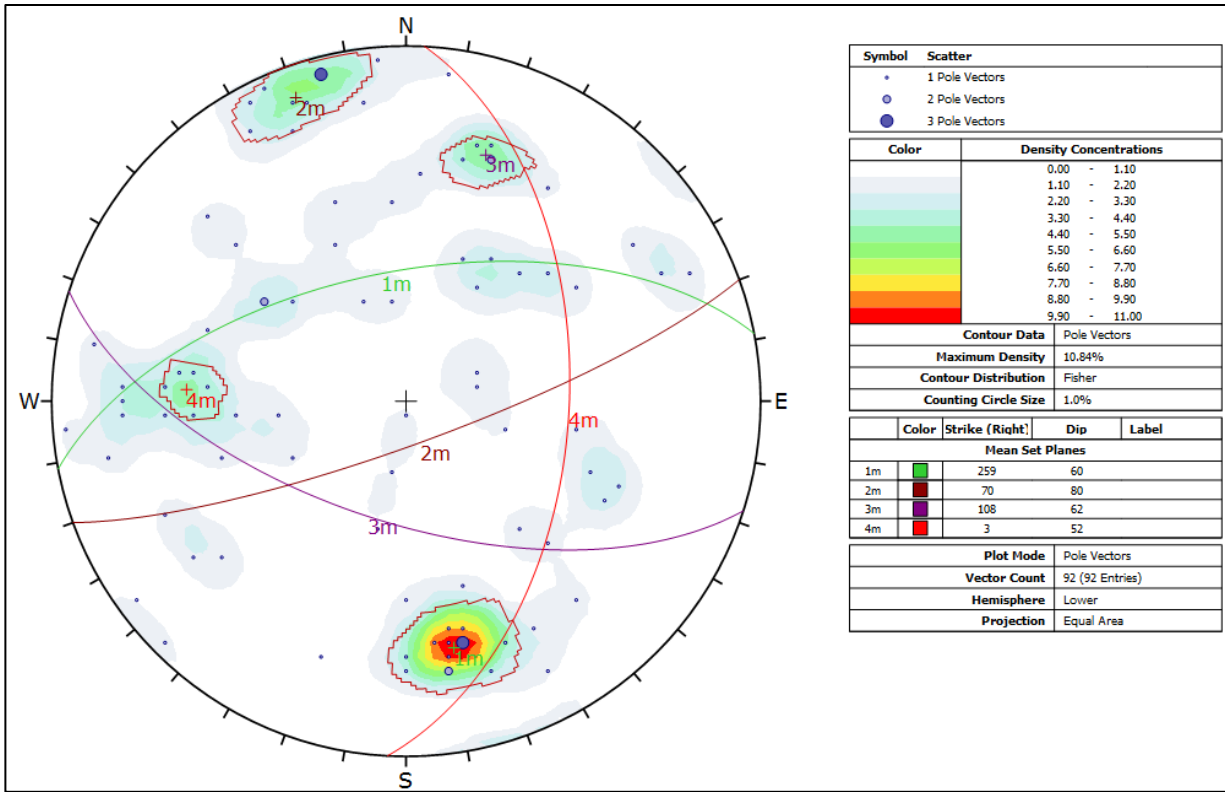


Figure 14: DIPS stereonet projection with density contour and primary joint sets. A larger view of the stereonet is available in Appendix F.

Four distinct joint sets were found in the stereographic projection (Table XI).

Table XI: Average strike and dip measurements selected in DIPS.

| Joint Set | Strike | Dip |
|-----------|--------|-----|
| 1 | 259 | 60 |
| 2 | 070 | 80 |
| 3 | 108 | 62 |
| 4 | 003 | 52 |

5.4.2. RocScience Unwedge

Unwedge is a three-dimensional stability analysis program for underground excavations in rock that contains structural discontinuities (RocScience, 2017). Factor of Safety (FS) values are calculated for potentially unstable wedges that exist and varying support methods can be modeled using different patterns of bolting and shotcrete (RocScience, 2017). Since Unwedge is

a RocScience program, the distinct joint sets determined in the DIPS analysis can be directly imported into Unwedge to create the wedge shapes. Due to varying drift lengths underground, an arbitrary 50-foot tunnel length oriented North with 0 grade was used for all models. Input data for the Unwedge model is outlined in Table XII.

Table XII: Unwedge input data parameters

| | |
|-------------------------------------|--------------------------|
| Excavation Trend | 0° |
| Excavation Plunge | 0° |
| Design Factor of Safety (FS) | 2.0 |
| Unit Weight Rock | 0.0811 t/ft ³ |
| Unit Weight Water | 0.0312 t/ft ³ |
| Shear Strength Model | Mohr-Coulomb |
| Phi | 54° |
| Tensile Strength | 0 t/ft ² |
| Cohesion | 28 t/ft ² |
| Water Pressure | Ground Surface |
| Joint Structure | Infinite Continuity |

Average cohesion and phi values from the Mohr-Coulomb failure envelope were used in the analysis. The average cohesion value was converted from psi to tons per square foot to fit the model parameters. Since the UMEC does not experience unfavorable groundwater flow throughout the mine, water pressure is modeled at ground surface.

Drift dimensions for the model were obtained by tracing a polygon around a three-dimensional scanned UMEC surface in Maptek I-Site software. The dimensions were imported into Unwedge from a .dxf file created by exporting the traced polygon from I-Site. Four distinct wedges appeared based on the joint orientations of the UMEC granite (Figure 15). Additional perspective views and model geometry are available in Appendix F.

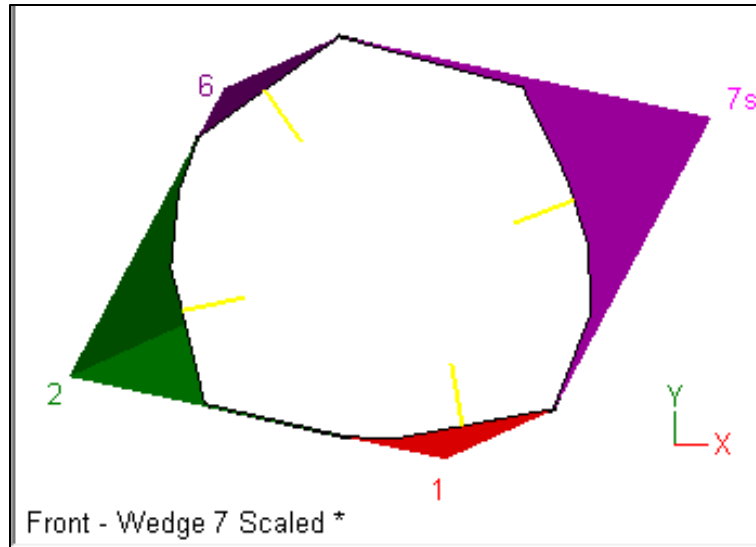


Figure 15: Unwedge predicted wedge failures.

Wedge 1 does not pose stability problems because it lies on the floor of the excavation. Wedge 2 possesses a Factor of Safety (FS) of almost 10, indicating that the wedge is stable within the ribs of the excavation. Wedge 6 and Wedge 7 have the potential for failure due to their orientation on the roof of the excavation. Due to the approximate volume of Wedge 6, spot bolting and mesh would mitigate the potential for falling out of the roof. Wedge 7 poses the highest threat to the excavation; therefore, additional bolting and mesh would be required to mitigate the risk of failure. Wedge parameters are provided in Table XIII.

Table XIII: Unwedge output.

| Parameter | Wedge 2 | Wedge 6 | Wedge 7s |
|---|--------------------|---------------|---------------|
| FS | 9.90 | 0.0 | 0.0 |
| Volume (ft ³) | 1.66 | 0.1 | 3.2 |
| Shear Force (tons) | 62.3 | 0.0 | 0.0 |
| Supporting Pressure (tons/ft ²) | 0.0 | 5.3 | 5.4 |
| Failure Mode | Sliding on Joint 1 | Falling wedge | Falling wedge |

The shear force indicated by Unwedge is the amount of force active in the direction of sliding. The support pressure indicates the amount of pressure required to achieve the design requirements with an FS of 2.0 if the FS is lowered, the support pressure required to stabilize

wedge 6 and wedge 7s would decrease. Since there are no frictional forces in the model, wedge 6 and wedge 7s would fall out due to lack of support.

The same tunnel parameters were used to model split-set bolt support. The UMEC uses standard 6-foot split set bolts and chain-link wire mesh for excavation stabilization. For modeling purposes, standard split set bolt parameters were set at the default values provided by Unwedge (Table XIV).

Table XIV: Unwedge input data parameters.

| Type | |
|-------------------------|-------|
| Tensile Capacity (tons) | 6 |
| Plate Capacity (tons) | 5 |
| Bond Strength (tons/ft) | 1 |
| Pattern Spacing | 3H,3V |

Once the bolt support was applied to the excavation, the FS values for Wedge 6 and Wedge 7s increased to 2.7 and 1.1, respectively (Figure 16). The resisting force required to maintain Wedge 7 in place is approximately 10 tons.

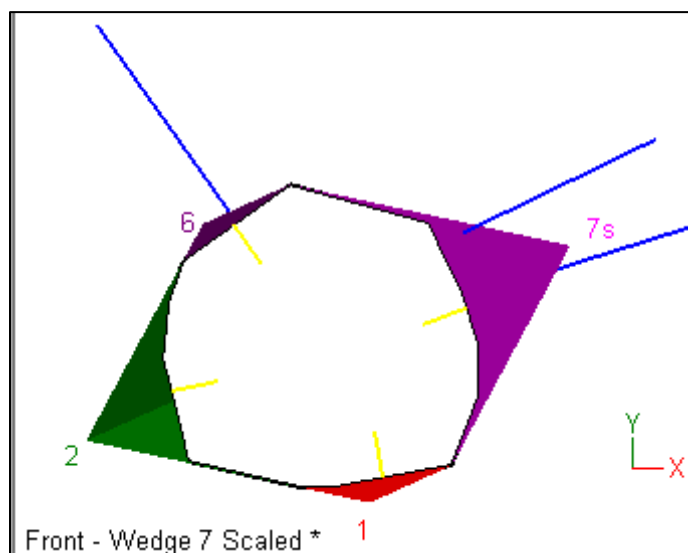


Figure 16: Unwedge predicted wedge failures with added bolt support. Additional views are available in Appendix H.

Additional Unwedge scenarios were modeled with tunnel directions of 45°, 90°, and 135° using the same 3H:3V bolt spacing for support. Graphics from each scenario are available in

Appendix H. Based on the analyses, the best driving direction for future excavations would be 90°.

5.4.2.1. Consideration of Numerical Model Development

A full-scale numerical model using either Finite Element Methods (FEM), Finite Difference Methods (FD), or Discrete Element Methods were considered; however, this type of modeling would be difficult because the rock mass is structurally controlled. Since RocScience Unwedge is a key block model program, it provides sufficient information to satisfy the requirements for the GCMP.

5.4.3. MapTek Vulcan

A geotechnical database was created in Vulcan in order to digitize the granitic characterization performed via field observations and laboratory analyses. The database was developed following the steps outlined in the Maptek Vulcan Help Manual (Maptek, 2015). The geotechnical database uses the known mine survey point orientation to properly orient the strike and dip measurements in three-dimensional space. Strike and dip measurement locations along the SLS tape were converted to Cartesian (x,y,z) coordinates using departure and latitude equations outlined by Ghilani and Wolf (2012). Once the geotechnical database is defined in Vulcan, strike and dip measurements can be viewed as a plane in the map (Figure 17).

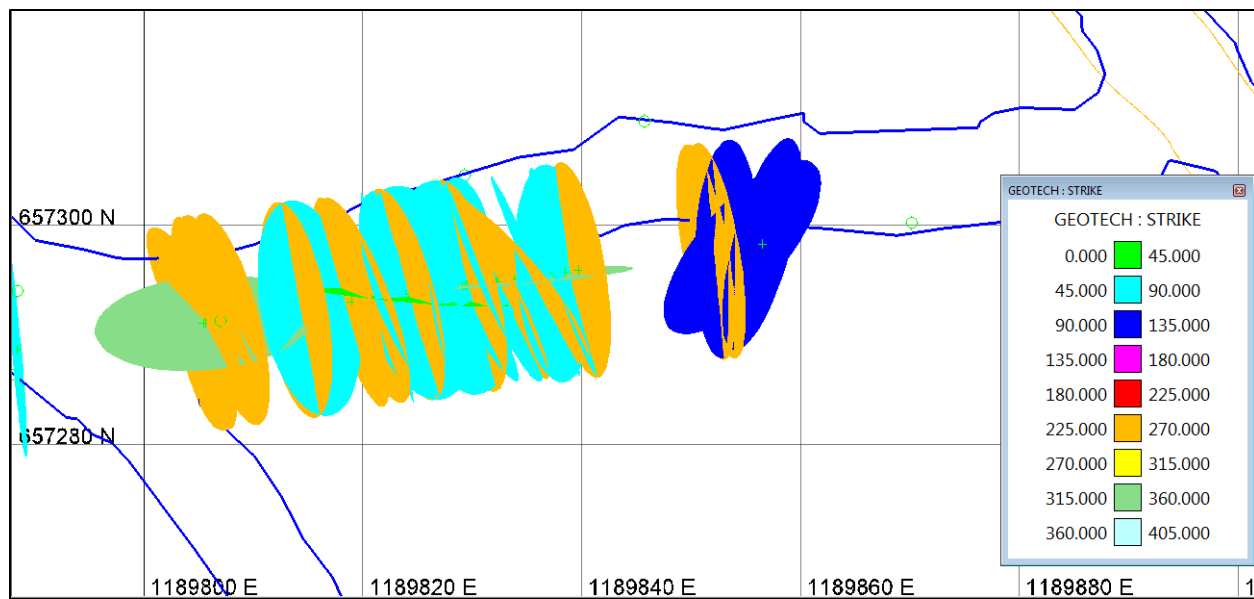


Figure 17: Zoomed in section of UMEC showing strike and dip projection planes. Full scale figure available in Appendix B.

6. UMEC Rock Classifications

6.1. Rock Quality Designation for UMEC Granite

Rock Quality Designation (RQD) was developed by Deere in 1967 to provide a quantitative estimate of rock mass quality from drill core logs (Hoek, 2007). RQD is defined as the percentage of intact core pieces longer than 4 inches in the total length of core (Hoek, 2007).

Core drilling was attempted at the UMEC with unfavorable results due to only having access to a handheld drill; therefore, no core was obtained. Since RQD can be directionally dependent based on the drill orientation, the use of empirical formulas to determine RQD can be applied when there is a lack of core, or drill orientation could disturb the interpretation of joint orientation. Two empirical formulas were used to determine the RQD for UMEC granite.

6.1.1. Palmström's RQD

Palmström (1982) suggested that if no core is available, but joint surfaces are visible on surface exposures or adits, RQD can be estimated from the number of discontinuities per unit volume (J_v) (Hoek, 2007). The relationship states:

$$RQD = 115 - 3.3J_v \quad (7)$$

where J_v is the sum of the number of joints per unit length of all joint sets known. The length is determined using an arbitrary one cubic meter rock mass that is projected onto the two-dimensional SLS surface (González de Vallejo and Ferrer, 2011). The number of joints that pass through this unit volume (independent of the joint set the joint belongs to), is recorded as the J_v . The J_v value used for the UMEC was determined by assigning a one cubic meter area to a section of the UMEC drift where the SLS was conducted. Survey location H50 possessed the most representative amount of joint sets; therefore, this section was used for the determination of J_v . The J_v was determined to equal four in the section of SLS survey chosen. Palmström (2005) suggested that if J_v is less than 4.5, the RQD equals to 100.

6.1.2. Priest and Hudson's RQD

Priest and Hudson (1976) proposed that RQD index can be estimated based on the discontinuity frequency. The equation approximates that:

$$RQD \approx e^{-0.1\lambda}(0.1\lambda + 1) \quad (8)$$

where λ is the inverse average spacing of the joints (González de Vallejo and Ferrer, 2011). The average spacing of the joints was determined by subtracting the location of the f_{n+1} fracture number from the initial fracture number (f) location along each survey point. All values for spacing were averaged. Appendix I contains a table with the average fracture spacing and associated calculations for RQD. Using Equation 8, an RQD of 99.92% was determined.

6.1.3. Differences in methodology

The RQD values determined by each method are different by 0.08%. Palmström's (1982) method provides a three dimensional interpretation of the two-dimensional ribs in the UMEC whereas Priest and Hudson's (1976) method allows for the determination of the RQD using the average joint spacing. Since RQD is primarily a rock core calculation, and no core was obtained in the UMEC, the results for the RQD are not representative of the UMEC granite. The average RQD estimated by these two methods suggests that the RQD in the UMEC is excellent when it is more realistically fair given the additional rock properties obtained during laboratory testing.

6.2. Rock Mass Rating for UMEC Granite

Bieniawski (1989) identified six parameters (Table XVII) that are used to classify rock through the Rock Mass Rating (RMR) system.

Table XV: RMR parameters (Modified from Bieniawski, 1989).

| Parameter | Symbol |
|--------------------------------|--------|
| Uniaxial Compressive Strength | UCS |
| Rock Quality Designation | RQD |
| Spacing of Discontinuities | J_s |
| Joint Condition | J_c |
| Groundwater conditions | J_w |
| Orientation of discontinuities | J_o |

Typically, the rock mass is divided into structural regions and each region is classified separately; however, since the granite at the UMEC is relatively uniform, the excavation will be evaluated as a whole, rather than in structural regions. Appendix I provides the RMR System classification parameters after Bieniawski (1989) and the selections made to determine the UMEC RMR. Table XVIII summarizes the selections made for the determination of the RMR.

Table XVI: RMR parameters and determined ratings.

| Symbol | Rating |
|----------------|-----------|
| UCS | 4 |
| RQD | 20 |
| J _s | 15 |
| J _c | 25 |
| J _w | 15 |
| J _o | -2 |
| RMR | 77 |
| Class Number | II |
| Description | Good Rock |

The RMR for the UMEC is 77, indicating that the granite is Class II good rock. Bieniawski (1989) provides guidelines for excavation and support of an excavation in Class II rock that recommend spot bolting when necessary with a 2.5 meter (8 feet) spacing with occasional wire mesh.

6.3. Q-System Classification for UMEC Granite

The Q-system for rock mass classification was developed at the Norwegian Geotechnical Institute (NGI) in 1974 as a quantitative classification system for estimating tunnel supports based on numerical assessment of rock mass quality (Palmström, 2015). The Q-System was updated by Grimstad and Barton in 1994 to include 1,000 case studies of Q-system tunnel classification. The Q is based on a numerical assessment of rock mass quality using the parameters outlined in Table XV.

Table XVII: Q-System input parameters (Modified from Hoek, 2007).

| Parameter | Symbol |
|---|--------|
| Rock Quality Designation | RQD |
| Number of Joint Sets | J_n |
| Roughness of most unfavorable joint or discontinuity | J_r |
| Degree of alteration or filling along weakest joint set | J_a |
| Water Inflow | J_w |
| Stress Reduction Factor | SRF |

These parameters are grouped into three quotients in order to determine the Q of a tunnel:

$$Q = \frac{RQD}{J_n} * \frac{J_r}{J_a} * \frac{J_w}{SRF} \quad (9)$$

The first quotient represents the overall structure of the rock mass, the second quotient serves as an indicator of the inter-block shear strength, and the third quotient represents the active stresses (Hoek, 2007). Table XVI outlines the parameters obtained to perform the Q-system calculations.

Table XVIII: Q-System input parameters.

| Symbol | Value |
|-------------|-------|
| RQD | 99% |
| J_n | 15 |
| J_r | 3 |
| J_a | 1.42 |
| J_w | 1 |
| SRF | 2.5 |
| Wall Height | 18 ft |
| ESR | 1.6 |

Generally, the J_a is the degree of alteration for the weakest joint; however, J_a was obtained by taking the average of all the joint alteration numbers gathered during the SLS. Appendix I contains the Q-system tables with selections of input parameters for UMEC Q-system calculations. A secondary quantity needed to determine the Q for the UMEC is the excavation support ratio (ESR). Since the UMEC is a permanent mine opening containing adits and drifts, an ESR of 1.6 is used for calculating the Q. The calculated Q-value for the UMEC is 5.60. If the RQD and J_n parameters are modified to a fair RQD and a 2+ random joint sets, respectively, the Q increases from 5.60 to 8.50, providing a range for the UMEC granite. Figure 18 shows the plot for the UMEC Q.

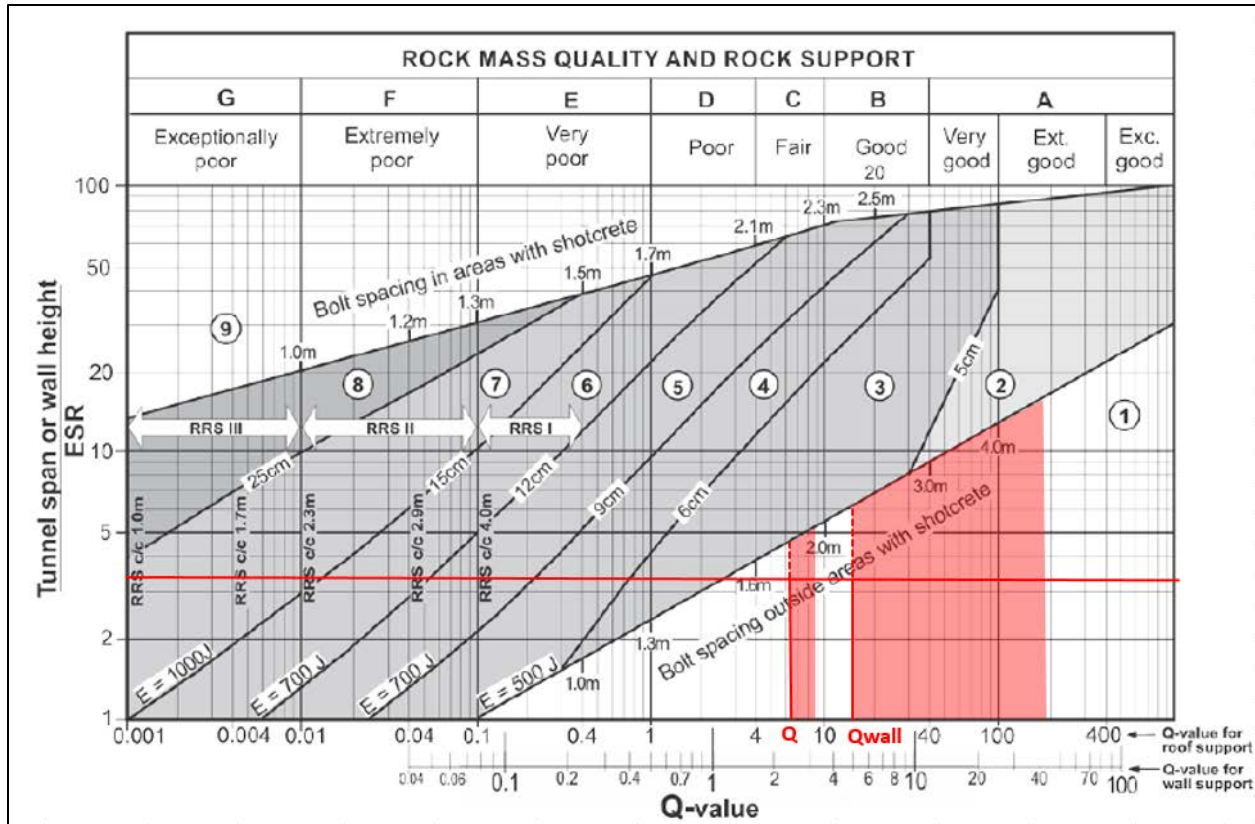


Figure 18: UMEC Q and Q_{wall} . Extrapolated values indicated with dashed red line. Q and Q_{wall} range are indicated by red shaded area.

The Q range for the UMEC falls within zone 1, indicating that the support required for the UMEC is no support or spot bolting. While the Q indicates that there does not need to be any additional support for the UMEC, the longevity of the facility requires more than spot bolting for problematic areas. If the Q-value is extrapolated above the intersection on the y-axis, a recommended bolt spacing for the UMEC is approximately 1.8 meters (6 feet).

An additional quantity derived from the Q-system calculation is the Q_{wall} , or the wall support, which is found by applying wall height into the Q equation. Since the Q-value for the UMEC ranged between 0.1 – 10.0, the following equation is used to determine Q_{wall} :

$$Q_{wall} = 2.5Q \quad (10)$$

The Q_{wall} for the UMEC is 14.0, which also plots in zone 1 on the Rock Mass Quality and Rock Support chart (Figure 18). If the value is extrapolated to the line above, it is recommended

that a bolt spacing of 2.2 meters (7.2 feet) be used. Since 7.2 feet is an unrealistic bolt spacing to measure due to the mining methods used in the UMEC, a 7.0 bolt spacing could be used.

6.4. Applications of the Rock Structure Rating (RSR)

Hoek (2007) outlines the use of a classification scheme known as the Rock Structure Rating (RSR) for relatively small tunnels supported by the use of steel sets, shotcrete, and rock bolts. Though the RSR is limited to small excavations, it provides additional classification information when the RQD and RMR do not fully identify the material limitations in an excavation. The RSR states:

$$RSR = A + B + C \quad (11)$$

where, A is defined as geologic parameters, B is the material geometry parameter, and C is the effect of groundwater. RSR selections are in Appendix I. Table XIX summarizes the RSR selections for the UMEC.

Table XIX: RSR selection summary.

| Parameter | Value |
|-----------|-------|
| A | 18 |
| B | 25 |
| C | 18 |
| Total | 61 |

Once the RSR value is determined, the value is plotted on a curve to determine the average bolt spacing recommended for the excavation (Figure 19).

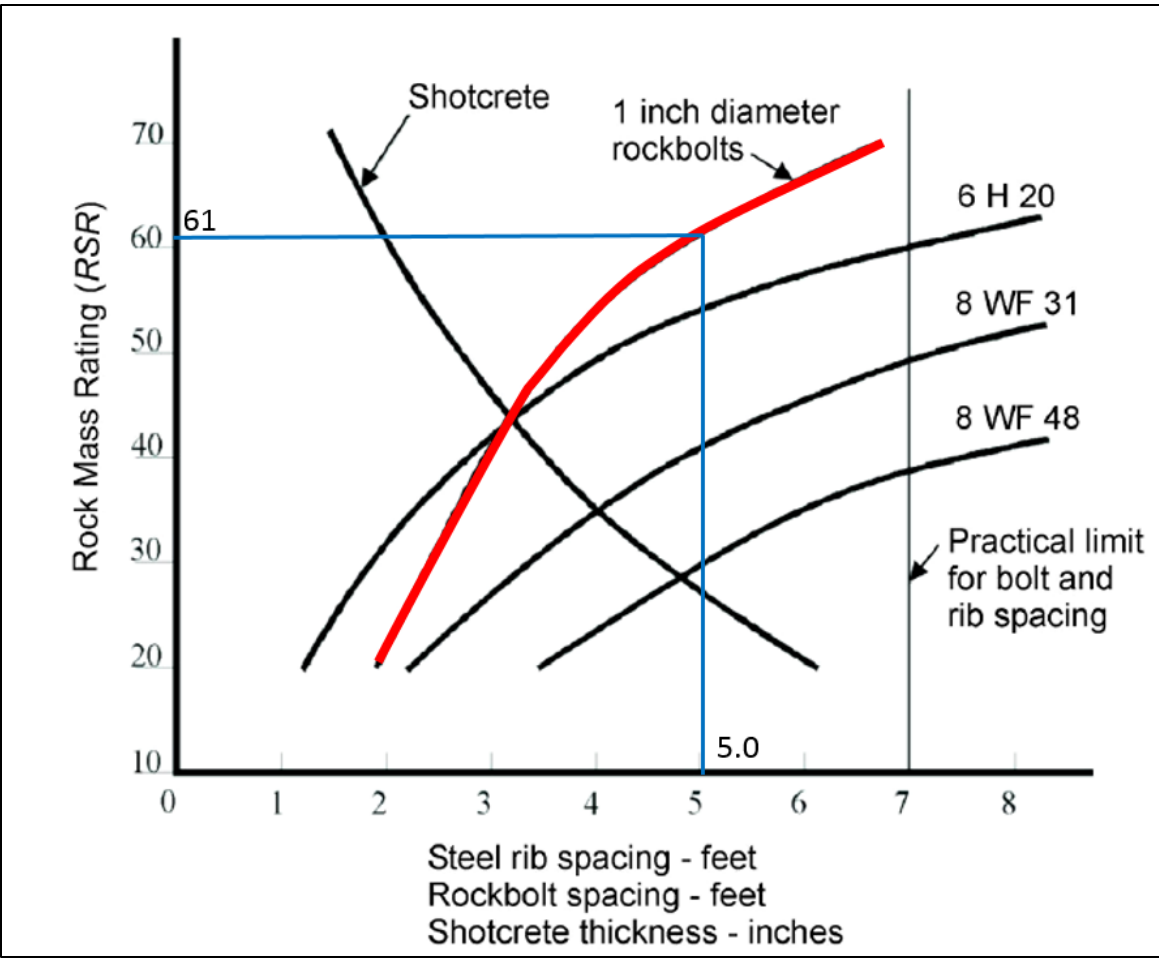


Figure 19: RSR value for the UMEC. Red line indicates the type of bolt used.

The recommended bolt spacing based on the RSR is 5.0 feet. This value more representative of the bolt spacing required to maintain an excavation in the UMEC; however, it is still recommended that a spacing of 3Hx3V be used when bolting in the UMEC to prevent falling wedges. A table summarizing each interpretation method is available in Appendix I.

7. Development of Ground Control Management Plan

Ground control management is essential for all operating mines to ensure the safety of personnel and equipment working in and around the area. Rock properties and geologic data are used to develop a best fit GCMP in conjunction with mining activity.

Based on the results of the triaxial tests, adding 150 psi of confining pressure to the UMEC granite significantly improves the strength. Six-foot split-set bolts do not add additional confining pressures to the rock; however, the bolts will maintain the current confining pressure that the rock in the excavation is experiencing. The use of wire mesh in conjunction with the split-set bolts contains the wedges created by the rock joint surfaces. Recommended bolt spacing will be outlined in the GCMP located in Appendix J.

8. Conclusions

The following conclusions were determined based on the results of the study:

- Average weathering grade of UMEC granite based on granitic mapping is Grade 2,
- The average UCS, based on lab testing, for UMEC granite is 2,070 psi,
- Visual identification for weathering grade in the UMEC may not be enough to properly identify the strength parameters of the rock,
- The average axial stress at failure, when increasing the confining pressure to 150 or 500 psi in triaxial strength testing, increases to 5,370 psi and 7,590 psi respectively for UMEC granite,
- Grade I granite possesses a cohesion of 362 psi and a friction angle of 63°,
- Grade II granite possesses a cohesion of 402 psi and a friction angle of 54°,
- Grade III granite possesses a cohesion of 396 psi and a friction angle of 47°,
- The addition of confining pressure significantly increases the strength of the granite,
- Brazilian test results are consistent with UCS test and triaxial test results, indicating that the compressive strength is five times the tensile strength,
- PLT test results are inconsistent with the UCS test results,
- Four distinct joint sets exist within the UMEC granite: Joint Set 1 striking 259°, dipping 60°; Joint Set 2 striking 70°, dipping 80°; Joint Set 3 striking 108°, dipping 62°; and Joint Set 4 striking 3°, dipping 52°,
- One wedge solid poses a threat to the UMEC based on the joint geometry when the excavation direction is oriented directly north (0°),

- Possible wedge failures are stabilized with the use of 6-foot split set bolts and wire mesh,
- Unwedge modeling indicates that an tunnel orientation of 90° would be best for future excavations,
- The RMR for the UMEC is 69, indicating the UMEC granite is Class II, good rock,
- The Q-value for the UMEC ranges from 5.6 to 8.5 and lies in zone 1 of the Rock Mass Quality and Rock Support graph, indicating that the UMEC does not require a distinct bolting scheme and could go unsupported,
- A recommended bolt spacing based on the Q-value for the UMEC is six feet,
- The Q_{wall} value for the UMEC ranges from 14.0 to 21.0 and lies in zone 1 of the Rock Mass Quality and Rock Support graph, indicating that the UMEC does not need extensive wall support or bolting,
- A recommended bolt spacing based on the Q_{wall} is seven feet,
- An eight feet bolt spacing with occasional wire mesh is recommended base on the RMR, and
- The RSR value for the UMEC is 61, indicating that the recommended bolt spacing to maintain an open excavation is 5.0 feet.

9. Recommendations

The following are recommendations based on the results of this study:

- The GCMP will be an active document that is updated every other year unless a significant circumstances require an immediate update to the document,
- Based on the mining rate of the Practical Underground Mining class, samples should be collected and tested once every two years by a competent person in the Mining Engineering Department or Geological Engineering Department,
- Quarterly inspections of wire mesh and rock bolts should be conducted to look for signs of squeezing or corrosion,
- Mapping of the UMEC should be conducted on an annual basis unless significant mining activity is performed by the Practical Underground Mining class,
- Necessary software interpretations (DIPS, Unwedge) and the Vulcan geotechnical database should be updated once mapping is completed,
- Though the Q-value indicates that there is no need for systematic bolting, a bolting scheme should be implemented to maintain the longevity and increase the safety of the facility,
- Through the RMR recommends the use of occasional wire mesh and an eight feet bolt spacing, wire mesh should be used at all times to maintain the longevity and increase the safety of the facility. Bolt spacing provided based on the RMR can be used as a guideline but should be modified if there is an undesirable wedge in the roof, and
- It is recommended that the next orientation to begin new excavations is 90°.

10. References Cited

- ASTM Standard D7012 (2010). Standard Test Method for Compressive Strength and Elastic Moduli of Intact Rock Core Specimens under Varying States of Stress and Temperatures. In. West Conshohocken, PA.
- Barton, N. (1978). Suggested methods for the quantitative description of discontinuities in rock masses. *International Journal of Rock Mechanics and Mining Sciences & Geomechanics Abstracts*, 15(6), 319-368.
- Bates, R. L., & Jackson, J. A. (Eds.). (1984) *Dictionary of Geological Terms* (3 ed.). New York: Anchor Books [Prepared by The American Geological Institute].
- Bieniawski, Z. T. (1975). The point-load test in geotechnical practice. *Engineering Geology*, 9(1), 1-11. Retrieved from <http://mtproxy.lib.umt.edu:3048/login?url=http://search.proquest.com/docview/52356870?accountid=28080>
- Bieniawski, Z. T. (1989) *Engineering rock mass classifications*. Canada: John Wiley & Sons, Incorporated.
- Carlisle, S. (April 6, 2015). Orphan Boy Facility Visit. [Memorandum]. Greenwood Village, Colorado: Newmont Mining Corporation.
- Chaleen, N.E., Hooper, A.G., & Rugh, R.F. (1981). *The Orphan Girl Mine – The World Museum of Mining: A living history*. Butte, Montana: Hell Roarin' Gulch Print Shop.
- Daly, W. B., Gillie, J., Bruce, J. L., Berrien, C. L., & Braly, N. B. (1925). *Mining Methods in the Butte District* American Institute of Mining, Metallurgical, and Petroleum Engineers, 234-287.
- Dunshee, B. H. (1913). *Timbering in the Butte Mines*. Transactions of the American Institute of Mining Engineers.
- Foster, D. A., Grice, W. C., & Kalakay, T. J. (2010). Extension of the Anaconda metamorphic core complex: 40Ar/39Ar thermochronology and implications for Eocene tectonics of the northern Rocky Mountains and the Boulder batholith. *Lithosphere*, 2(4), 232.
- GCTS Testing Systems. (2016). ULT-100 Ultrasonic velocity measurement system. Retrieved from <http://www.gcts.com/pdf/ULT-100.pdf>
- Goodman, R.E. (1989). *Introduction to rock mechanics*. New York: Wiley.
- González de Vallejo, L. I. G., Ferrer, M., & De Freitas, M. H. (2011). *Geological engineering*. CRC Press.

- Ghilani, C. D., & Wolf, P. R. (2012). *Elementary Surveying: An Introduction to Geomatics* (13 ed.). Upper Saddle River, New Jersey: Pearson Education Incorporated.
- Guilbert, J., & Park, C., Jr. (1986). *The Geology of Ore Deposits*. Long Grove, Illinois: Waveland Press, Incorporated.
- Hoek, E. (2007). *Practical Rock Engineering*. Retrieved from <https://www.rocscience.com/learning/hoek-s-corner/books>
- Houston, R. A., & Dilles, J.H. (2013). Structural Geologic Evolution of the Butte District, Montana. *Economic Geology*, 108, 1397-1424.
- Kermy, J., Mofya, E., Holmlund, J., & Ahlgren, S. (2002, April). Digital imaging for rock mass characterization. In *Proceedings of the 2nd Annual Conference on the Application of Geophysical and NDT Methodologies to Transportation Facilities and Infrastructure*, Los Angeles.
- Lund, K., Aleinkoff, J., Kunk, M., Unruh, D., Zeihen, G., Hodges, W., O'Neill, J. M. (2002). SHRIMP U-Pb and $^{40}\text{Ar}/^{39}\text{Ar}$ Age Constraints for Relating Plutonism and Mineralization in the Boulder Batholith Region, Montana. *Economic Geology*, 97.
- Palmström, A. (1982). The volumetric joint count - A useful and simple measure of the degree of rock mass jointing. *IV Congress International Association of Engineering Geology*, 2.
- Palmström, A. (2005). Measurements and Correlations between block size and Rock Quality Designation (RQD). *Tunnels and Underground Space Technology*, 20(4), 616.
- Palmström, A. (2015). *Classification Systems*. Retrieved from http://www.rockmass.net/articles/classification/classification_systems.html
- Pariseau, W. (2012). *Design Analysis in Rock Mechanics* (M. McKinnon Ed. 2 ed.). London, UK: CRC Press.
- Patton, F.D. & Deere, D.U. (1971). Significant geologic factors in rock slope stability. *Proceedings – Symposium on Planning open pit mines*, 143-151.
- Priest, S.D. & Hudson, J.A. (1976). Discontinuity spacings in rock. *International Journal of Rock Mechanics*, Vol. 13, 135-148.
- Read, J., & Stacey, P. (2009). *Guidelines for Open Pit Slope Design* (A. de Kretser Ed. 1 ed.). Collingwood, Australia: CSIRO.
- RocScience. (2017a). *DIPS Online Help*. Retrieved from <https://www.rocscience.com/help/dips/webhelp7/Dips.htm>

- RocScience. (2017b). Unwedge Online Help. Retrieved from <https://www.rocscience.com/help/unwedge/webhelp4/Unwedge.htm>
- Rosenthal, S. (2015). Personal Communication [Thesis Discussion].
- Rosenthal, S. (2016). Personal Communication [Thesis Discussion].
- Rusnak, J. A., & Mark, C. (2000). Using the point load test to determine the uniaxial compressive strength of coal measure rock. *Proceedings - International Conference on Ground Control in Mining*, 19, 362-371. Retrieved from <http://mtproxy.lib.umt.edu:3048/login?url=http://search.proquest.com/docview/51896729?accountid=28080>
- Sales, R. H. (1913). *Ore deposits at Butte, Montana*. American Institute of Mining, Metallurgical, and Petroleum Engineers.
- Salman, M., & Al-Amawee, A. (2006). The Ratio between Static and Dynamic Modulus of Elasticity in Normal and High Strength Concrete. *Journal of Engineering and Development*, 10(2), 163-174.
- Sawkins, F. (1972). Sulfide Ore Deposits in Relation to Plate Tectonics. *Journal of Geology*, 80(4), 20.
- Tunnell, H. R. (1922). *Handling Ore in Mines of Butte District*. Transaction of the American Institute of Mining and Metallurgical Engineers.
- Vulcan, Maptek. (2015) *ISIS Database Generation Language*.

Appendix A: Weathering Grades Observed at UMEC

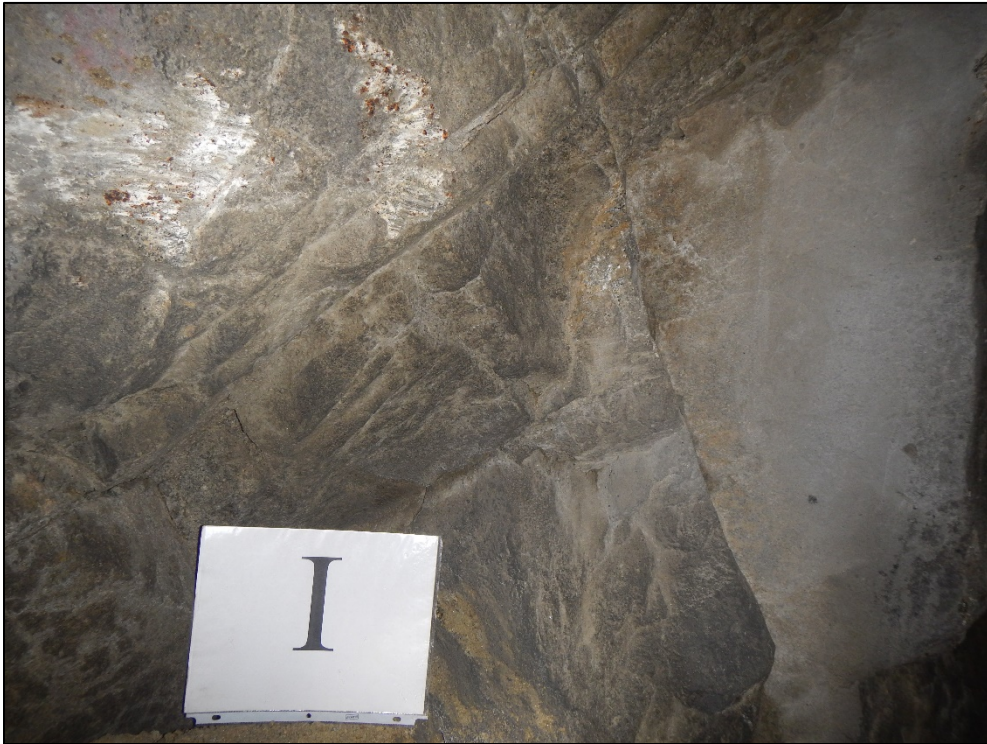


Figure 20: Weathering Grade I observed at UMEC.



Figure 21: Weathering Grade II observed at UMEC.



Figure 22: Weathering Grade III observed at UMEC.



Figure 23: Weathering Grade IV observed at UMEC.



Figure 24: Weathering Grade V observed at UMEC.



Figure 25: Weathering Grade VI observed at UMEC.

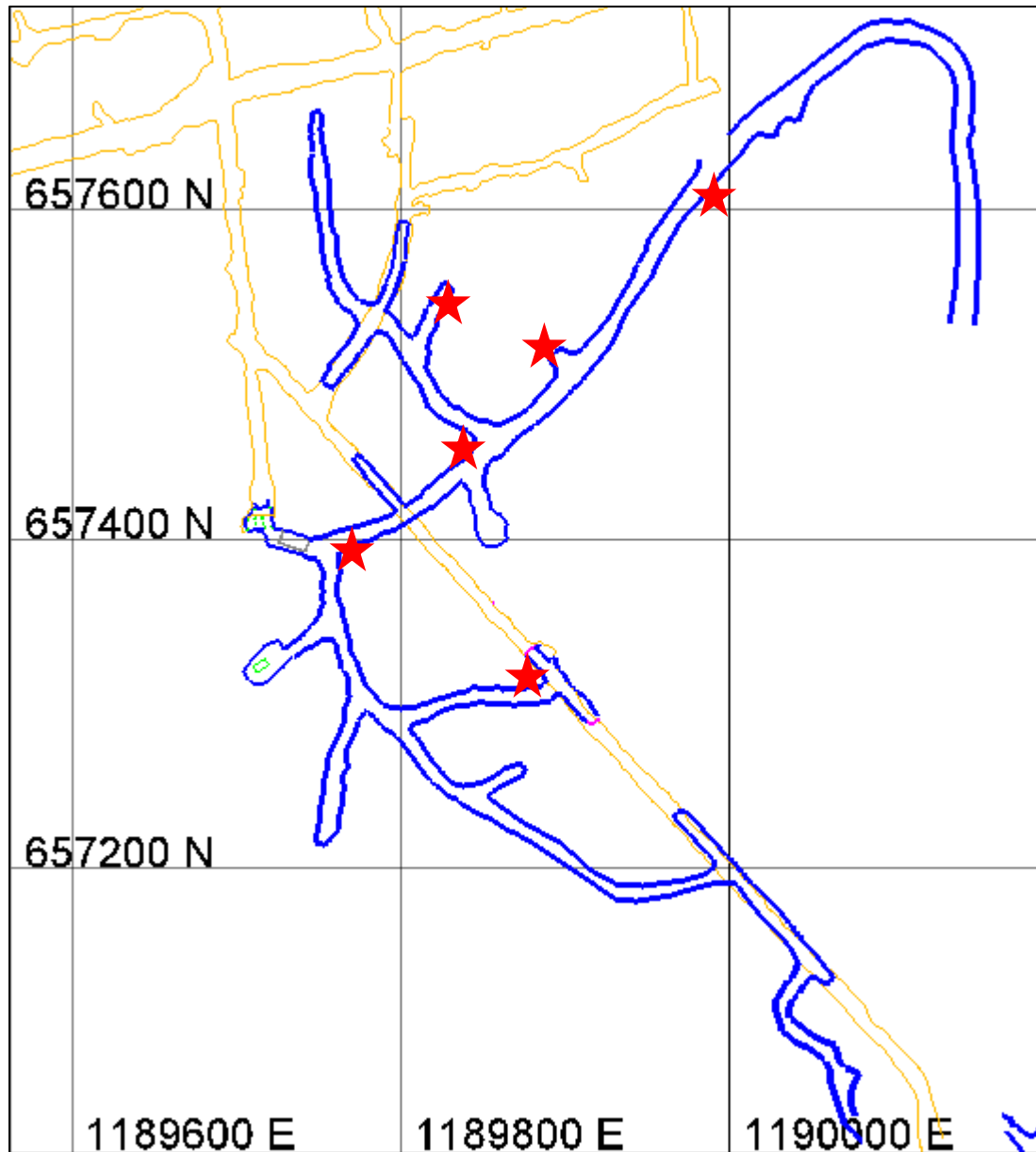
Appendix B: Additional Maps

Figure 26: UMEC map with sample locations indicated by red star..

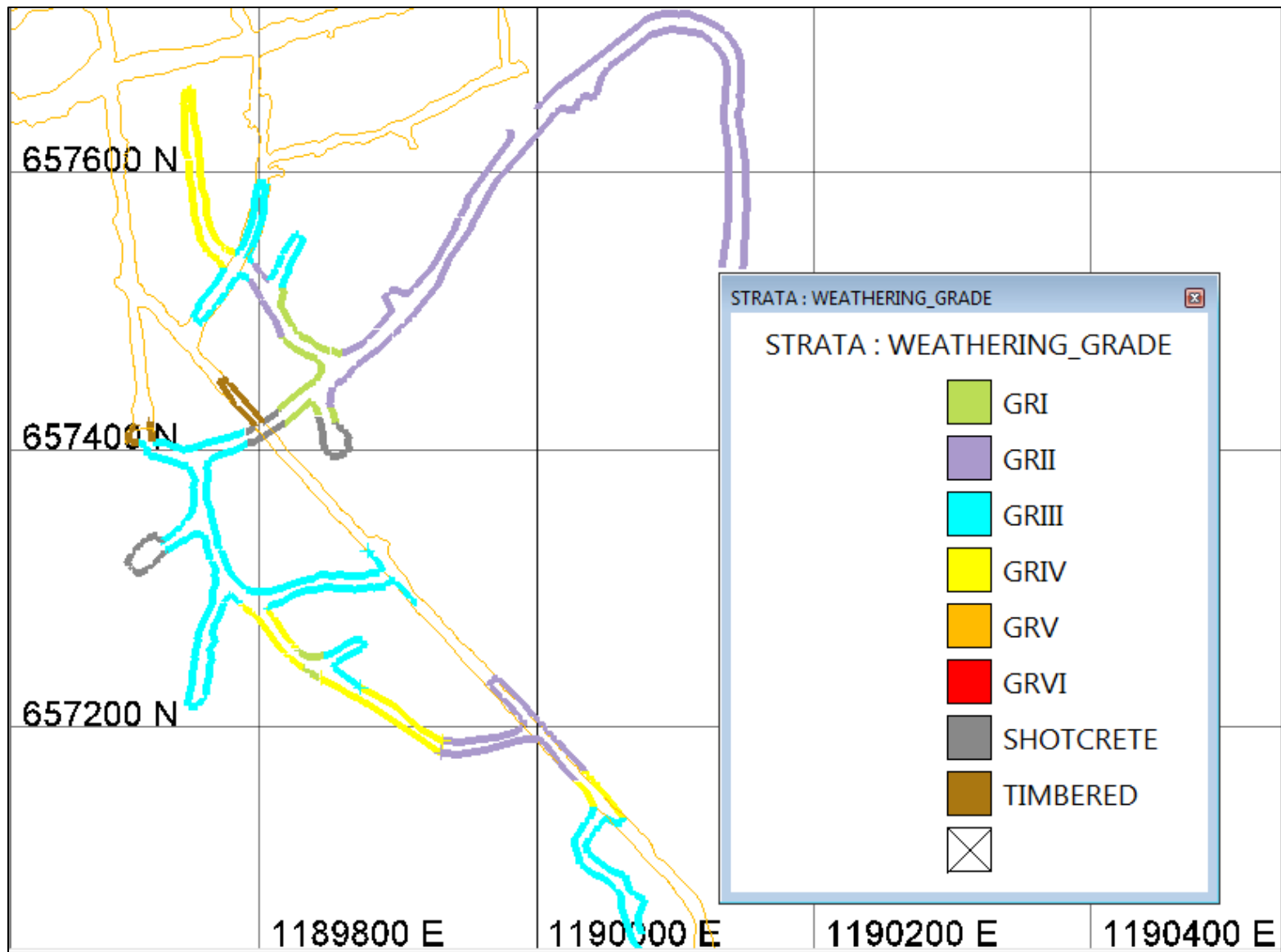


Figure 27: UMEC weathering grade map.

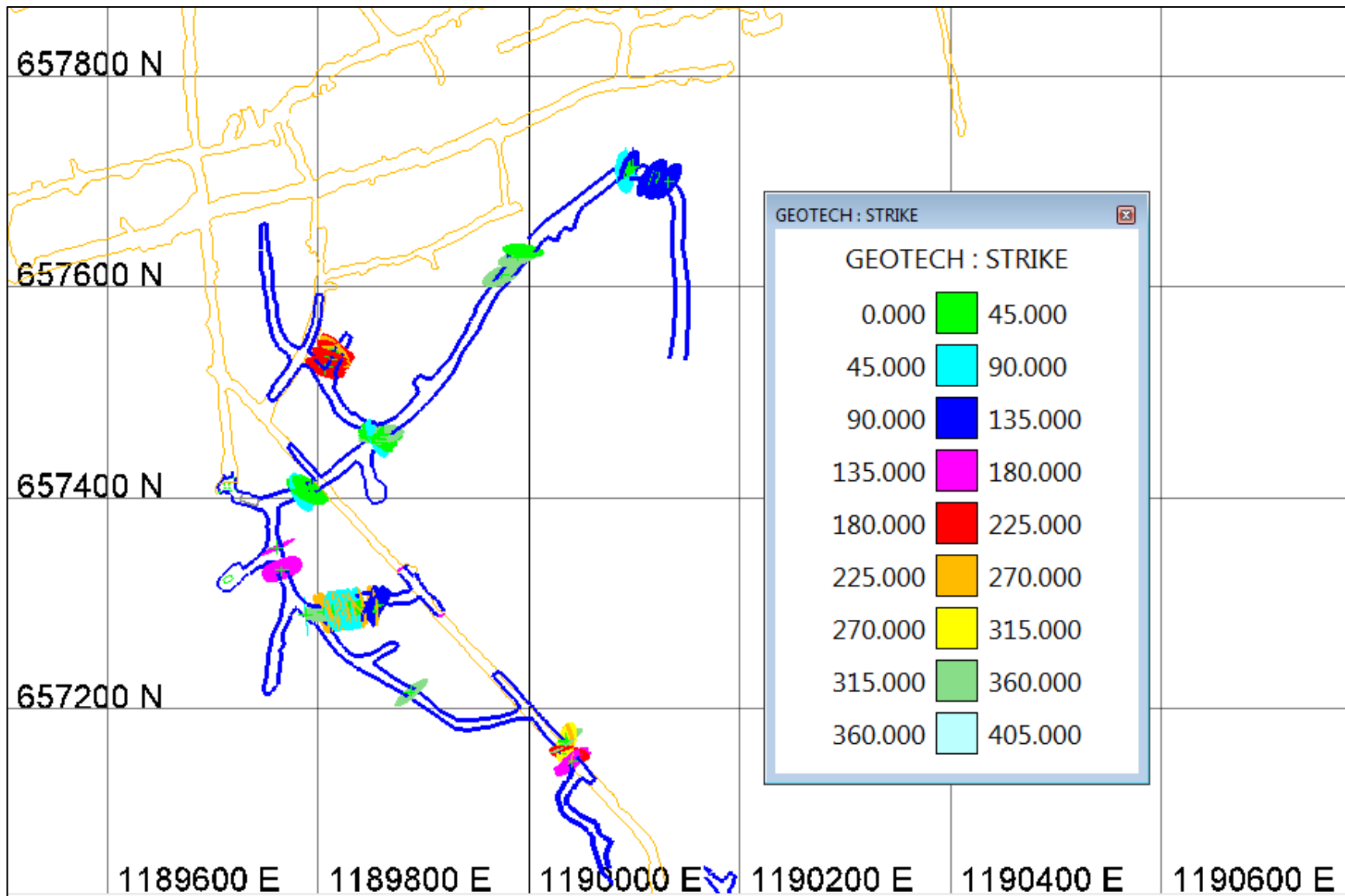


Figure 28: UMEC with strike and dip planes.

Appendix C: Cumulative Core Data

Table XX: Core sample parameters.

| SUITE | Diameter (in) | Length (in) | Mass (g) | Volume (in ³) | Density (g/in ³) | Density (g/cm ³) |
|-----------|---------------|-------------|----------|---------------------------|------------------------------|------------------------------|
| G | 1.722 | 4.218 | 421.840 | 9.82 | 42.94 | 2.620 |
| J | 1.722 | 4.082 | 409.770 | 9.51 | 43.10 | 2.630 |
| K | 1.724 | 4.111 | 410.330 | 9.60 | 42.76 | 2.609 |
| L1 | 1.722 | 4.175 | 415.920 | 9.72 | 42.78 | 2.610 |
| O | 1.723 | 3.880 | 392.73 | 9.05 | 43.41 | 2.649 |
| | | | | | | |
| A | 1.726 | 3.537 | 359.440 | 8.28 | 43.43 | 2.650 |
| B | 1.725 | 4.314 | 435.610 | 10.09 | 43.21 | 2.637 |
| D | 1.723 | 3.887 | 395.190 | 9.06 | 43.60 | 2.661 |
| E | 1.725 | 3.957 | 399.760 | 9.25 | 43.23 | 2.638 |
| F | 1.725 | 3.598 | 365.730 | 8.41 | 43.49 | 2.654 |
| | | | | | | |
| P1 | 1.723 | 4.044 | 411.03 | 9.43 | 43.59 | 2.660 |
| P2 | 1.729 | 3.483 | 350.060 | 8.18 | 42.81 | 2.612 |
| P4 | 1.725 | 3.395 | 402.760 | 7.93 | 50.76 | 3.098 |
| Q1 | 1.723 | 3.711 | 377.150 | 8.65 | 43.59 | 2.660 |

Table XXI: ULT Testing Results. Values that are not listed were unable to be obtained during testing.

| Sample | P-Wave (m/s) | S-Wave (m/s) | Poisson's Ratio | Young's Modulus (x10 ⁷ KPa) | Young's Modulus (x10 ⁶ psi) |
|----------------|--------------|--------------|-----------------|--|--|
| G | 1,294 | | | | |
| J | 1,222 | | | | |
| K | 1,047 | | | | |
| L1 | 2,992 | 1,345 | 0.37 | 1.31 | 1.89 |
| | | | | | |
| A | 1,590 | 1,138 | | 6.77 | 9.81 |
| B | 1,553 | 1,057 | 0.07 | 4.95 | 7.17 |
| D | 1,769 | 1,293 | | 8.35 | 1.21 |
| E | 1,276 | 946 | | 4.25 | 6.16 |
| F | 1,570 | 1,202 | | 6.19 | 8.98 |
| | | | | | |
| P2 | 3,207 | 1,985 | 0.19 | 2.51 | 3.63 |
| P4 | 2,471 | 1,425 | 0.25 | 1.35 | 1.95 |
| Q1 | 2,790 | 1,647 | 0.23 | 1.78 | 2.59 |
| | | | | | |
| AVERAGE | 1,900 | 1,340 | 0.22 | 3.62 | 5.25 |

Table XXII: UCS Test and Triaxial Test results.

| Sample | Diameter (in) | Confining Pressure (psi) | Peak Force (lbf) | UCS or Axial stress at failure (psi.) | Young's Modulus (x10 ⁶ psi) | Poisson's Ratio |
|--------|---------------|--------------------------|------------------|---------------------------------------|--|-----------------|
| G | 1.722 | NA | 3,584 | 1,539 | 0.99 | |
| J | 1.722 | NA | 5,204 | 2,234 | 1.47 | 0.26 |
| K | 1.724 | NA | 3,018 | 1,293 | 0.82 | |
| L1 | 1.722 | 500 | 11,101 | 4,766 | 1.98 | |
| O | 1.723 | 150 | 9,872 | 4,234 | 2.28 | |
| | | | | | | |
| A | 1.726 | NA | 7,324 | 3,130 | 2.44 | |
| B | 1.725 | NA | 4,091 | 1,750 | 1.31 | |
| D | 1.723 | 500 | 16,075 | 6,894 | 4.14 | |
| E | 1.725 | NA | 4,776 | 1,915 | 1.29 | |
| F | 1.725 | 150 | 11,057 | 4,731 | 2.96 | |
| | | | | | | |
| P1 | 1.723 | NA | 2,482 | 1,064 | 2.18 | |
| P2 | 1.729 | NA | 8,541 | 3,638 | 3.75 | |
| P4 | 1.725 | 500 | 25,959 | 11,107 | 7.78 | |
| Q1 | 1.723 | 150 | 16,678 | 7,153 | 5.73 | |

Table XXIII: Brazilian test results.

| Sample ID | Suite | Diameter (mm) | Diameter (in) | Thickness (mm) | Thickness (in) | Valid? |
|-----------|-------|---------------|---------------|----------------|----------------|--------|
| A | 2 | 43.69 | 1.720 | 27.135 | 1.068 | Y |
| B | | 43.72 | 1.721 | 21.115 | 0.831 | N |
| C1 | | 43.71 | 1.721 | 21.045 | 0.829 | N |
| C2 | | 43.62 | 1.717 | 18.025 | 0.710 | N |
| E | | 43.74 | 1.722 | 28.86 | 1.136 | Y |
| F1 | 1 | 43.81 | 1.725 | 24.545 | 0.966 | Y |
| F2 | | 43.73 | 1.722 | 14.96 | 0.589 | N |
| G1 | | 43.66 | 1.719 | 19.195 | 0.756 | N |
| G2 | | 43.71 | 1.721 | 17.775 | 0.700 | Y |
| G3 | | 43.69 | 1.720 | 19.75 | 0.778 | Y |
| H | | 43.83 | 1.726 | 23.38 | 0.920 | N |
| K | | 43.76 | 1.723 | 19.285 | 0.759 | N |
| J | | 43.62 | 1.717 | 30.59 | 1.204 | Y |
| M | | 43.62 | 1.717 | 18.77 | 0.739 | Y |
| P1 | | 3 | 43.62 | 1.717 | 18.36 | 0.723 |
| P2 | 43.65 | | 1.719 | 19.44 | 0.765 | Y |
| P3 | 43.65 | | 1.719 | 17.49 | 0.689 | Y |
| Q1 | 43.71 | | 1.721 | 23.1 | 0.909 | Y |
| Q2 | 43.66 | | 1.719 | 18.01 | 0.709 | Y |

Table XXIV: Brazilian test results continued.

| Sample ID | Force (kN) | Force (N) | Force (lbf) | Tensile Strength (psi) |
|------------------------------|------------|-----------|-------------|------------------------|
| A | 3.41 | 3410 | 767 | 265.60 |
| B | 1.18 | 1180 | 265 | 118.03 |
| C1 | 2.35 | 2350 | 528 | 235.90 |
| C2 | 1.67 | 1670 | 375 | 196.13 |
| E | 4.93 | 4930 | 1,108 | 360.62 |
| F1 | 3.39 | 3390 | 762 | 291.10 |
| F2 | 1.43 | 1430 | 321 | 201.84 |
| G1 | 2.39 | 2390 | 537 | 263.34 |
| G2 | 2.03 | 2030 | 456 | 241.26 |
| G3 | 2.51 | 2510 | 564 | 268.60 |
| H | 3.02 | 3020 | 679 | 272.13 |
| K | 1.37 | 1370 | 308 | 149.90 |
| J | 1.99 | 1990 | 447 | 137.71 |
| M | 7.04 | 7040 | 1,583 | 793.97 |
| P1 | 7.71 | 7710 | 1,733 | 888.95 |
| P2 | 3.46 | 3460 | 778 | 376.51 |
| P3 | 5.19 | 5190 | 1,167 | 627.73 |
| Q1 | 5.12 | 5120 | 1,151 | 468.23 |
| Q2 | 4.85 | 4850 | 1,090 | 569.54 |
| | | | | |
| Total AVERAGE | 3.42 | 3,420 | 770 | 354 |
| Valid Results AVERAGE | 4.30 | 4,300 | 970 | 440 |

Table XXV: Point Load Test results.

| Sample ID | Diameter (mm) | Length (mm) | Pressure (kN) | Pressure (N) |
|-----------|---------------|-------------|---------------|--------------|
| C | 43.72 | 89.55 | 4.28 | 962 |
| F5 | 43.90 | 89.24 | 6.31 | 1,419 |
| H | 43.85 | 87.74 | 0.5 | 112 |
| I | 43.73 | 91.24 | 0.55 | 124 |
| M | 43.88 | 89.56 | 3.09 | 695 |

Table XXVI: Point Load Test results continued.

| Sample ID | Diameter (in) | Length (in) | Pressure (lbf) | I _s | F | I _{s50} | UCS |
|----------------|---------------|-------------|----------------|----------------|------|------------------|-------|
| C | 1.721 | 3.526 | 962 | 324.8 | 0.22 | 71.3 | 1,712 |
| F5 | 1.728 | 3.513 | 1,419 | 474.9 | 0.22 | 104.5 | 2,507 |
| H | 1.726 | 3.454 | 112 | 37.7 | 0.22 | 8.3 | 199 |
| I | 1.722 | 3.592 | 124 | 41.7 | 0.22 | 9.2 | 220 |
| M | 1.728 | 3.526 | 695 | 232.8 | 0.22 | 51.2 | 1,229 |
| AVERAGE | | | | | | | 1,173 |

Table XXVII: Cumulative Mohr Circle failure envelope results.

| Grade | Cohesion (psi) | Phi (°) |
|----------------|----------------|---------|
| I | 363 | 63 |
| II | 402 | 53 |
| III | 396 | 47 |
| AVERAGE | 387 | 54 |

Appendix D: GCTS ULT-100 Testing Results

ULT Testing Results for Suite 1 shown in Figures 29-36.

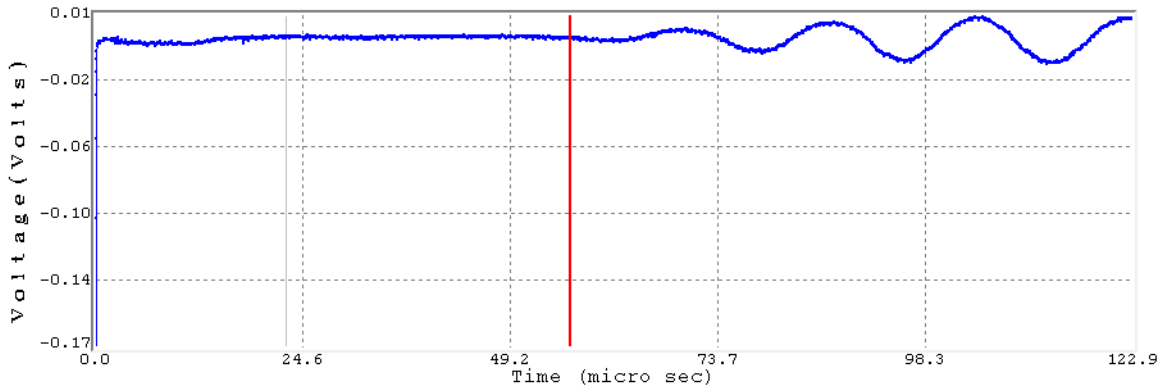


Figure 29: P-Wave response for Sample A at 1,590 meters per second.

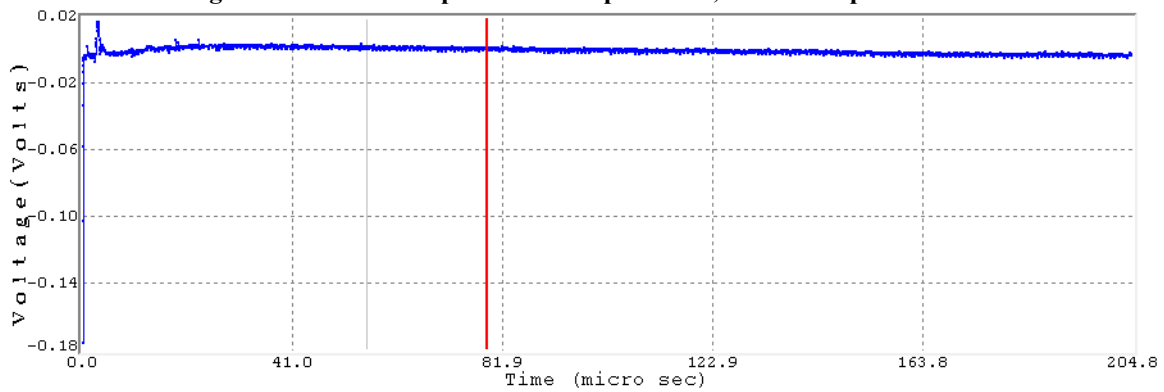


Figure 30: S-Wave response for Sample G is unresponsive.

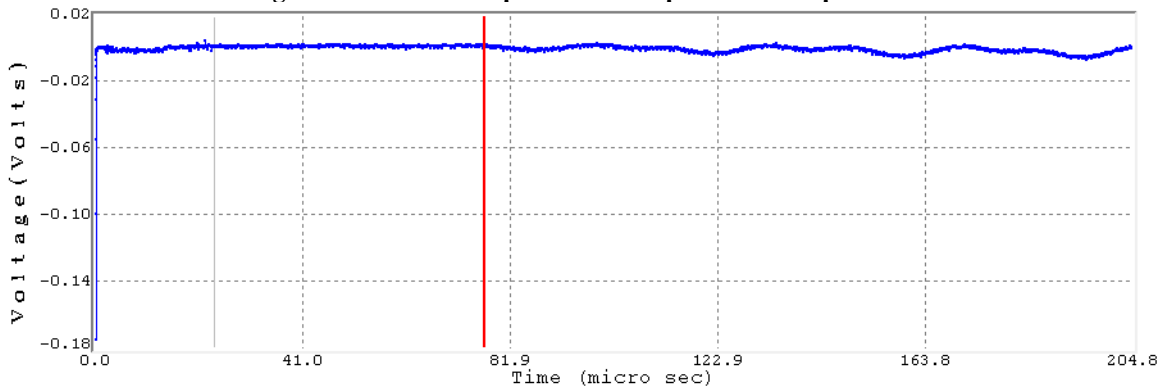
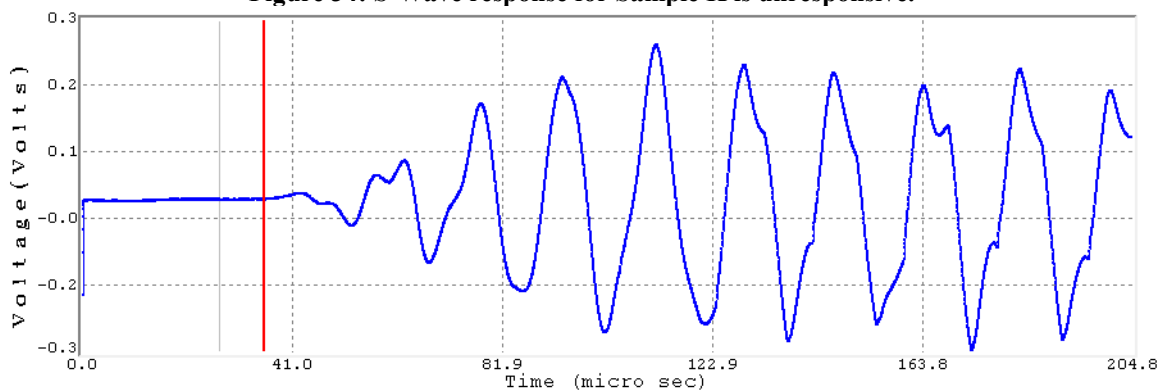
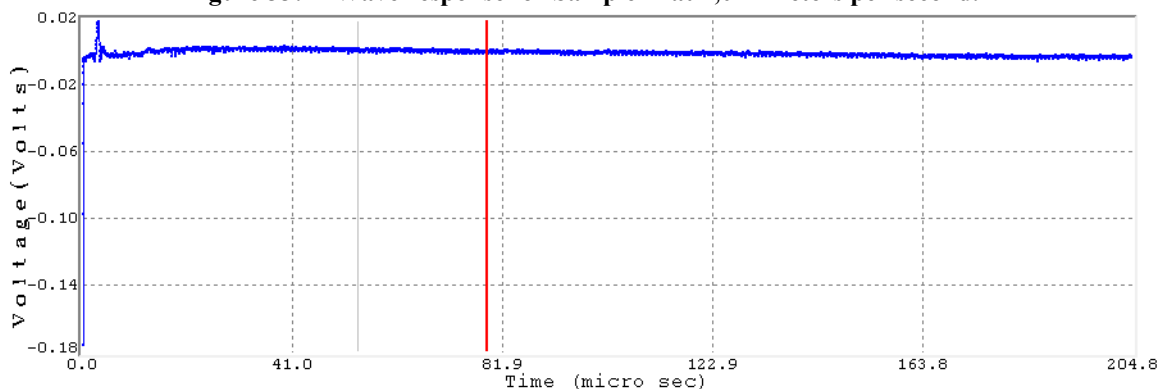
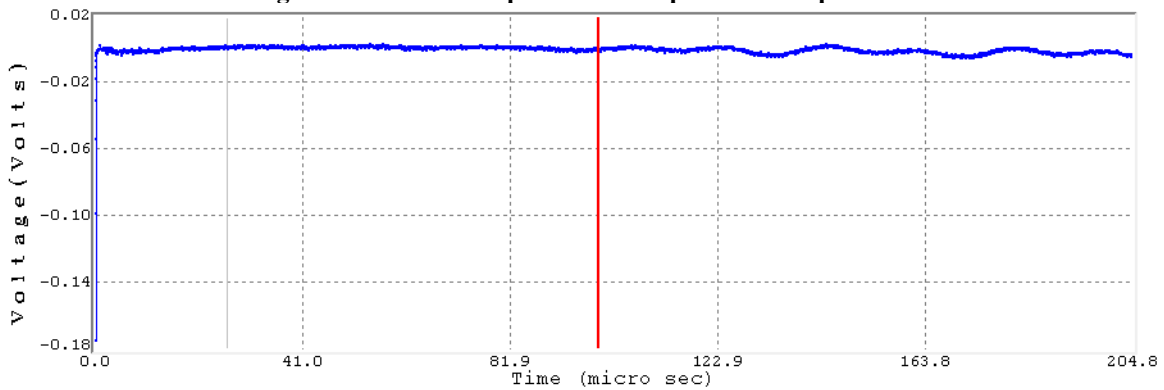
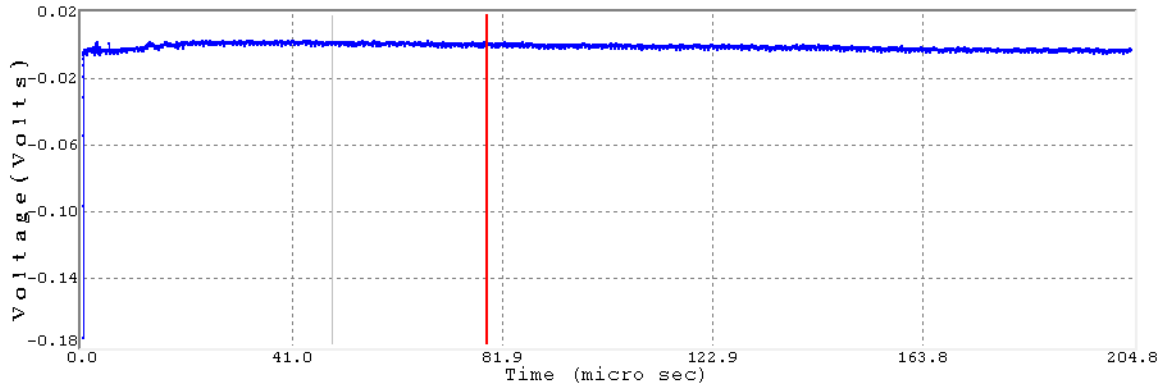


Figure 31: P-Wave response for Sample J at 1,222 meters per second.



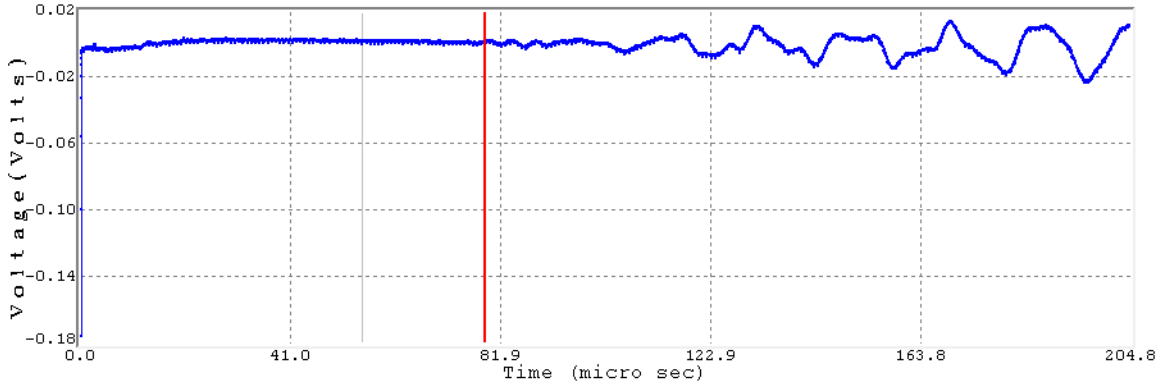


Figure 36: S-Wave response for Sample L1 at 1,345 meters per second.

ULT Testing Results for Suite 2 shown in Figures 37-46.

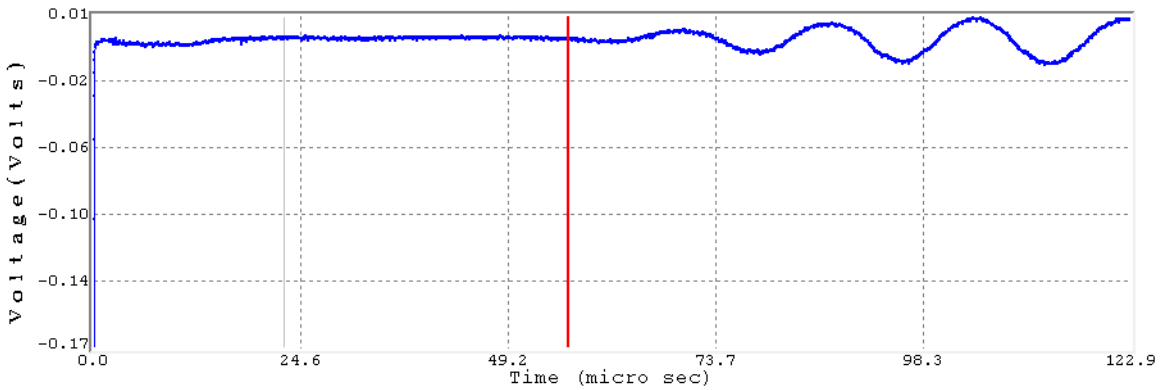


Figure 37: P-Wave response for Sample A at 1,590 meters per second.

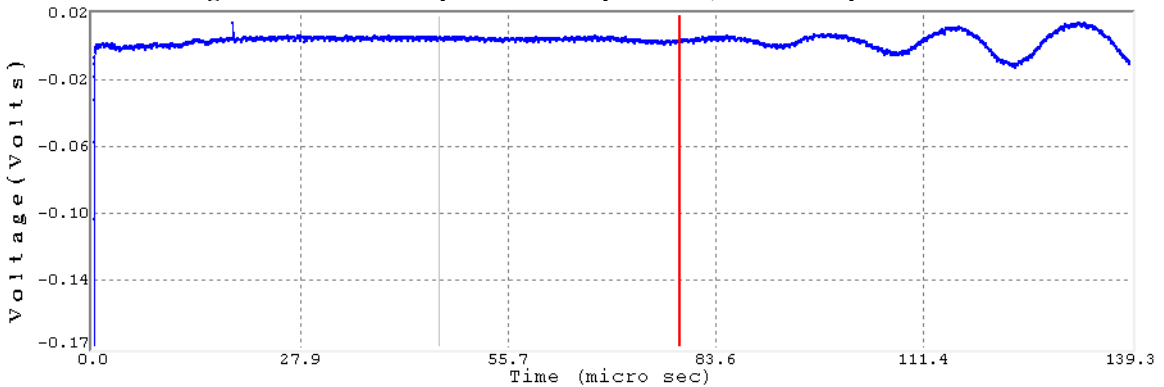


Figure 38: S-Wave response for Sample A at 1,138 meters per second.

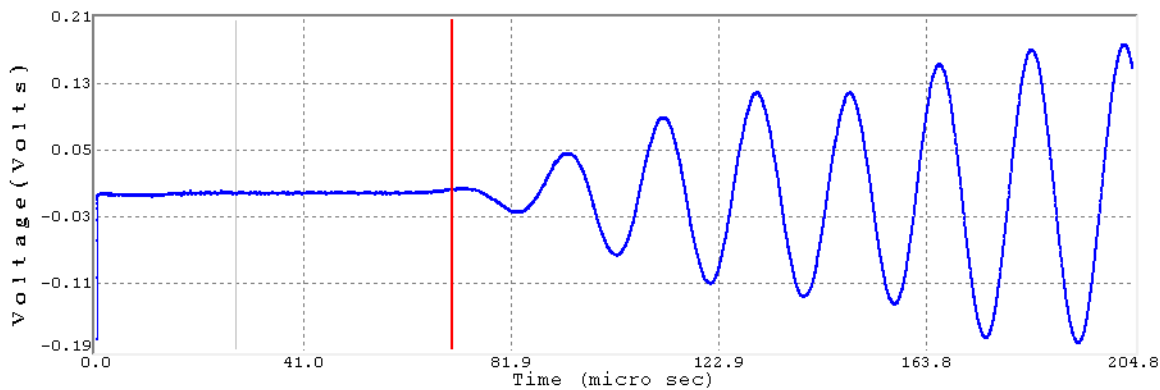


Figure 39: P-Wave response for Sample B at 1,553 meters per second.

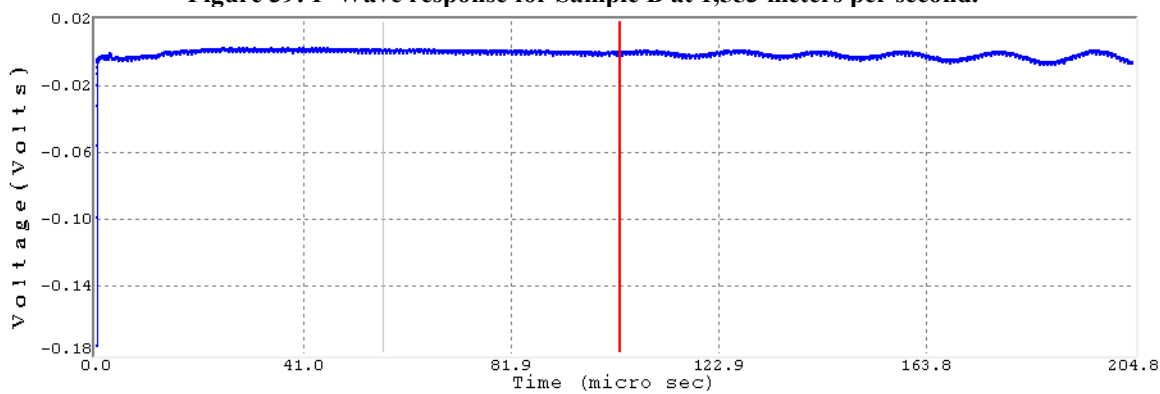


Figure 40: S-Wave response for Sample B at 1,057 meters per second.

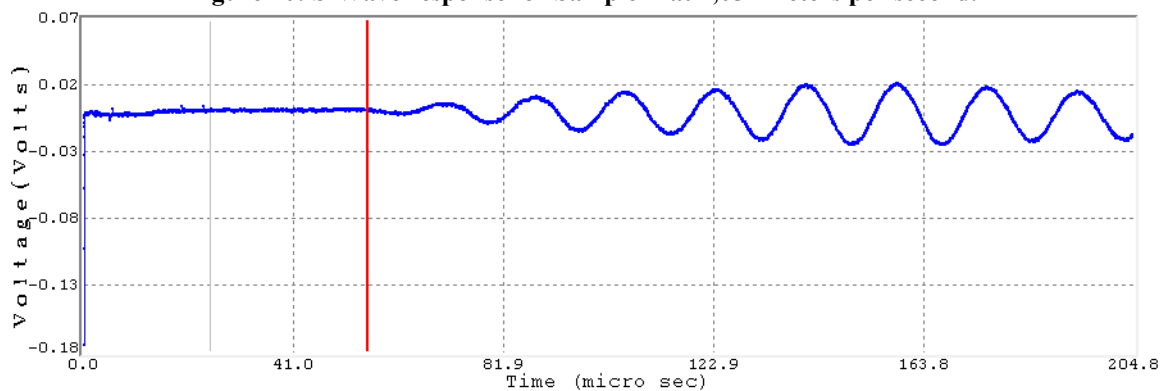


Figure 41: P-Wave response for Sample D at 1,769 meters per second.

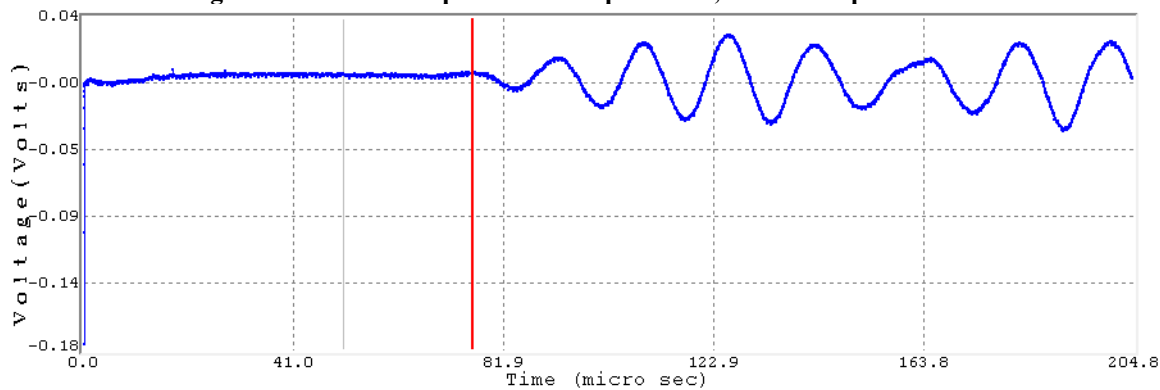


Figure 42: S-Wave response for Sample D at 1,293 meters per second.

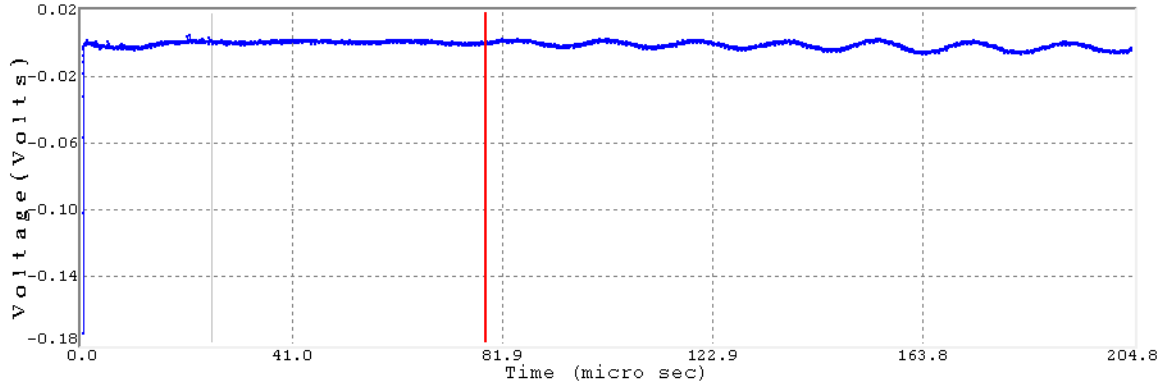


Figure 43: P-Wave response for Sample E at 1,296 meters per second.

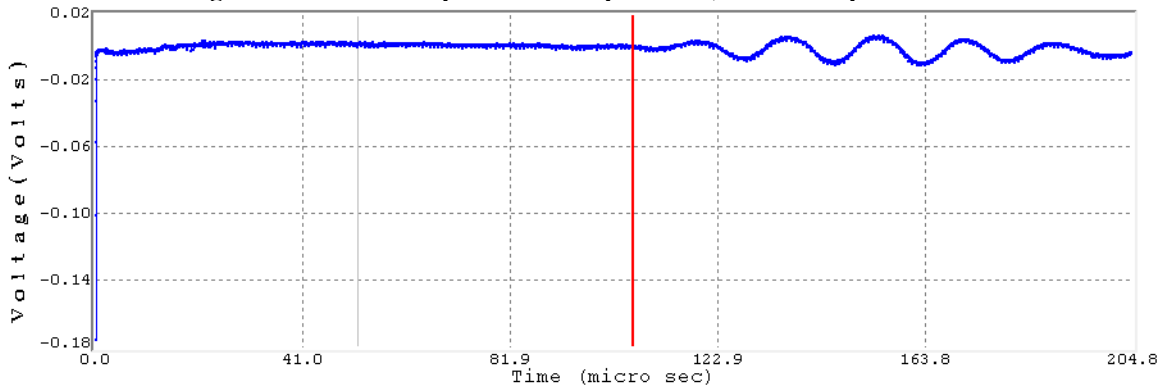


Figure 44: S-Wave response for Sample E at 946 meters per second.

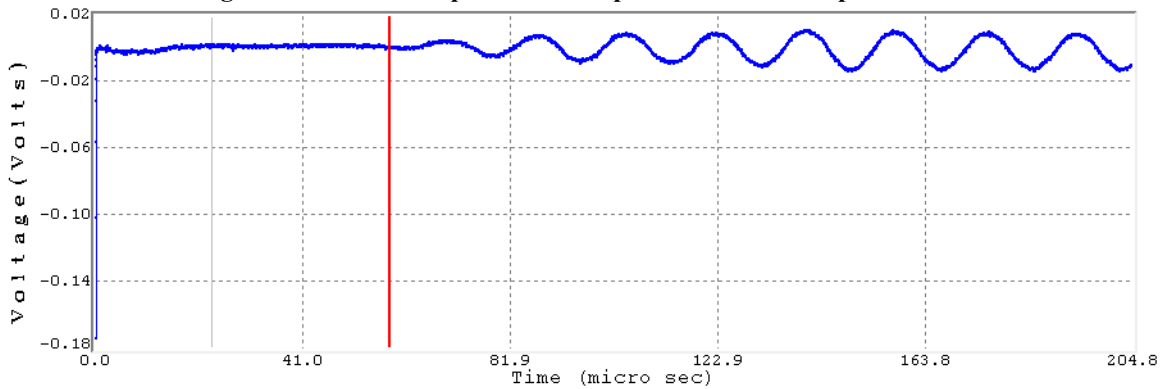


Figure 45: P-Wave response for Sample F at 1,570 meters per second.

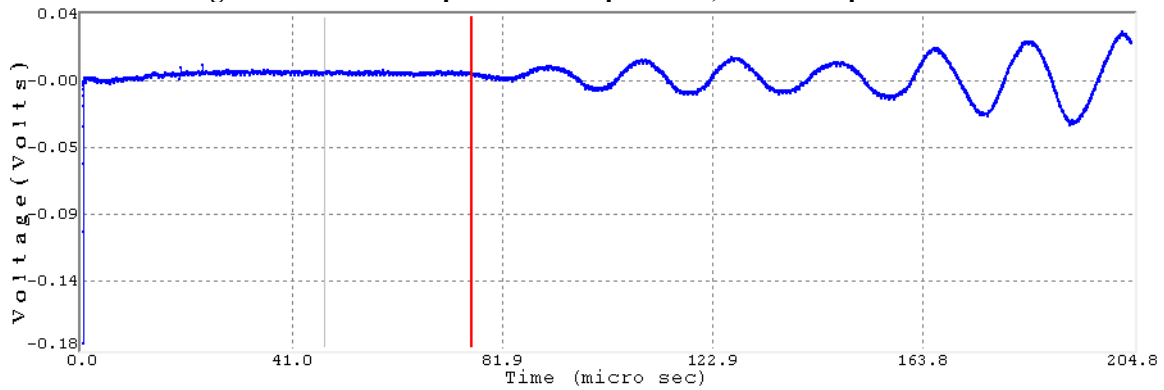


Figure 46: S-Wave response for Sample F at 1,202 meters per second.

ULT Testing Results for Suite 3 shown in Figures 47-52.

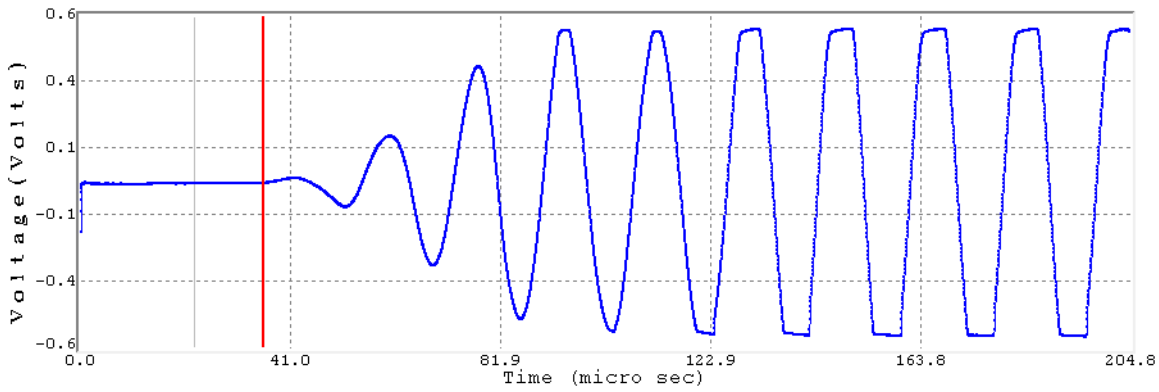


Figure 47: P-Wave response for Sample P2 at 2,471 meters per second.

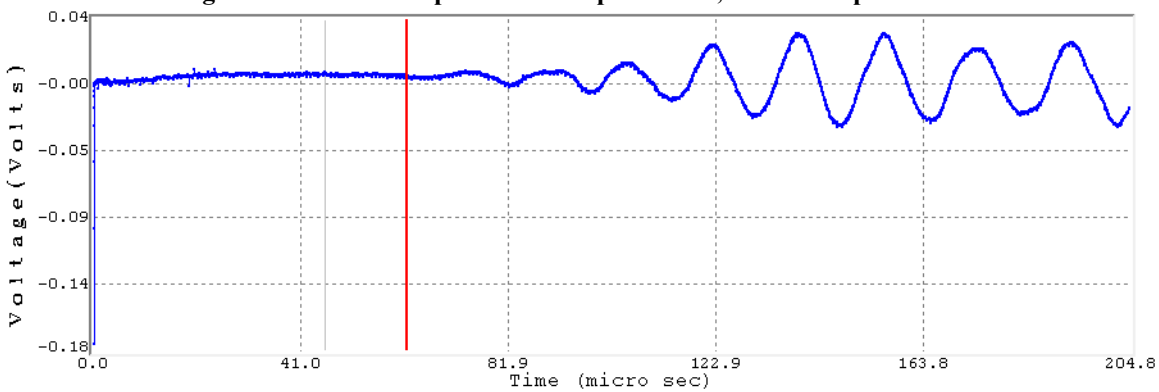


Figure 48: S-Wave response for Sample P2 at 1,425 meters per second.

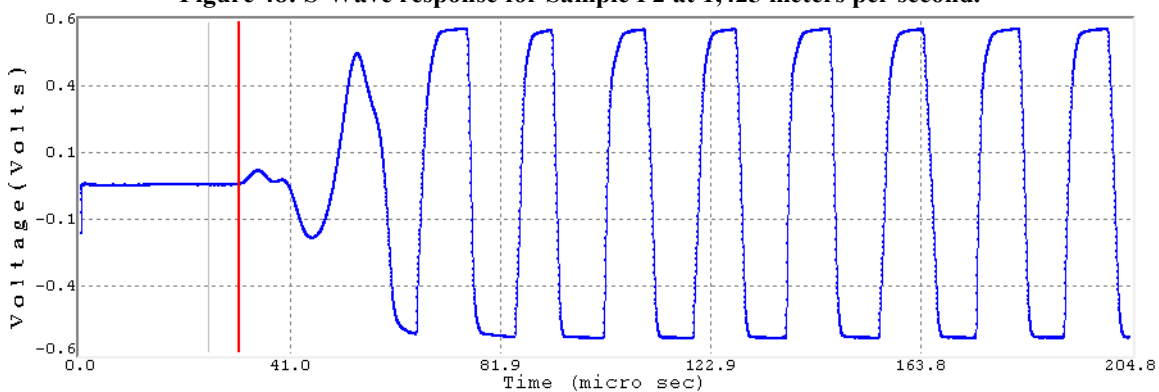


Figure 49: P-Wave response for Sample P4 at 3,207 meters per second.

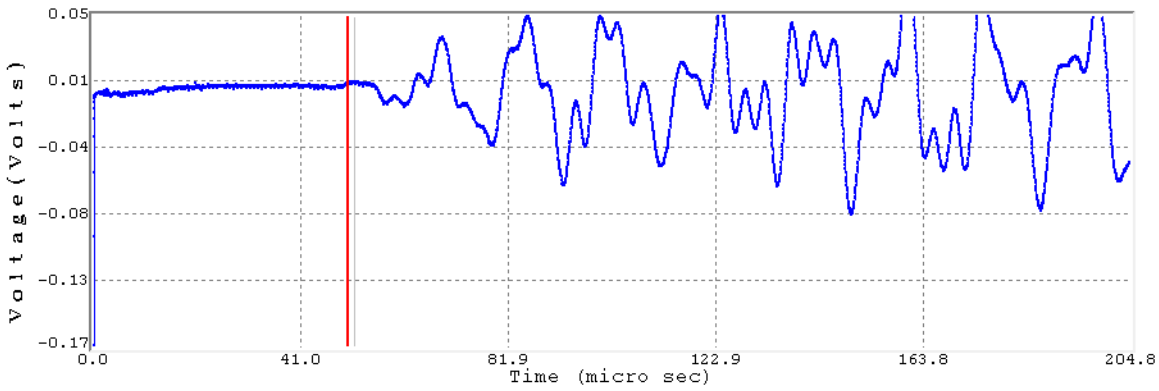


Figure 50: S-Wave response for Sample P4 at 1,985 meters per second.

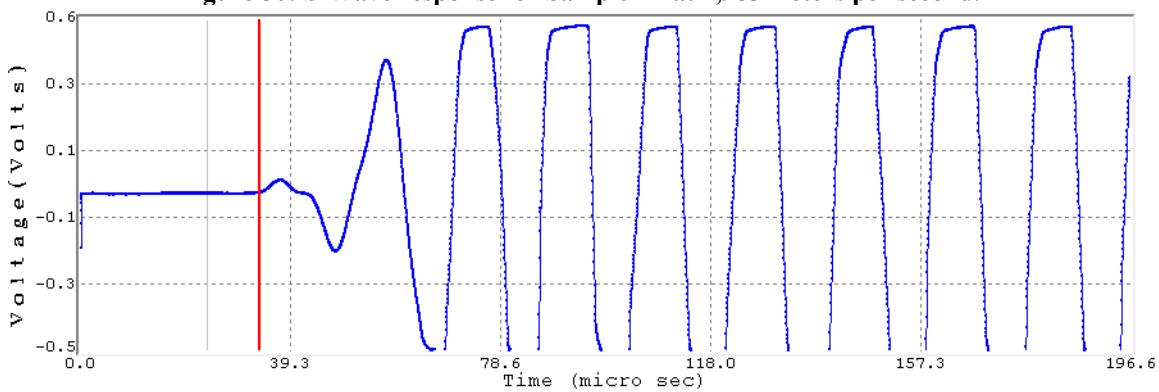


Figure 51: P-Wave response for Sample Q1 at 2,790 meters per second.

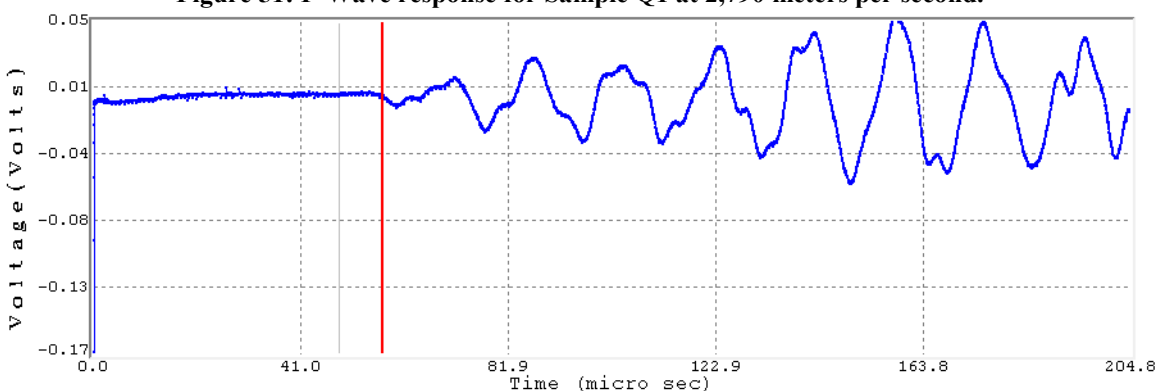


Figure 52: S-Wave response for Sample Q1 at 1,647 meters per second.

Appendix E: UCS Test Core Sample Results

Suite 1 core sample results:

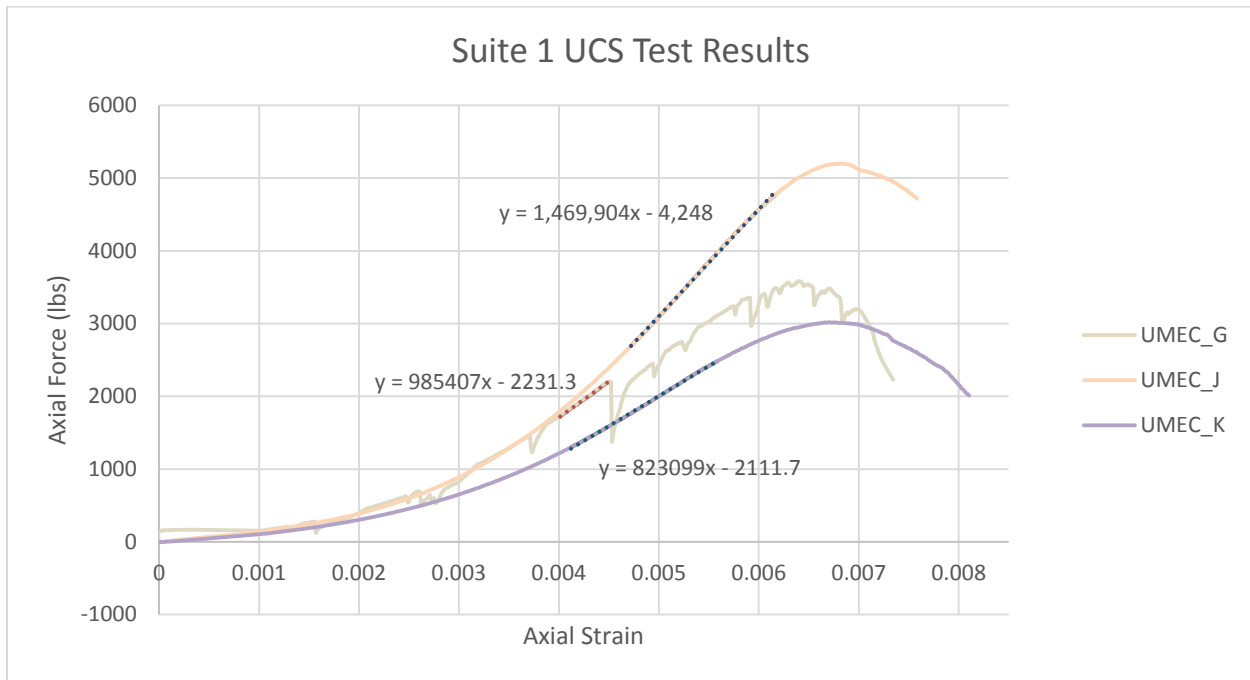


Figure 53: Plot of the Stress versus Strain curves produced using the TerraTek software for the UCS tests.



Figure 54: Sample G prior to axial load. No distinct cracks present in core.



Figure 55: Sample G after axial load. Sample continuously compressed, causing force to undulate until nonviolent shear failure occurred.



Figure 56: Sample J prior to axial load. No distinct cracks present in core.



Figure 57: Sample J after axial load. Sample compressed until nonviolent failure occurred. Failure crack indicated with pencil.



Figure 58: Sample K prior to axial load. No distinct cracks present in core.

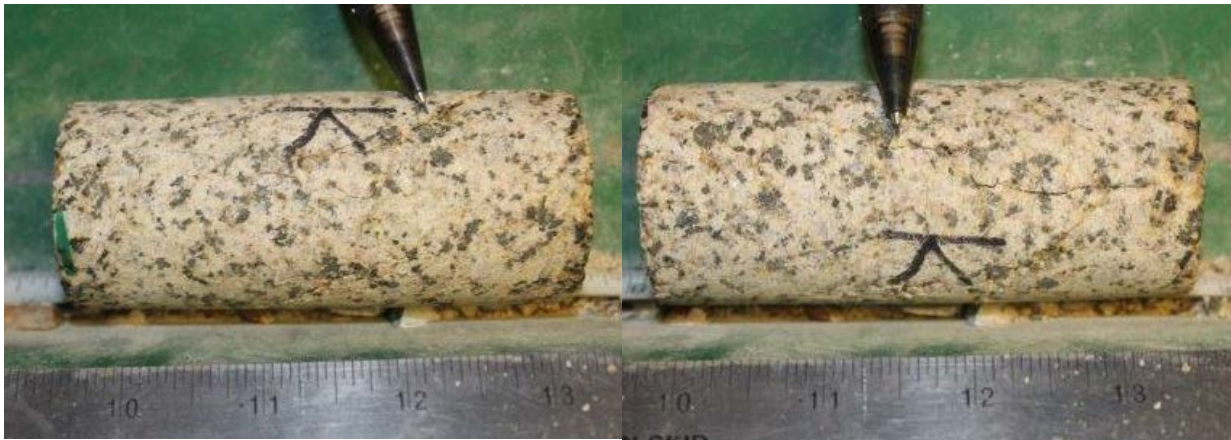


Figure 59: Sample K after axial load. Sample compressed until nonviolent failure occurred. Failure crack indicated with pencil.

Suite 2 core sample results:

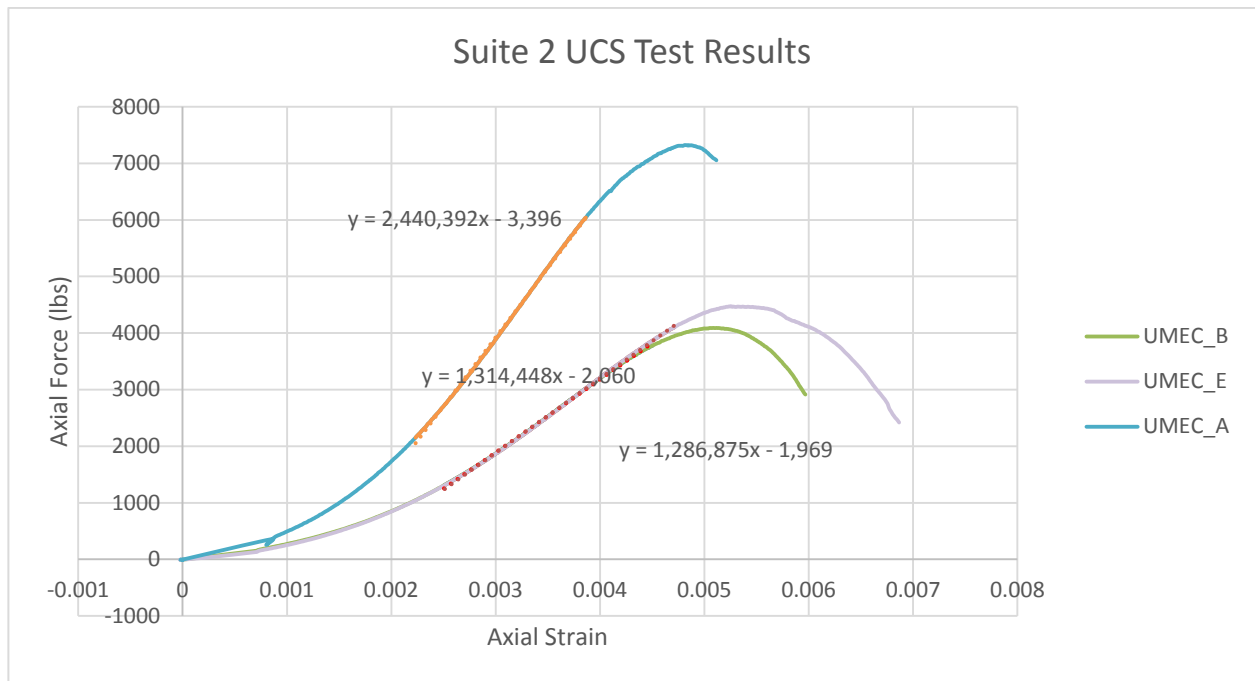


Figure 60: Plot of the Stress versus Strain curves produced using the TerraTek software for the UCS tests.



Figure 61: Sample A prior to axial load. No distinct cracks present in core.



Figure 62: Sample A after axial load. Sample compressed until nonviolent failure occurred. Failure crack indicated with pencil.



Figure 63: Sample B prior to axial load. No distinct cracks present in core.



Figure 64: Sample B after axial load. Sample compressed until nonviolent failure occurred. Failure crack indicated with pencil.



Figure 65: Sample E after axial load. No photograph was taken prior to axial load. Sample compressed until nonviolent failure occurred. Multiple axial splits developed while under load. Failure crack indicated with pencil.

Suite 3 core sample results:

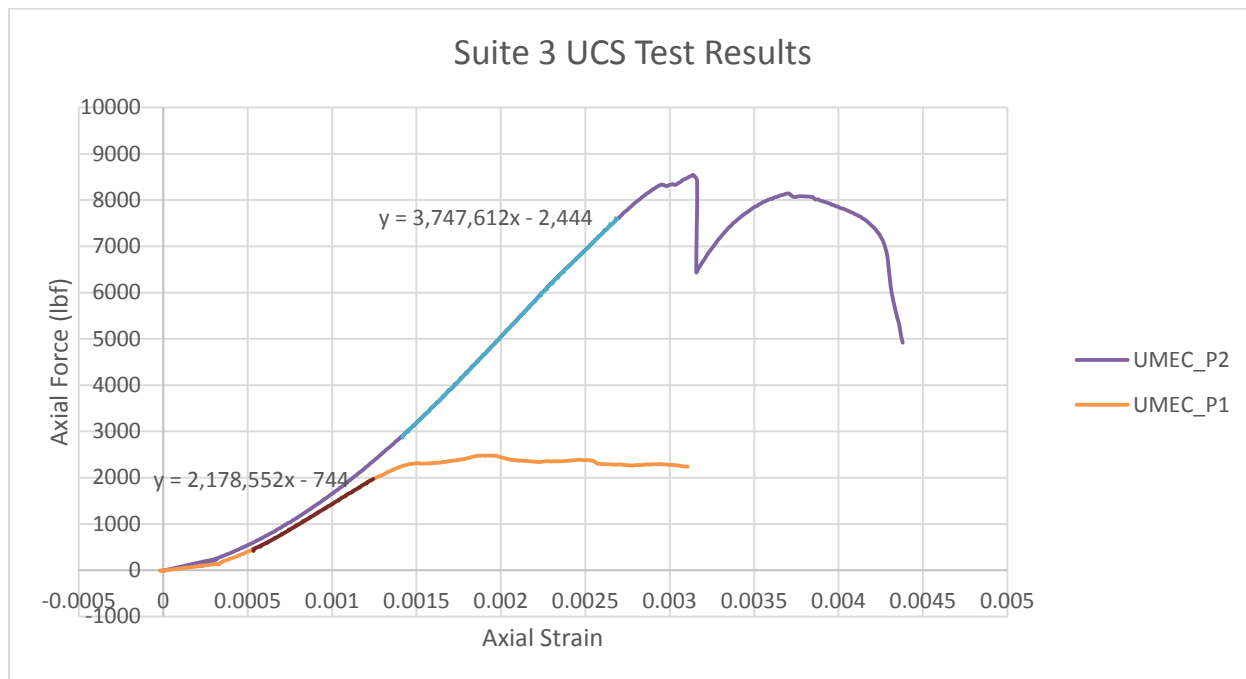


Figure 66: Plot of the Stress versus Strain curves produced using the TerraTek software for the UCS tests.



Figure 67: Sample P1 prior to axial load. Large crack approximately 30° from vertical.



Figure 68: Sample P1 after axial load. Sample compressed until brittle failure occurred along major discontinuity.



Figure 69: Sample P2 prior to axial load. Small fracture indicated with pencil.



Figure 70: Sample P2 after axial load. Sample compressed until first brittle cracking occurred along major discontinuity, causing sharp drop in axial pressure. Failure occurred shortly after, causing additional cracking to form throughout the core sample.

Appendix F: Triaxial Test Core Sample Results

Results for triaxial testing with 500 psi confining pressure:

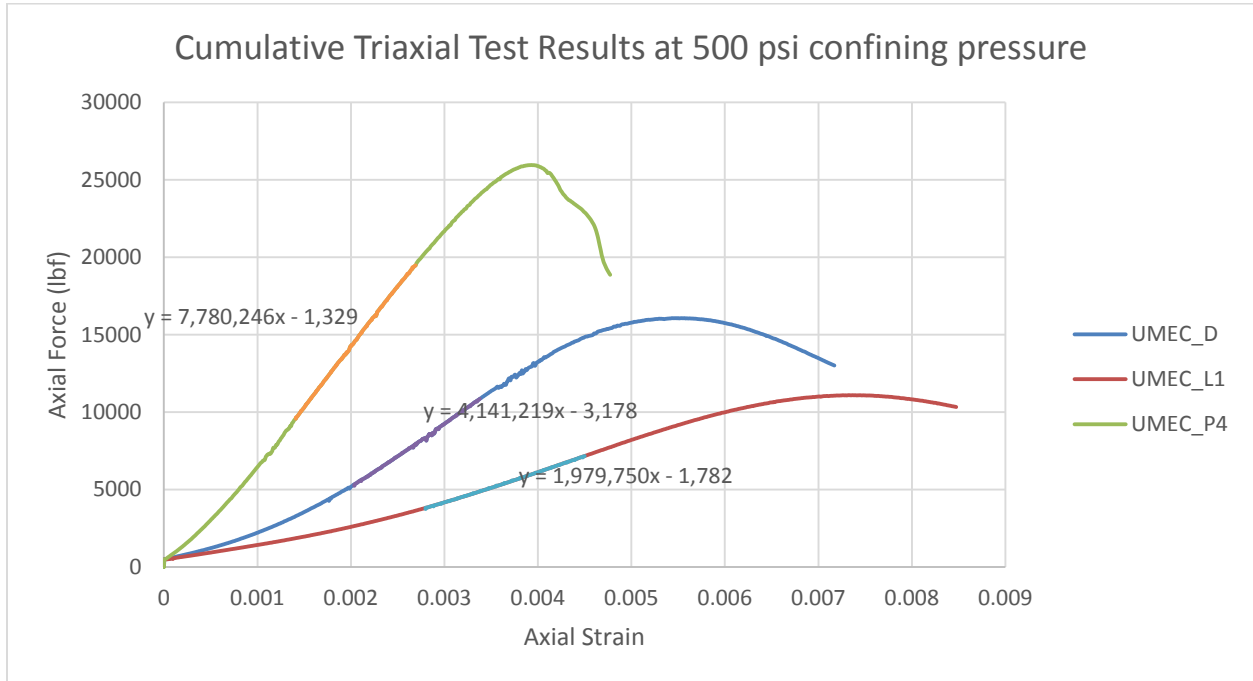


Figure 71: Plot of the Stress versus Strain curves produced using the TerraTek software for the triaxial tests at 500 psi confining pressure.



Figure 72: Sample D prior to triaxial load. No distinct cracks present in core.



Figure 73: Sample D after triaxial load. Sample failed nonviolently, no distinct shear planes present.



Figure 74: Sample L1 prior to triaxial load. No distinct cracks present in core. Small cracks patched with bolt anchor sulfaset yellow: high speed expansive anchoring compound.



Figure 75: Sample L1 after triaxial load. Sample failed nonviolently, no distinct shear planes present.



Figure 76: Sample P4 prior to triaxial load. No distinct cracks present in core.



Figure 77: Sample P4 after triaxial load. Sample failed nonviolently. Small shear fracture indicated with pencil.

Results for triaxial testing with 150 psi confining pressure:

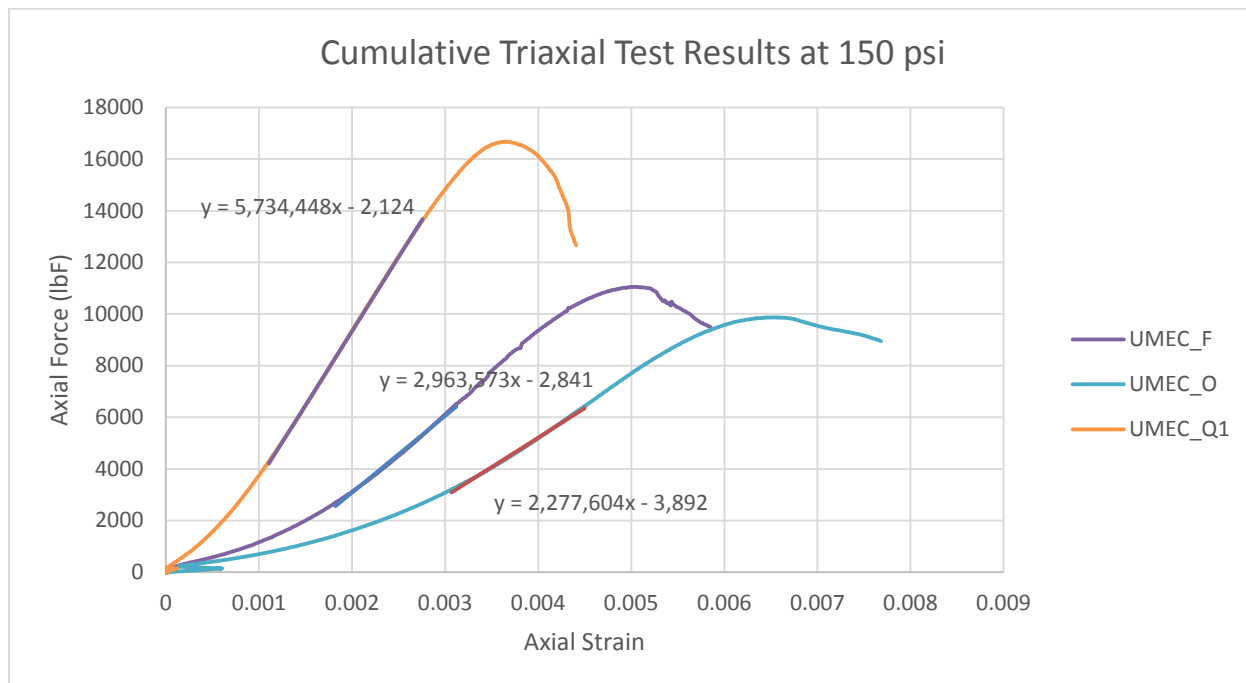


Figure 78: Plot of the Stress versus Strain curves produced using the TerraTek software for the triaxial tests at 150 psi confining pressure.

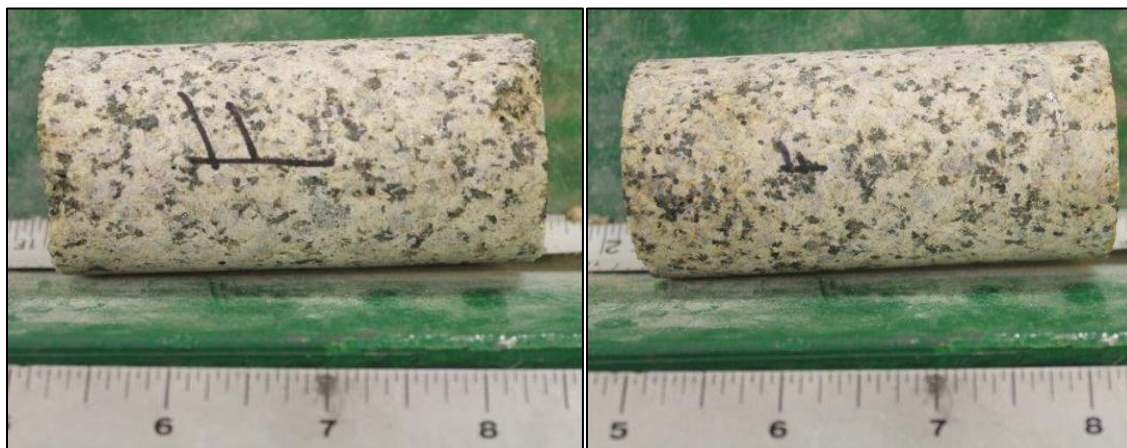


Figure 79: Sample F prior to triaxial load. No distinct cracks present in core.



Figure 80: Sample F after triaxial load. Sample failed nonviolently. Small shear fracture indicated with pencil.

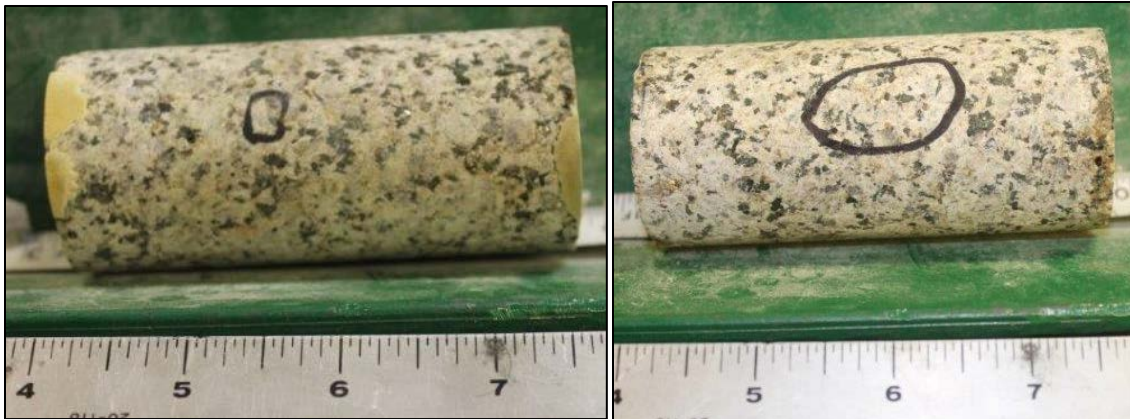


Figure 81: Sample O prior to triaxial load. No distinct vertical cracks present in core. Small cracks patched with bolt anchor sulfaset yellow: high speed expansive anchoring compound.



Figure 82: Sample O after triaxial load. Sample failed nonviolently. Small shear fracture indicated with pencil.

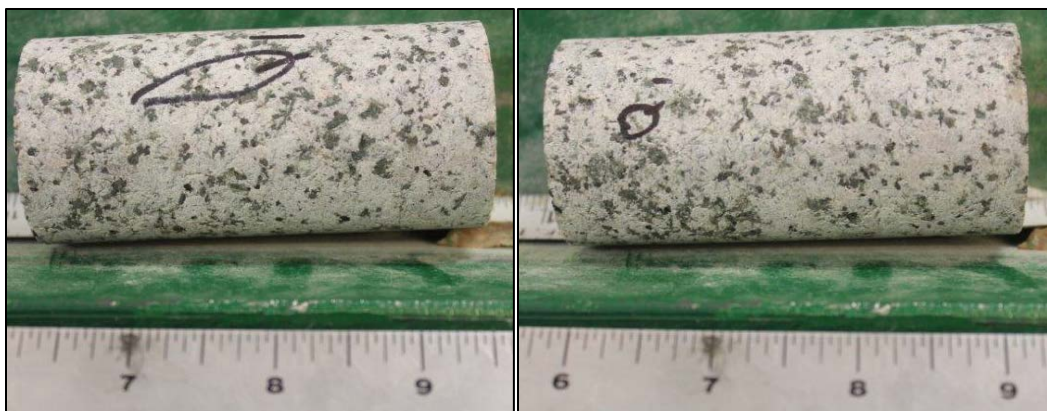


Figure 83: Sample Q1 prior to triaxial load. No distinct cracks present in core.



Figure 84: Sample Q1 after triaxial load. Sample failed nonviolently. No shear fracture planes are visible.

Appendix G: Brazilian Test and Point Load Test Core Sample Results



Figure 85: Brazilian test results.

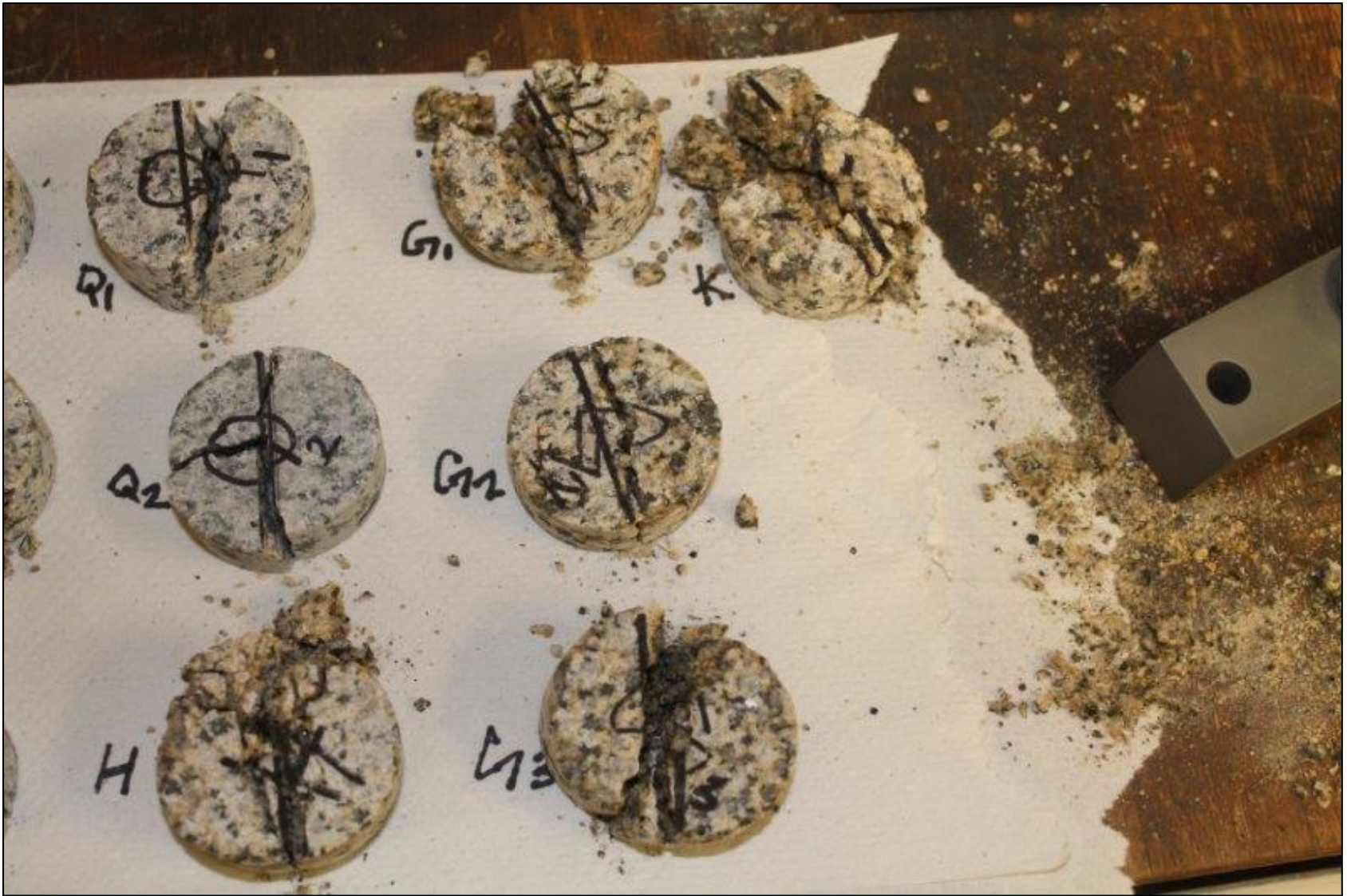


Figure 86: Brazilian test results.

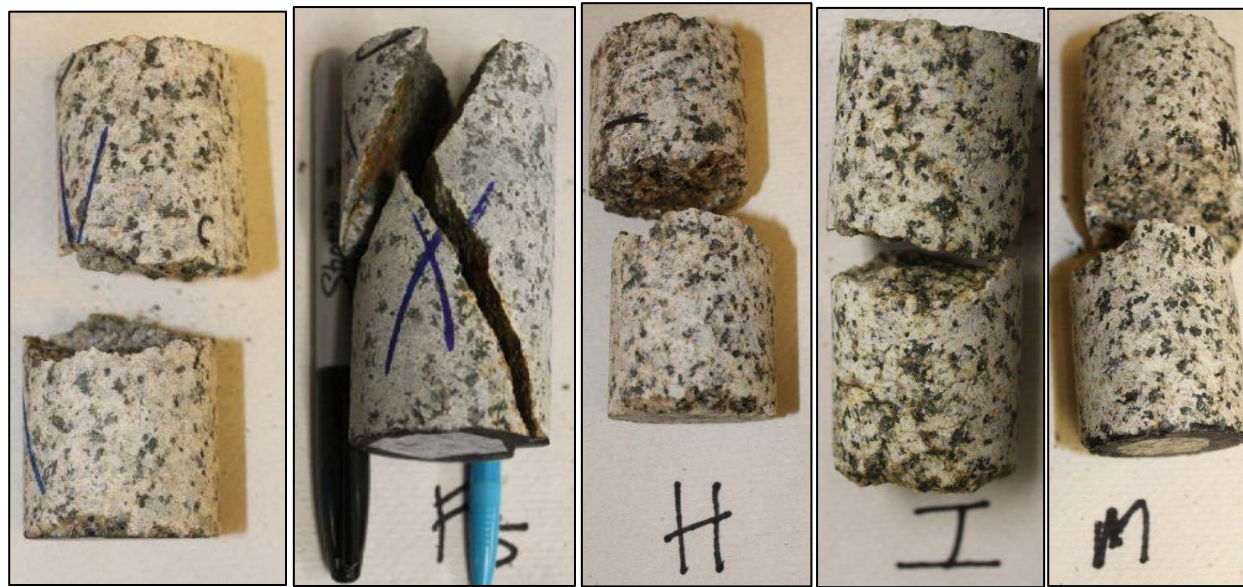


Figure 87: Point load test results.

Appendix H: Supplemental Software Figures

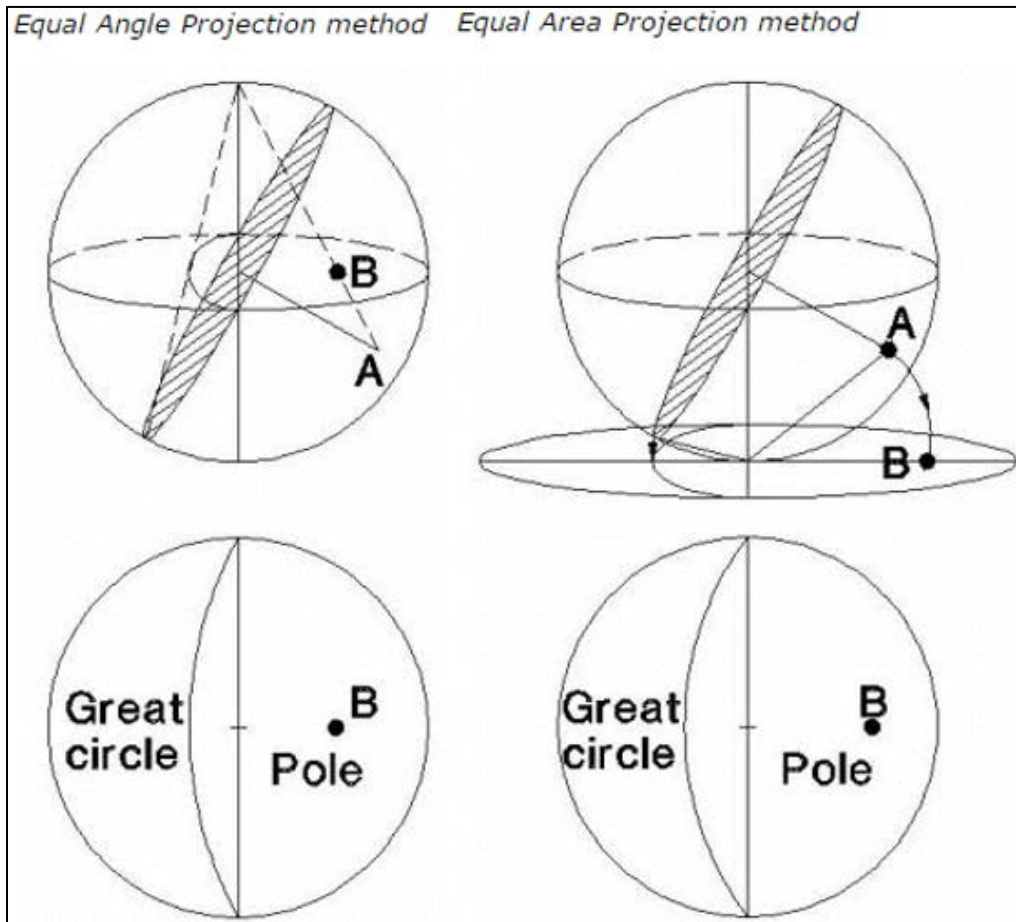


Figure 88: Difference in equal angle and equal area stereonet projection methods (Modified from RocScience, 2017).

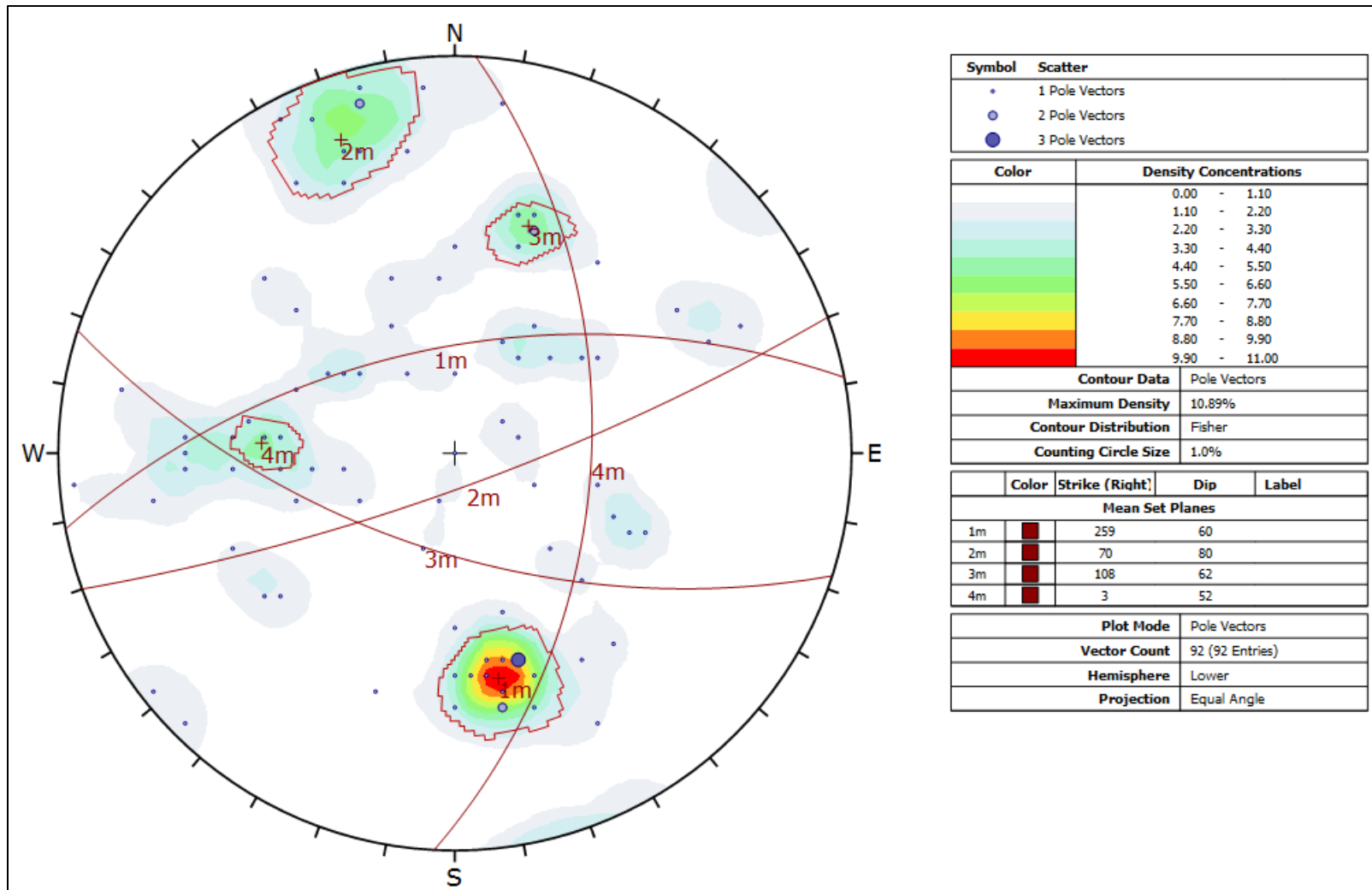


Figure 89: DIPS stereonet projection with density contour and primary joint sets.

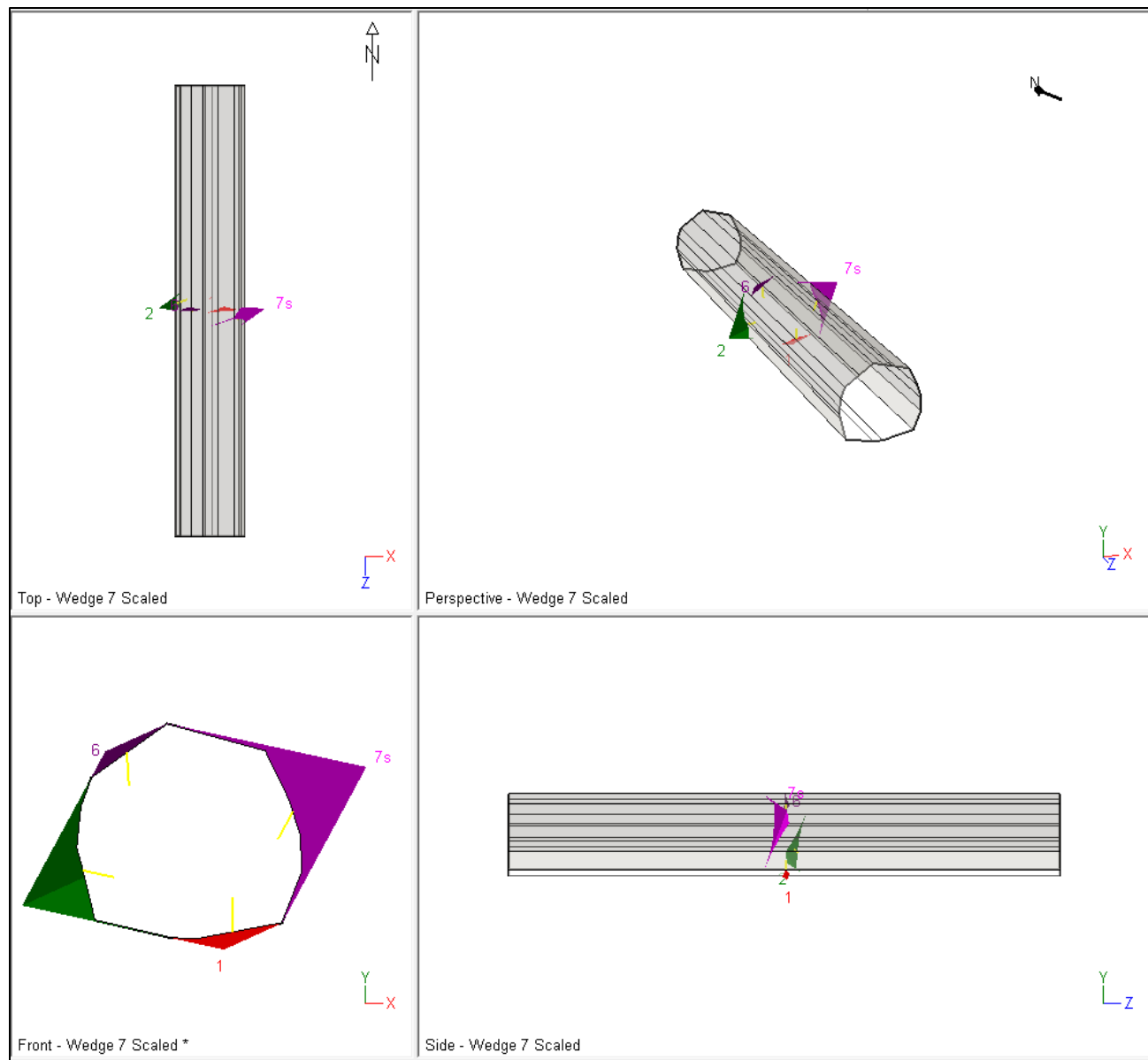


Figure 90: Unwedge model with different views.

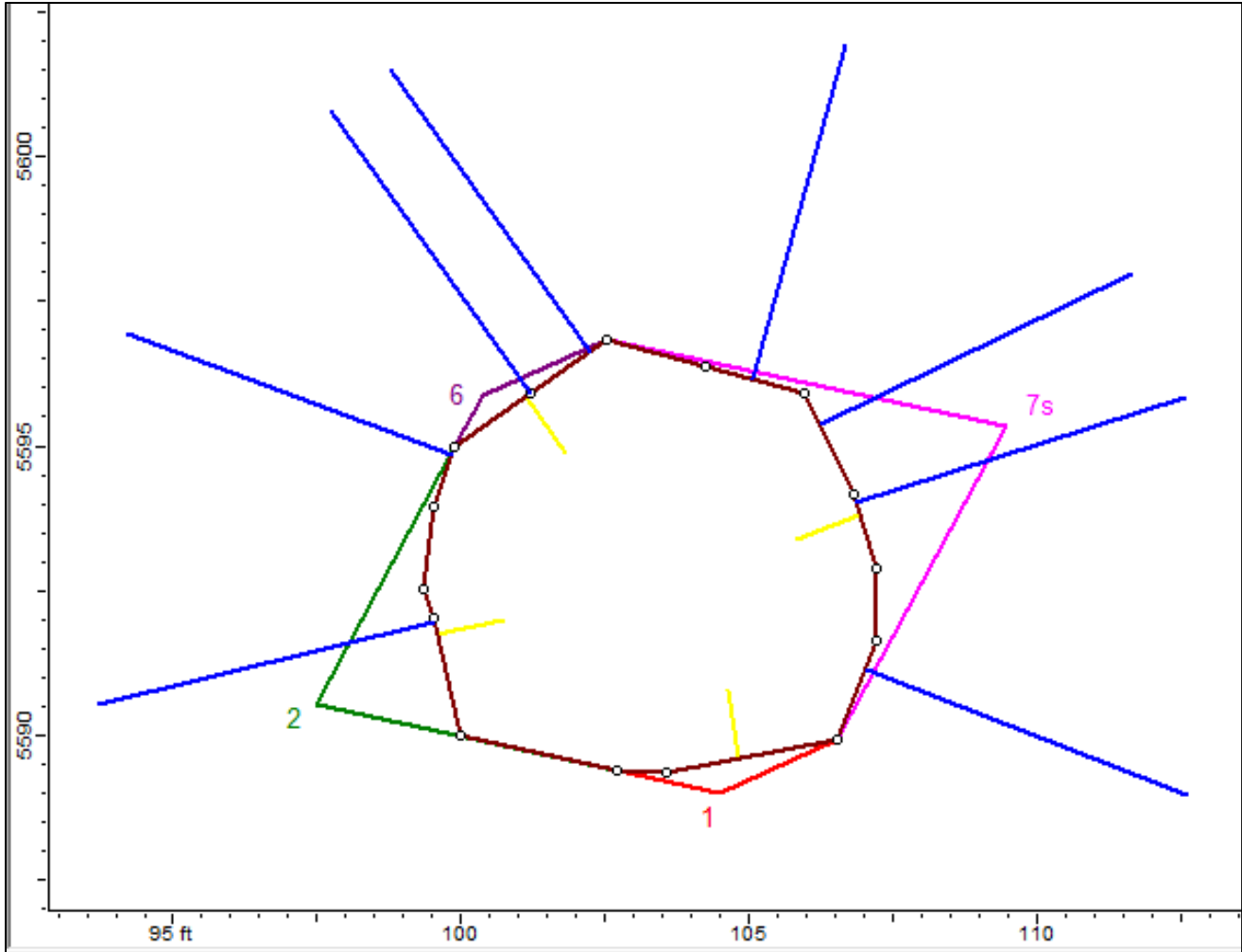


Figure 91: Unwedge model with added bolt support.

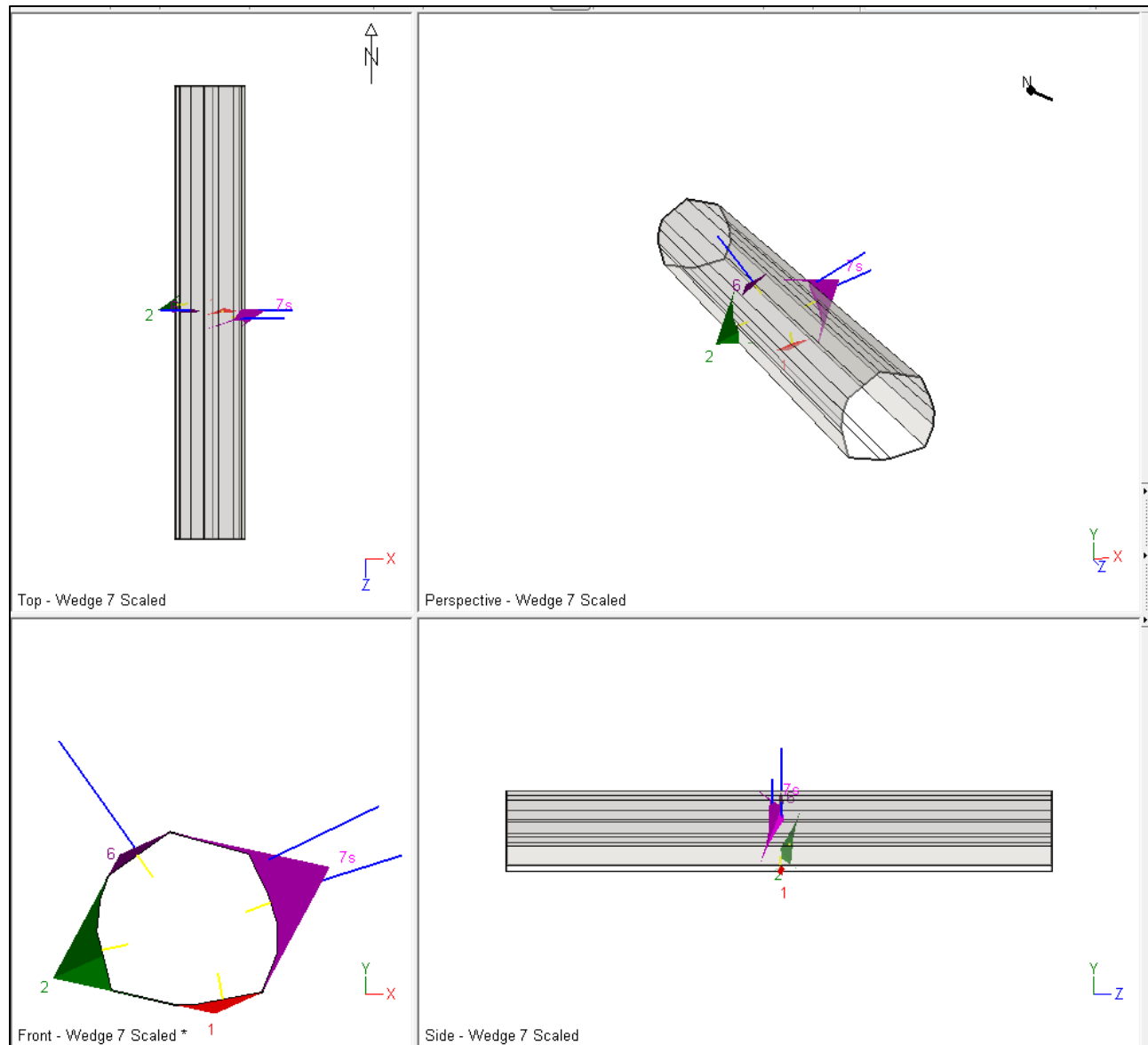


Figure 92: Cross section view of Unwedge model with bolt supports.

Unwedge model 45° tunnel direction:

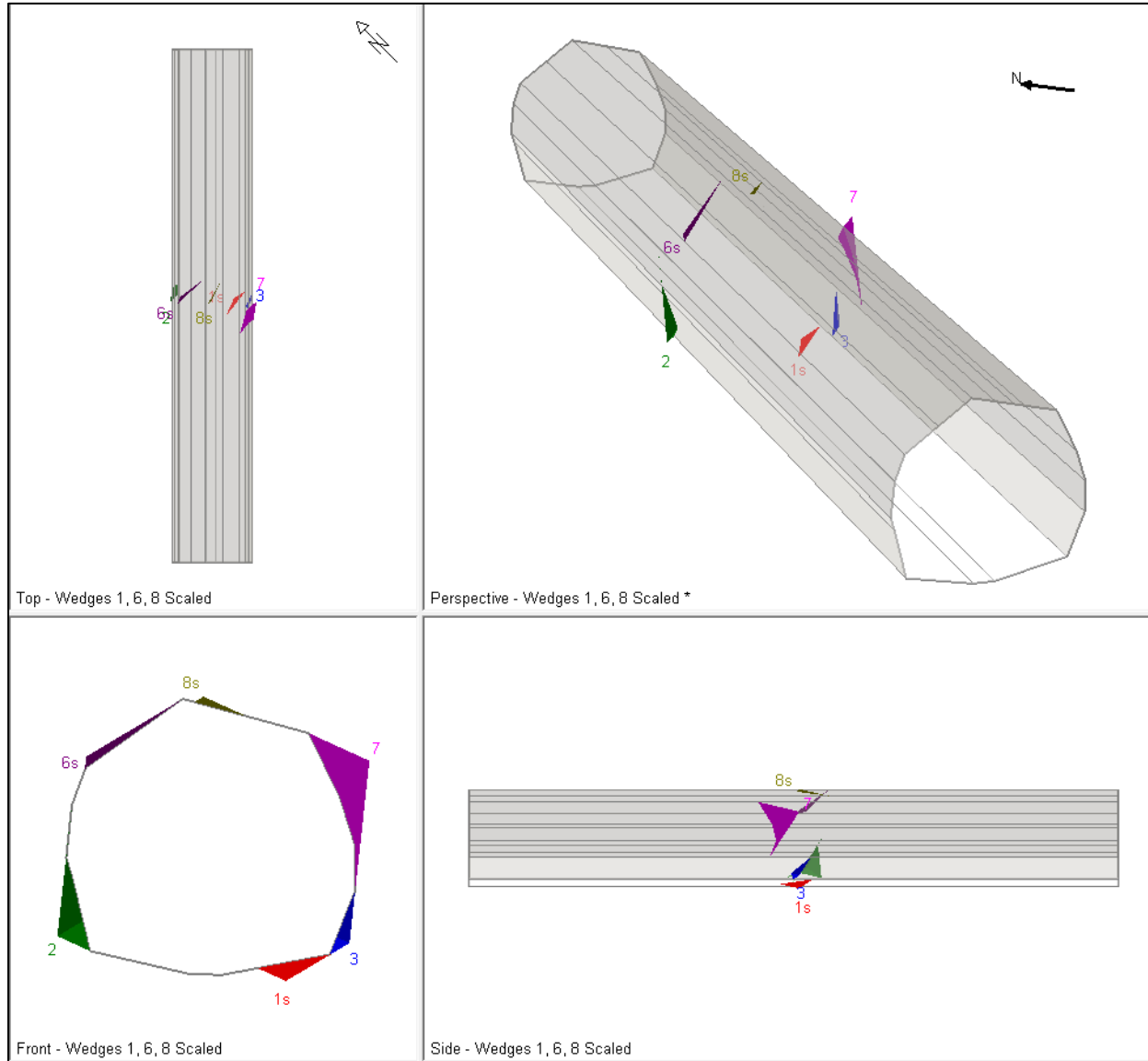


Figure 93: 45° Unwedge model with different views.

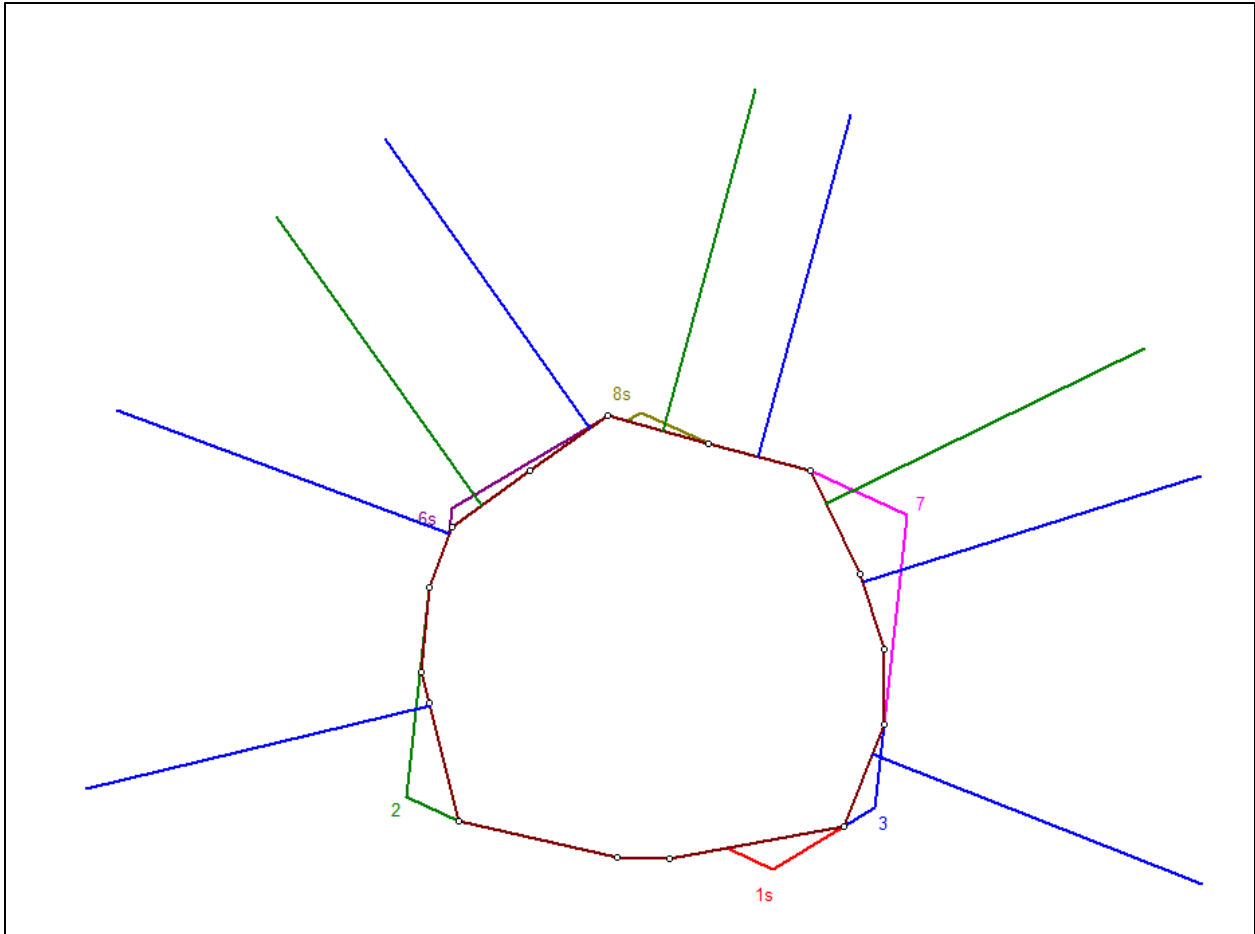


Figure 94: 45° Unwedge model with added bolt support. Bolt pattern indicated in blue, spot bolts indicated in green.

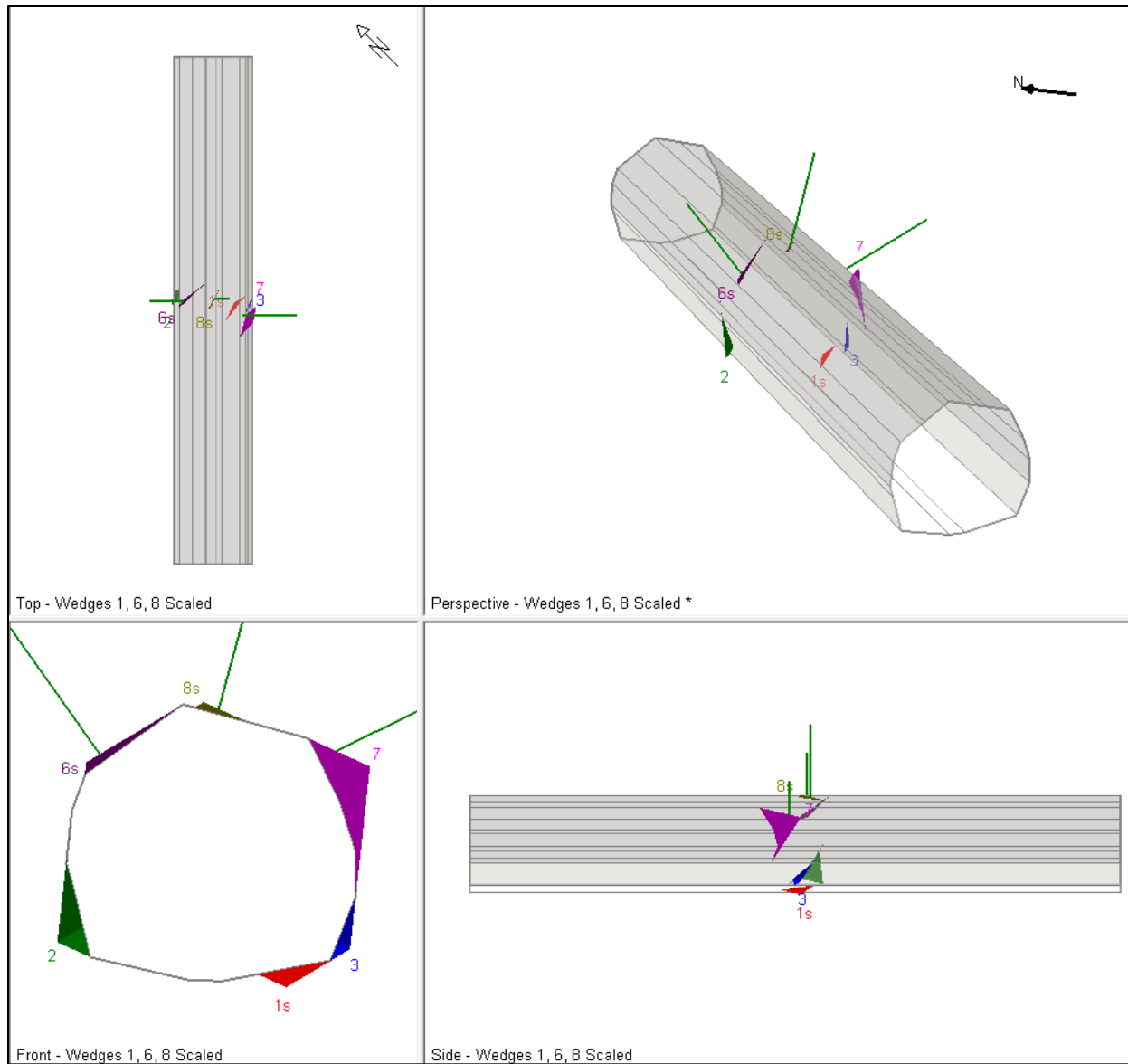


Figure 95: 45° Unwedge model with added bolt support with different views.

Unwedge model 90° tunnel direction:

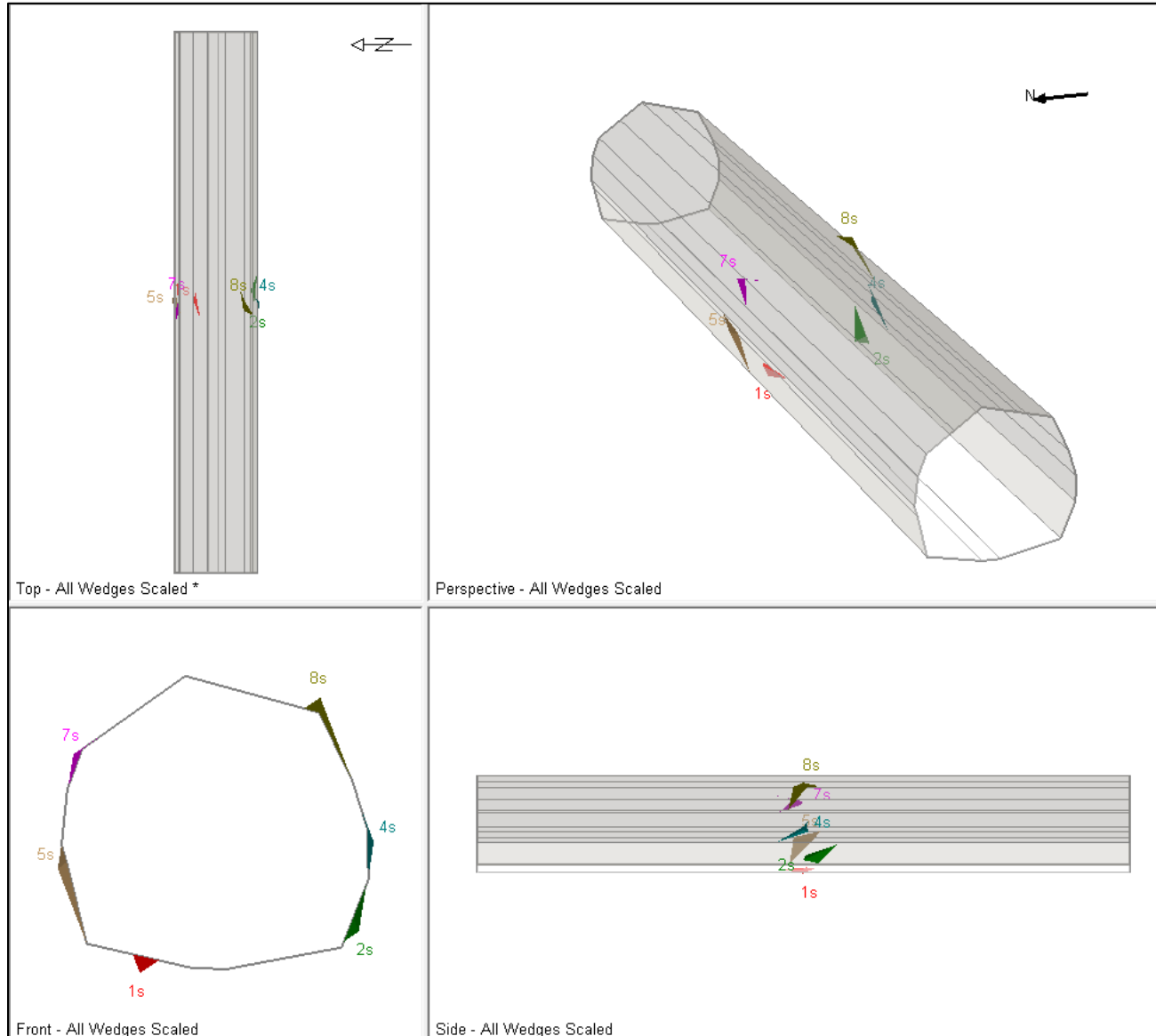


Figure 96: 90° Unwedge model with different views.

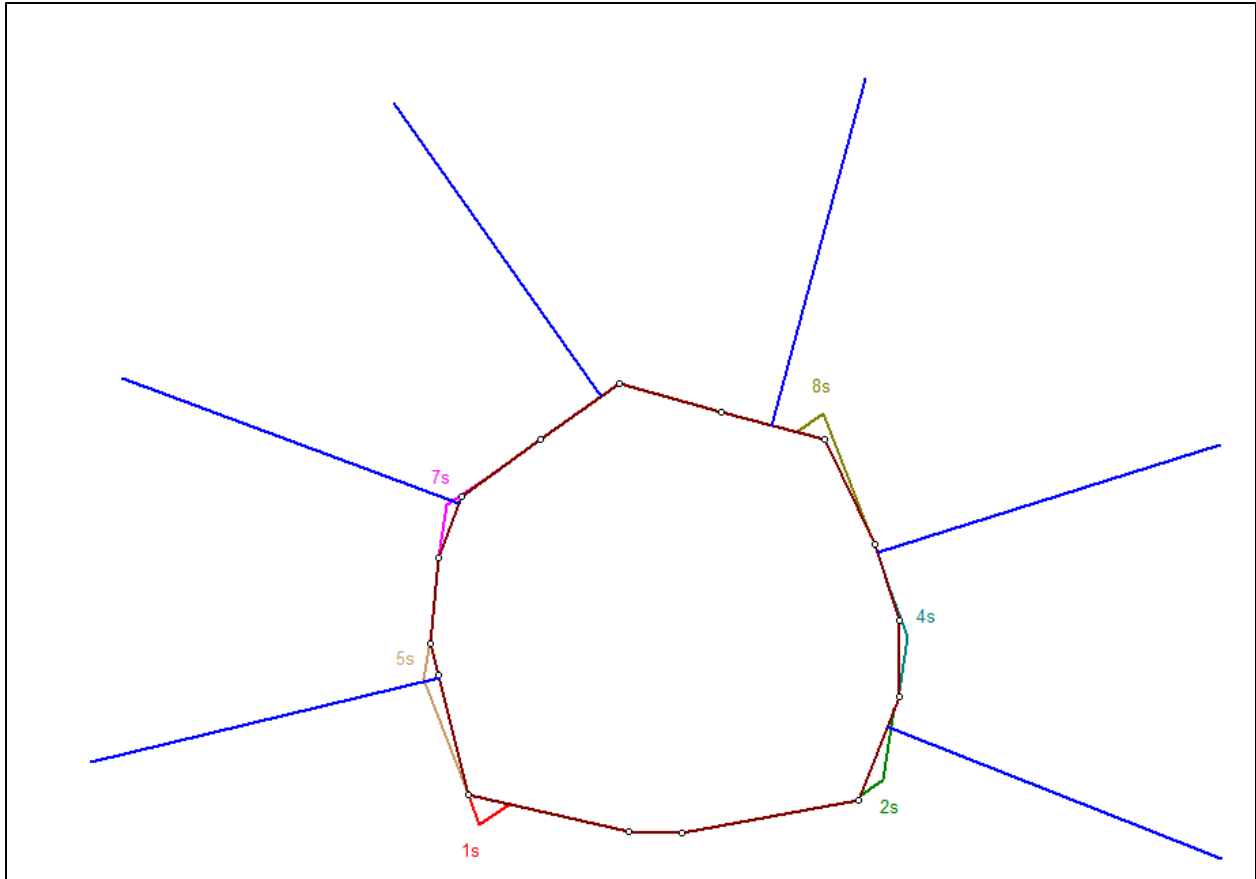


Figure 97: 90° Unwedge model with added bolt support. Bolt pattern indicated in blue, no spot bolts are necessary in this direction.

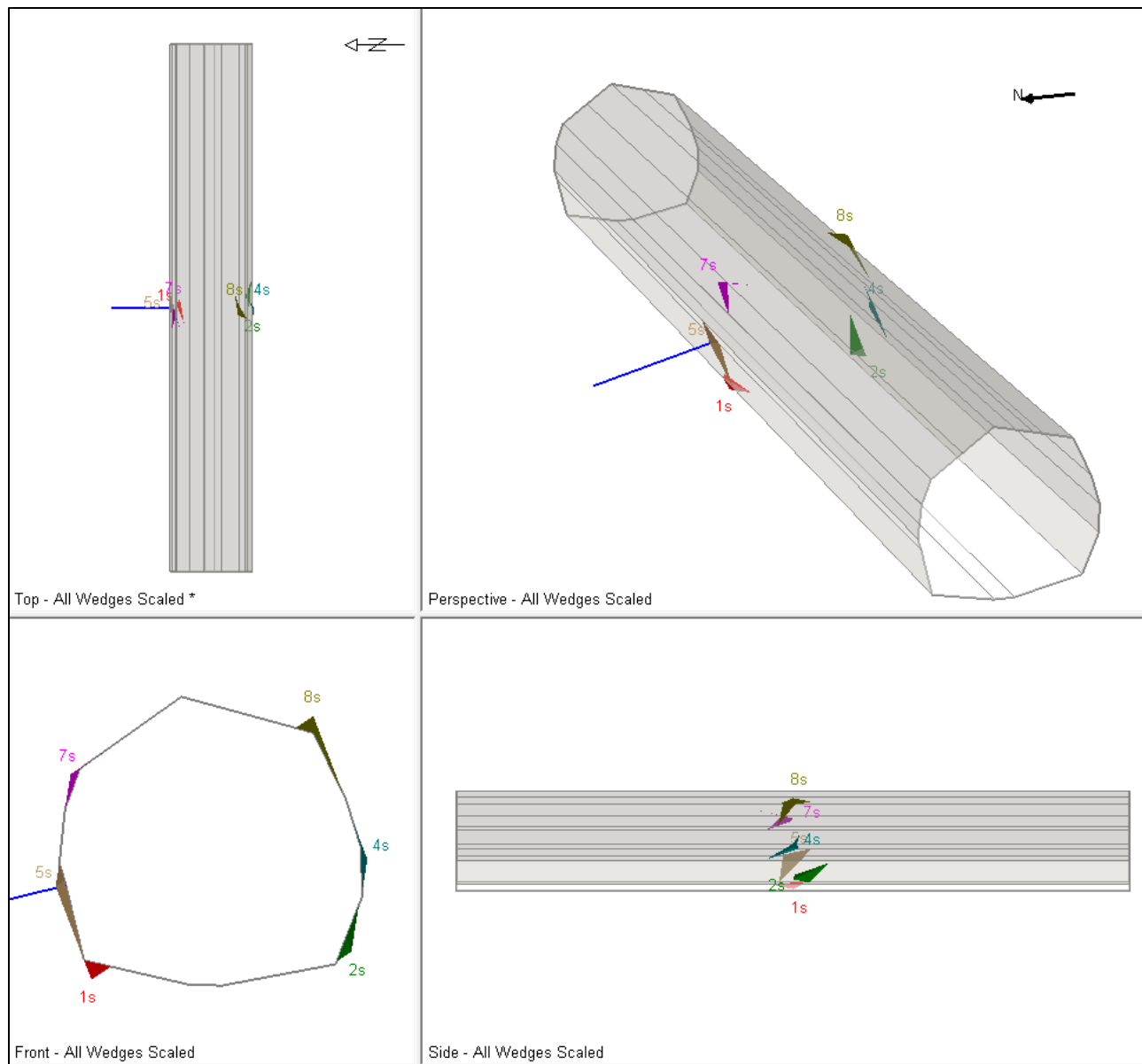


Figure 98: 90° Unwedge model with added bolt support with different views.

Unwedge model 135° tunnel direction:

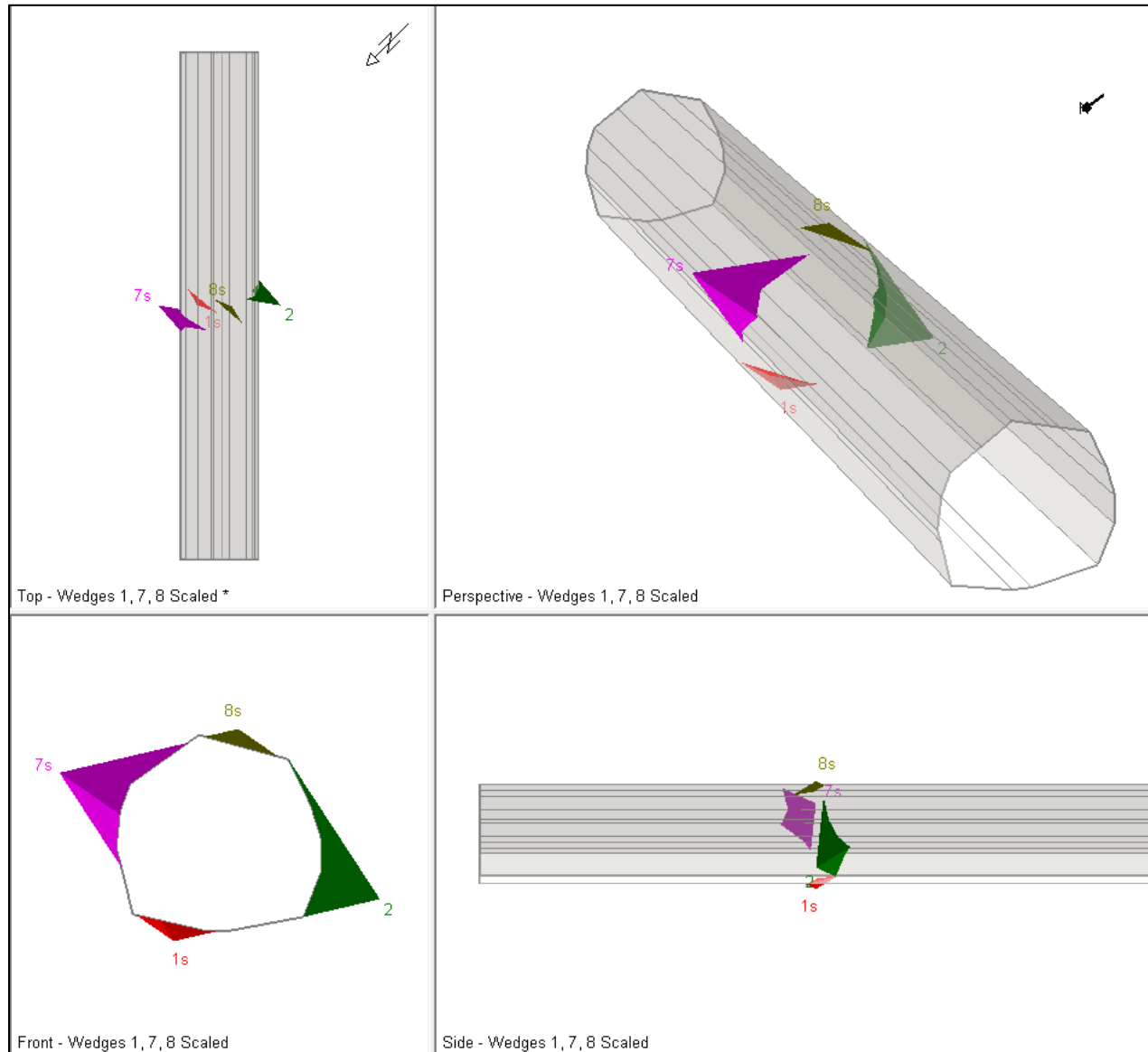


Figure 99: 135° Unwedge model with different views.

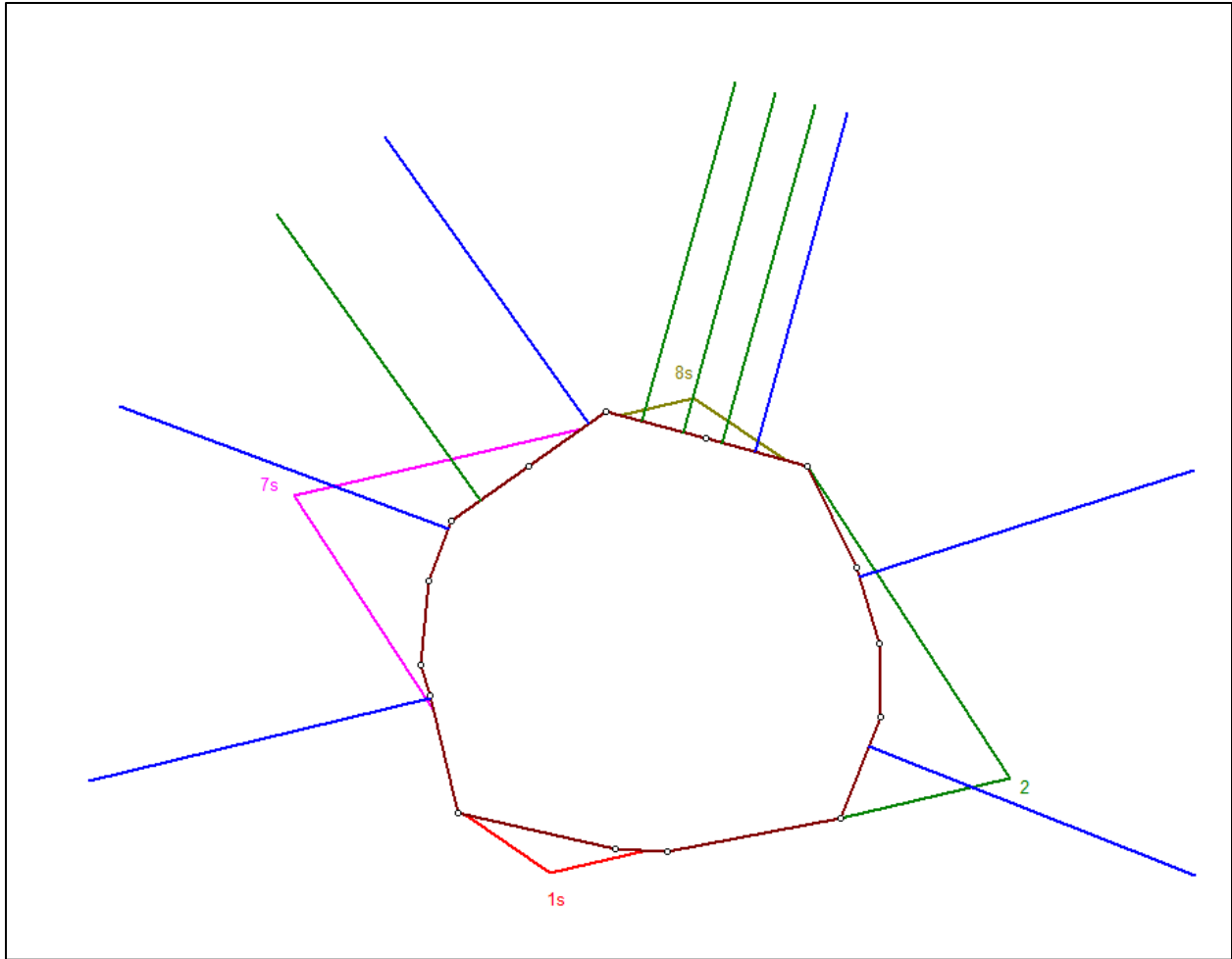


Figure 100: 135° Unwedge model with added bolt support. Bolt pattern indicated in blue, spot bolts indicated in green.

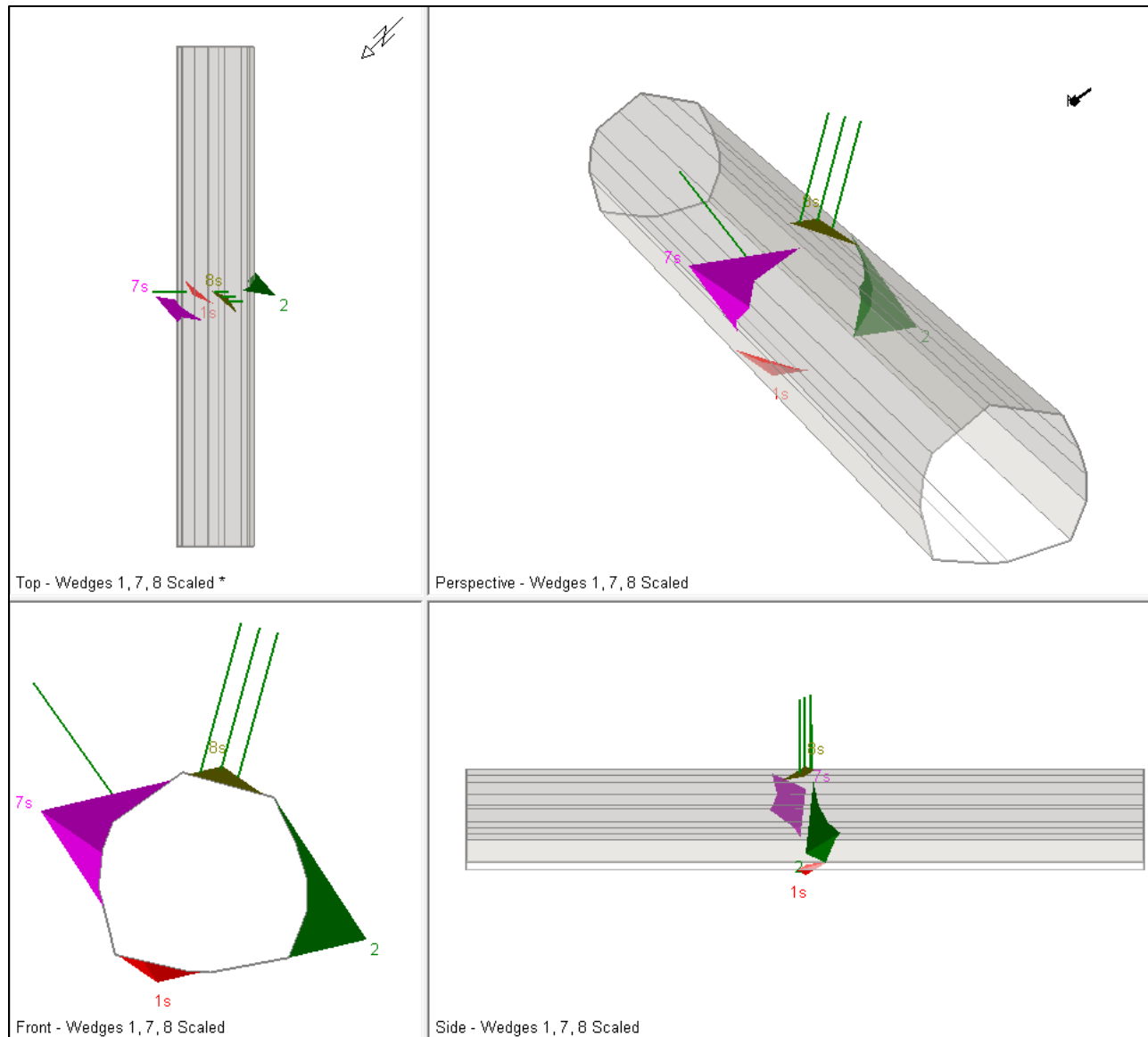


Figure 101: 135° Unwedge model with added bolt support with different views.

Appendix I: Additional Calculations

Palmström's RQD Determination:

$$J_v = \quad (12)$$

$$RQD = 115 - 3.3J_v$$

$$RQD = 115 - 3.3 * \quad (13)$$

$$RQD = \%$$

Priest and Hudson RQD Determination:

$$\lambda = \frac{1}{\text{average joint spacing}} \quad (14)$$

$$\lambda = \frac{1}{2.54}$$

$$\lambda = 0.39$$

$$RQD \approx e^{-0.01\lambda}(0.1\lambda + 1)$$

$$RQD \approx e^{-0.01*0.39}((0.1 * 0.39) + 1) \quad (15)$$

$$RQD \approx 99.92\%$$

Q-System selections for UMEC.

RQD (Rock Quality Designation)

| | |
|--|-----------------|
| Very poor | RQD = 0 - 25% |
| Poor | 25 - 50 |
| Fair | 50 - 75 |
| Good | 75 - 90 |
| Excellent | 90 - 100 |
| Notes: | |
| (i) Where RQD is reported or measured as < 10 (including 0), a nominal value of 10 is used to evaluate Q | |
| (ii) RQD intervals of 5, i.e. 100, 95, 90, etc. are sufficiently accurate | |

Jn (joint set number)

| | |
|---|--------------|
| Massive, no or few joints | Jn = 0.5 - 1 |
| One joint set | 2 |
| One joint set plus random joints | 3 |
| Two joint sets | 4 |
| Two joint sets plus random joints | 6 |
| Three joint sets | 9 |
| Three joint sets plus random joints | 12 |
| Four or more joint sets, heavily jointed, "sugar-cube", etc. | 15 |
| Crushed rock, earthlike | 20 |
| Notes: (i) For tunnel intersections, use (3.0 x Jn); (ii) For portals, use (2.0 x Jn) | |

Jr (joint roughness number)

| | | | |
|---|----------|---|--|
| a) Rock-wall contact, | | c) No rock-wall contact when sheared | |
| b) rock-wall contact before 10 cm shear | | Zone containing clay minerals thick enough to prevent rock-wall contact | |
| Discontinuous joints | Jr = 4 | Sandy, gravelly or crushed zone thick enough to prevent rock-wall contact | |
| Rough or irregular, undulating | 3 | 1.0 | |
| Smooth, undulating | 2 | | |
| Slickensided, undulating | 1.5 | | |
| Rough or irregular, planar | 1.5 | | |
| Smooth, planar | 1.0 | | |
| Slickensided, planar | 0.5 | | |
| Note: i) Descriptions refer to small scale features, and intermediate scale features, in that order | | Notes: | |
| | | i) Add 1.0 if the mean spacing of the relevant joint set is greater than 3 m | |
| | | ii) Jr = 0.5 can be used for planar, slickensided joints having lineations, provided the lineations are oriented for minimum strength | |

Ja (joint alteration number)

| Contact between joint walls | JOINT WALL CHARACTER | | Condition | Wall contact | |
|-------------------------------|-------------------------|--------------------------|---|--|----------------------------------|
| | CLEAN JOINTS | Healed or welded joints: | | filling of quartz, epidote, etc. | Ja = 0.75 |
| Fresh joint walls: | | | no coating or filling, except from staining (rust) | 1 | |
| Slightly altered joint walls: | | | non-softening mineral coatings, clay-free particles, etc. | 2 | |
| COATING OR THIN FILLING | Friction materials: | | sand, silt, calcite, etc. (non-softening) | 3 | |
| | Cohesive materials: | | clay, chlorite, talc, etc. (softening) | 4 | |
| Some or no wall contact | FILLING OF: | | Type | Some wall contact Thin filling (< 5 mm) | No wall contact Thick filling |
| | Friction materials | | sand, silt calcite, etc. (non-softening) | Ja = 4 | Ja = 8 |
| | Hard cohesive materials | | compacted filling of clay, chlorite, talc, etc. | 6 | 5 - 10 |
| | Soft cohesive materials | | medium to low overconsolidated clay, chlorite, talc | 8 | 12 |
| | Swelling clay materials | | filling material exhibits swelling properties | 8 - 12 | 13 - 20 |

Jw (joint water reduction factor)

| | | |
|---|---------------------------|------------|
| Dry excavations or minor inflow, i.e. < 5 l/min locally | $p_w < 1 \text{ kg/cm}^2$ | Jw = 1 |
| Medium inflow or pressure, occasional outwash of joint fillings | 1 - 2.5 | 0.66 |
| Large inflow or high pressure in competent rock with unfilled joints | 2.5 - 10 | 0.5 |
| Large inflow or high pressure, considerable outwash of joint fillings | 2.5 - 10 | 0.3 |
| Exceptionally high inflow or water pressure at blasting, decaying with time | > 10 | 0.2 - 0.1 |
| Exceptionally high inflow or water pressure continuing without noticeable decay | > 10 | 0.1 - 0.05 |
| Note: (i) The last four factors are crude estimates. Increase Jw if drainage measures are installed | | |
| (ii) Special problems caused by ice formation are not considered | | |

SRF (Stress Reduction Factor)

| | | | | |
|---|---|-------------------------------|-----------------------|-----------|
| Weakness zones intersecting excavation | Multiple weakness zones with clay or chemically disintegrated rock, very loose surrounding rock (any depth) | SRF = 10 | | |
| | Single weakness zones containing clay or chemically disintegrated rock (depth of excavation < 50 m) | 5 | | |
| | Single weakness zones containing clay or chemically disintegrated rock (depth of excavation > 50 m) | 2.5 | | |
| | Multiple shear zones in competent rock (clay-free), loose surrounding rock (any depth) | 7.5 | | |
| | Single shear zones in competent rock (clay-free), loose surrounding rock (depth of excavation < 50 m) | 5 | | |
| | Single shear zones in competent rock (clay-free), loose surrounding rock (depth of excavation > 50 m) | 2.5 | | |
| Loose, open joints, heavily jointed or "sugar-cube", etc. (any depth) | | 5 | | |
| Note: (i) Reduce these SRF values by 25 - 50% if the relevant shear zones only influence, but do not intersect the excavation. | | | | |
| Competent rock, rock stress problems | | σ_c / σ_1 | σ_2 / σ_c | SRF |
| | Low stress, near surface, open joints | > 200 | < 0.01 | 2.5 |
| | Medium stress, favourable stress condition | 200 - 10 | 0.01 - 0.3 | 1 |
| | High stress, very tight structure. Usually favourable to stability, may be except for walls | 10 - 5 | 0.3 - 0.4 | 0.5 - 2 |
| | Moderate slabbing after > 1 hour in massive rock | 5 - 3 | 0.5 - 0.65 | 5 - 50 |
| | Slabbing and rock burst after a few minutes in massive rock | 3 - 2 | 0.65 - 1 | 50 - 200 |
| Heavy rock burst (strain burst) and immediate dynamic deformation in massive rock | | < 2 | > 1 | 200 - 400 |
| Notes: (ii) For strongly anisotropic stress field (if measured): when $5 < \sigma_1 / \sigma_3 < 10$, reduce σ_c to $0.75 \sigma_c$. When $\sigma_1 / \sigma_3 > 10$, reduce σ_c to $0.5 \sigma_c$. | | | | |
| (iii) Few case records available where depth of crown below surface is less than span width. Suggest SRF increase from 2.5 to 5 for low stress cases | | | | |
| Squeezing rock | Plastic flow of incompetent rock under the influence of high pressure | Mild squeezing rock pressure | 1 - 5 | 5 - 10 |
| | | Heavy squeezing rock pressure | > 5 | 10 - 20 |
| Swelling rock | Chemical swelling activity depending on presence of water | Mild swelling rock pressure | | 5 - 10 |
| | | Heavy swelling rock pressure | | 10 - 15 |

| Type or use of underground opening | ESR |
|---|-----------|
| Temporary mine openings | 3.5 |
| Vertical shafts, rectangular and circular respectively | 2.0 - 2.5 |
| Water tunnels, permanent mine openings, adits, drifts | 1.6 |
| Storage caverns, road tunnels with little traffic, access tunnels, etc. | 1.3 |
| Power stations, road and railway tunnels with heavy traffic, civil defence shelters, etc. | 1.0 |
| Nuclear power plants, railroad stations, sport arenas, etc. | 0.8 |

For $Q > 10$ use $Q_{wall} = 5Q$

For $0.1 < Q < 10$ use $Q_{wall} = 2.5Q$

For $Q < 0.1$ use $Q_{wall} = Q$

Figure 102: Q-system selections (Modified from Palmström, 2015).

Additional Q-System selections for UMEC.

RQD (Rock Quality Designation)

| | |
|--|---------------|
| Very poor | RQD = 0 - 25% |
| Poor | 25 - 50 |
| Fair | 50 - 75 |
| Good | 75 - 90 |
| Excellent | 90 - 100 |
| Notes: | |
| (i) Where RQD is reported or measured as < 10 (including 0), a nominal value of 10 is used to evaluate Q | |
| (ii) RQD intervals of 5, i.e. 100, 95, 90, etc. are sufficiently accurate | |

Jn (joint set number)

| | |
|---|--------------|
| Massive, no or few joints | Jn = 0.5 - 1 |
| One joint set | 2 |
| One joint set plus random joints | 3 |
| Two joint sets | 4 |
| Two joint sets plus random joints | 6 |
| Three joint sets | 9 |
| Three joint sets plus random joints | 12 |
| Four or more joint sets, heavily jointed, "sugar-cube", etc. | 15 |
| Crushed rock, earthlike | 20 |
| Notes: (i) For tunnel intersections, use (3.0 x Jn); (ii) For portals, use (2.0 x Jn) | |

Jr (joint roughness number)

| | | | |
|---|--------|---|----------|
| a) Rock-wall contact, b) rock-wall contact before 10 cm shear | | c) No rock-wall contact when sheared | |
| Discontinuous joints | Jr = 4 | Zone containing clay minerals thick enough to prevent rock-wall contact | Jr = 1.0 |
| Rough or irregular, undulating | 3 | Sandy, gravelly or crushed zone thick enough to prevent rock-wall contact | 1.0 |
| Smooth, undulating | 2 | Notes: | |
| Slickensided, undulating | 1.5 | i) Add 1.0 if the mean spacing of the relevant joint set is greater than 3 m | |
| Rough or irregular, planar | 1.5 | ii) Jr = 0.5 can be used for planar, slickensided joints having lineations, provided the lineations are oriented for minimum strength | |
| Smooth, planar | 1.0 | | |
| Slickensided, planar | 0.5 | | |
| Note: i) Descriptions refer to small scale features, and intermediate scale features, in that order | | | |

Ja (joint alteration number)

| Contact between joint walls | JOINT WALL CHARACTER | | Condition | Wall contact | |
|-------------------------------|-------------------------|--------------------------|---|--|----------------------------------|
| | CLEAN JOINTS | Healed or welded joints: | | filling of quartz, epidote, etc. | Ja = 0.75 |
| Fresh joint walls: | | | no coating or filling, except from staining (rust) | 1 | |
| Slightly altered joint walls: | | | non-softening mineral coatings, clay-free particles, etc. | 2 | |
| COATING OR THIN FILLING | Friction materials: | | sand, silt, calcite, etc. (non-softening) | 3 | |
| | Cohesive materials: | | clay, chlorite, talc, etc. (softening) | 4 | |
| Some or no wall contact | FILLING OF: | | Type | Some wall contact Thin filling (< 5 mm) | No wall contact Thick filling |
| | Friction materials | | sand, silt calcite, etc. (non-softening) | Ja = 4 | Ja = 8 |
| | Hard cohesive materials | | compacted filling of clay, chlorite, talc, etc. | 6 | 5 - 10 |
| | Soft cohesive materials | | medium to low overconsolidated clay, chlorite, talc | 8 | 12 |
| | Swelling clay materials | | filling material exhibits swelling properties | 8 - 12 | 13 - 20 |

Jw (joint water reduction factor)

| | | |
|---|---------------------------|------------|
| Dry excavations or minor inflow, i.e. < 5 l/min locally | $p_w < 1 \text{ kg/cm}^2$ | Jw = 1 |
| Medium inflow or pressure, occasional outwash of joint fillings | 1 - 2.5 | 0.66 |
| Large inflow or high pressure in competent rock with unfilled joints | 2.5 - 10 | 0.5 |
| Large inflow or high pressure, considerable outwash of joint fillings | 2.5 - 10 | 0.3 |
| Exceptionally high inflow or water pressure at blasting, decaying with time | > 10 | 0.2 - 0.1 |
| Exceptionally high inflow or water pressure continuing without noticeable decay | > 10 | 0.1 - 0.05 |
| Note: (i) The last four factors are crude estimates. Increase Jw if drainage measures are installed | | |
| (ii) Special problems caused by ice formation are not considered | | |

RMR system selections for the UMEC.

| A. CLASSIFICATION PARAMETERS AND THEIR RATINGS | | | | | | | | | |
|---|--------------------------------------|--|---|--|--|--|--|-----------|---------|
| Parameter | | | Range of values | | | | | | |
| 1 | Strength of intact rock material | Point-load strength index | >10 MPa | 4 - 10 MPa | 2 - 4 MPa | 1 - 2 MPa | For this low range - uniaxial compressive test is preferred | | |
| | | Uniaxial comp. strength | >250 MPa | 100 - 250 MPa | 50 - 100 MPa | 25 - 50 MPa | 5 - 25 MPa | 1 - 5 MPa | < 1 MPa |
| | | Rating | 15 | 12 | 7 | 4 | 2 | 1 | 0 |
| 2 | Drill core Quality RQD | | 90% - 100% | 75% - 90% | 50% - 75% | 25% - 50% | < 25% | | |
| | Rating | | 20 | 17 | 13 | 8 | 3 | | |
| 3 | Spacing of | | > 2 m | 0.6 - 2 . m | 200 - 600 mm | 60 - 200 mm | < 60 mm | | |
| | Rating | | 20 | 15 | 10 | 8 | 5 | | |
| 4 | Condition of discontinuities (See E) | | Very rough surfaces Not continuous No separation Unweathered wall rock | Slightly rough surfaces Separation < 1 mm Slightly weathered walls | Slightly rough surfaces Separation < 1 mm Highly weathered walls | Slickensided surfaces or Gouge < 5 mm thick or Separation 1-5 mm Continuous | Soft gouge >5 mm thick or Separation > 5 mm Continuous | | |
| | Rating | | 30 | 25 | 20 | 10 | 0 | | |
| 5 | Groundwater | Inflow per 10 m tunnel length (l/m) | None | < 10 | 10 - 25 | 25 - 125 | > 125 | | |
| | | (Joint water press/ (Major principal σ)) | 0 | < 0.1 | 0.1, - 0.2 | 0.2 - 0.5 | > 0.5 | | |
| | | General conditions | Completely dry | Damp | Wet | Dripping | Flowing | | |
| | Rating | | 15 | 10 | 7 | 4 | 0 | | |
| B. RATING ADJUSTMENT FOR DISCONTINUITY ORIENTATIONS (See F) | | | | | | | | | |
| Strike and dip orientations | | | Very favourable | Favourable | Fair | Unfavourable | Very Unfavourable | | |
| Ratings | Tunnels & mines | | 0 | -2 | -5 | -10 | -12 | | |
| | Foundations | | 0 | -2 | -7 | -15 | -25 | | |
| | Slopes | | 0 | -5 | -25 | -50 | | | |
| C. ROCK MASS CLASSES DETERMINED FROM TOTAL RATINGS | | | | | | | | | |
| Rating | | | 100 ← 81 | 80 ← 61 | 60 ← 41 | 40 ← 21 | < 21 | | |
| Class number | | | I | II | III | IV | V | | |
| Description | | | Very good rock | Good rock | Fair rock | Poor rock | Very poor rock | | |
| D. MEANING OF ROCK CLASSES | | | | | | | | | |
| Class number | | | I | II | III | IV | V | | |
| Average stand-up time | | | 20 yrs for 15 m span | 1 year for 10 m span | 1 week for 5 m span | 10 hrs for 2.5 m span | 30 min for 1 m span | | |
| Cohesion of rock mass (kPa) | | | > 400 | 300 - 400 | 200 - 300 | 100 - 200 | < 100 | | |
| Friction angle of rock mass (deg) | | | > 45 | 35 - 45 | 25 - 35 | 15 - 25 | < 15 | | |
| E. GUIDELINES FOR CLASSIFICATION OF DISCONTINUITY conditions | | | | | | | | | |
| Discontinuity length (persistence) | | | < 1 m | 1 - 3 m | 3 - 10 m | 10 - 20 m | > 20 m | | |
| Rating | | | 6 | 4 | 2 | 1 | 0 | | |
| Separation (aperture) | | | None | < 0.1 mm | 0.1 - 1.0 mm | 1 - 5 mm | > 5 mm | | |
| Rating | | | 6 | 5 | 4 | 1 | 0 | | |
| Roughness | | | Very rough | Rough | Slightly rough | Smooth | Slickensided | | |
| Rating | | | 6 | 5 | 3 | 1 | 0 | | |
| Infilling (gouge) | | | None | Hard filling < 5 mm | Hard filling > 5 mm | Soft filling < 5 mm | Soft filling > 5 mm | | |
| Rating | | | 6 | 4 | 2 | 2 | 0 | | |
| Weathering | | | Unweathered | Slightly weathered | Moderately weathered | Highly weathered | Decomposed | | |
| Ratings | | | 6 | 5 | 3 | 1 | 0 | | |
| F. EFFECT OF DISCONTINUITY STRIKE AND DIP ORIENTATION IN TUNNELLING** | | | | | | | | | |
| Strike perpendicular to tunnel axis | | | | | Strike parallel to tunnel axis | | | | |
| Drive with dip - Dip 45 - 90° | | Drive with dip - Dip 20 - 45° | | | Dip 45 - 90° | | Dip 20 - 45° | | |
| Very favourable | | Favourable | | | Very unfavourable | | Fair | | |
| Drive against dip - Dip 45-90° | | | | | Dip 0-20 - Irrespective of strike° | | | | |
| Fair | | Unfavourable | | | Fair | | | | |

Figure 104: RMR selections (Modified from Bieniawski, 1989).

RSR system selections for the UMEC.

Table 1: Rock Structure Rating: Parameter A: General area geology

| | Basic Rock Type | | | | Geological Structure | | | |
|-------------|-----------------|--------|------|------------|----------------------|-----------|------------|-------------|
| | Hard | Medium | Soft | Decomposed | | | | |
| Igneous | 1 | 2 | 3 | 4 | | Slightly | Moderately | Intensively |
| Metamorphic | 1 | 2 | 3 | 4 | | Folded or | Folded or | Folded or |
| Sedimentary | 2 | 3 | 4 | 4 | Massive | Faulted | Faulted | Faulted |
| Type 1 | | | | | 30 | 22 | 15 | 9 |
| Type 2 | | | | | 27 | 20 | 13 | 8 |
| Type 3 | | | | | 24 | 18 | 12 | 7 |
| Type 4 | | | | | 19 | 15 | 10 | 6 |

Table 2: Rock Structure Rating: Parameter B: Joint pattern, direction of drive

| | Strike \perp to Axis | | | | | Strike \parallel to Axis | | |
|---------------------------------|--------------------------------------|----------|----------|-------------|----------|----------------------------|---------|----------|
| | Direction of Drive | | | | | Direction of Drive | | |
| | Both | With Dip | | Against Dip | | Either direction | | |
| Average joint spacing | Dip of Prominent Joints ^a | | | | | Dip of Prominent Joints | | |
| | Flat | Dipping | Vertical | Dipping | Vertical | Flat | Dipping | Vertical |
| 1. Very closely jointed, < 2 in | 9 | 11 | 13 | 10 | 12 | 9 | 9 | 7 |
| 2. Closely jointed, 2-6 in | 13 | 16 | 19 | 15 | 17 | 14 | 14 | 11 |
| 3. Moderately jointed, 6-12 in | 23 | 24 | 28 | 19 | 22 | 23 | 23 | 19 |
| 4. Moderate to blocky, 1-2 ft | 30 | 32 | 36 | 25 | 28 | 30 | 28 | 24 |
| 5. Blocky to massive, 2-4 ft | 36 | 38 | 40 | 33 | 35 | 36 | 24 | 28 |
| 6. Massive, > 4 ft | 40 | 43 | 45 | 37 | 40 | 40 | 38 | 34 |

Table 3: Rock Structure Rating: Parameter C: Groundwater, joint condition

| | Sum of Parameters A + B | | | | | |
|---|------------------------------|------|------|---------|------|------|
| | 13 - 44 | | | 45 - 75 | | |
| Anticipated water inflow gpm/1000 ft of tunnel | Joint Condition ^b | | | | | |
| | Good | Fair | Poor | Good | Fair | Poor |
| None | 22 | 18 | 12 | 25 | 22 | 18 |
| Slight, < 200 gpm | 19 | 15 | 9 | 23 | 19 | 14 |
| Moderate, 200-1000 gpm | 15 | 22 | 7 | 21 | 16 | 12 |
| Heavy, > 1000 gp | 10 | 8 | 6 | 18 | 14 | 10 |

Figure 105: RSR selections (Modified from Hoek, 2007).

Cumulative interpretation table:

Table XXVIII: Interpretation summary

| Interpretation Method | Value | Recommendation |
|------------------------------|--------------|--|
| RMR | 77 | Spot bolting when necessary; 8-foot spacing with wire mesh. |
| Q | 5.60 | 6-foot bolt spacing with wire mesh; spot bolting when necessary. |
| Q _{wall} | 14.0 | 7-foot bolt spacing with wire mesh; spot bolting when necessary. |
| RSR | 61 | 5-foot bolt spacing with wire mesh; spot bolting when necessary. |

Appendix J: Ground Control Management Plan

Developed as a separate document with the intention that the separate document stay “live.” Document located in:

\\mtsmemg\Mining\02. Department Info\05.Research\2016_Rose_UMEC_GCMP\drafts\GCMP drafts

The first GCMP (completed March 2017), is included in this appendix.

Montana Tech Underground Mine Education Center (UMIEC)

Ground Control Management Plan (GCMP)

Updated (March 2017)

TABLE OF CONTENTS

| | | |
|------------|--|-----------|
| 1.0 | INTRODUCTION | 2 |
| 1.1 | COMMUNICATION OF GROUND CONTROL STRATEGIES | 2 |
| 1.1.1 | <i>Consideration of a Systematic Approach.....</i> | <i>2</i> |
| 1.2 | REVIEW PROCESSES | 2 |
| 1.3 | PROCESSES AND PROCEDURES FOR DEVELOPMENT | 3 |
| 2.0 | REQUIREMENTS FOR GROUND CONTROL MANAGEMENT PLAN..... | 3 |
| 3.0 | GROUND CONTROL MANAGEMENT PLAN DEVELOPMENT | 3 |
| 3.1 | APPLICATION AND STANDARDS | 4 |
| 4.0 | GEOLOGY AND GEOTECHNICAL CONSIDERATIONS IN FIELD AND LABORATORY ANALYSES..... | 4 |
| 4.1 | MINE GEOLOGY..... | 4 |
| 4.2 | GEOTECHNICAL CONSIDERATIONS | 5 |
| 4.2.1 | <i>Stress Conditions.....</i> | <i>5</i> |
| 4.3 | DATA COLLECTION | 5 |
| 4.3.1 | <i>Weathering Grade Mapping.....</i> | <i>5</i> |
| 4.3.2 | <i>Scanline Survey (SLS).....</i> | <i>6</i> |
| 4.4 | UMEC ANALYSIS METHODS | 6 |
| 4.5 | ROCK MASS CLASSIFICATION FOR ROCK SUPPORT AND REINFORCEMENT | 7 |
| 4.5.1 | <i>Tunneling Quality Index (Q).....</i> | <i>7</i> |
| 5.0 | GROUND CONTROL PROGRAM | 8 |
| 5.1 | GROUND SUPPORT MATERIAL DEFINITIONS..... | 8 |
| 5.2 | SPECIALIZED GROUND SUPPORT RECOMMENDATIONS..... | 9 |
| 5.3 | STANDARD OPERATING PROCEDURE FOR GROUND SUPPORT IN UMEC DRIFTS | 9 |
| 5.4 | STANDARD OPERATING PROCEDURE FOR BOLTING | 10 |
| 5.5 | INSTALLATION GUIDELINES | 10 |
| 5.6 | REMINDERS..... | 10 |
| 6.0 | FUTURE RECOMMENDATIONS | 11 |
| 7.0 | REFERENCES..... | 12 |

1.0 Introduction

The Ground Control Management Plan (GCMP) outlines systems developed to manage ground conditions present in the rock mass for underground mining activities at the Underground Mine Education Center (UMEC) on the Montana Tech Campus. This document addresses the primary goals of ground control management by focusing on the strategies for collection and utilization of important geotechnical information. This will be accomplished by:

- Providing geotechnical resources,
- Developing and implementing a GCMP to use at the UMEC, and
- Developing a ground awareness program to familiarize students with geotechnical hazards that exist underground at the UMEC and World Museum of Mining facilities.

An effective ground control management strategy is aimed at quantifying and reducing geotechnical risk in the UMEC while adhering to governing agency regulations¹ and ground support design. The ground control techniques described in this GCMP focus on a proactive and tactical approach by identifying ground control methods that effectively manage excavations without additional degradation or additional re-working of the excavation. The tactical approach described in this GCMP rely on the modification of ground support methods to maintain stability rather than changing the mining method used in the UMEC.

This GCMP has been created to make users of the UMEC facility aware of potentially hazardous ground conditions and ensure that ground control methods are properly implemented by students operating in the UMEC facility. Users of the facility include mining engineering and geological engineering department faculty, students (with special focus on students enrolled in the Practical Underground Mining course taught by the mining department).

1.1 Communication of Ground Control Strategies

Site-specific ground control awareness will be incorporated into the general underground induction for new people unfamiliar with underground operations at the UMEC. The information will be designed to give individuals the understanding of potential hazards presented by UMEC granite and how to identify potential hazards. Risk and risk mitigation is an integral part of the ground control strategy and should be considered during throughout mining operations and the implementation of the GCMP. The GCMP should be easily audible² and easy to understand, given the turn-over rate of students enrolled in the Practical Underground Mining Class.

1.1.1 Consideration of a Systematic Approach

This GCMP presents a systematic approach that allows the user to understand the important aspects of ground control for the UMEC. Factual information is clearly separated from inferred analytical decisions. A logical workflow from data collection, analysis, and design is presented in the subsequent sections.

1.2 Review Processes

The GCMP should be reviewed at a suitable interval based on the UMEC's hazards and risks. It is recommended that the GCMP is updated every other year unless significant

¹ While the UMEC is not covered under MSHA, it is important for students to be aware of the regulations and operate under the assumptions that the UMEC is an MSHA regulated facility.

² Easily audible forms of distribution would include a PowerPoint presentation given at the beginning of the Practical Underground Mining course.

circumstances require immediate changes to the document. Significant circumstances include changes in ground conditions and developments in ground control technology. The review process ensures that the GCMP contains relevant, up-to-date information that can be distributed to faculty of the Mining Engineering and Geological Engineering departments.

A competent person or persons should review the GCMP. A competent person is defined as any faculty member or student with experience in ground control or a student who is interested in gaining experience in the field of ground control.

1.3 Processes and Procedures for Development

Ground control management strategy is enacted by Ground Control Management Procedures outlined in Table 1.

Table 1. Ground control management procedure activities.

| Ground Control Management Procedure Activities | Summary of Activity |
|---|--|
| 1. Geotechnical Data Collection | Collection of relevant geological and geotechnical data for granitic characterization. This includes weathering grade mapping and a scanline survey (SLS) to obtain strike and dip measurements for new excavations in the UMEC. |
| 2. Modeling, Analysis and Design | Use of geotechnical engineering principles to design excavations that are fit for their intended use. Modeling includes the use of RocScience Unwedge and updating the Maptek Vulcan geotechnical database. |
| 3. Excavation Monitoring | Ensuring excavations are mined to appropriate dimensions and properly supported. |
| 4. Remediation | Determination of appropriate, effective techniques for post-failure treatment to regain control of excavations as necessary including rehabilitation of failed or old mining areas and ground support. |
| 5. Producing the GCMP | Incorporating the previous steps into an understandable document that can be used as a guide for student users of the UMEC. |

2.0 Requirements for Ground Control Management Plan

The UMEC should provide sufficient resources in order to maintain the subsequent ground control strategies. Equipment used for ground control will be inspected prior to use and must be appropriate for the intended use. Personnel performing ground control tasks must be aware of the ground control hazards and be deemed a competent person prior to ground control installation. It is the responsibility of the Montana Tech Mining Engineering and Geological Engineering Department faculty to assess the capabilities of personnel entering the UMEC in order to determine if s/he is deemed a competent person. Collection of data is the basis for building a usable GCMP. Adequate time should be spent in the data collection phase in order to develop a quality GCMP.

3.0 Ground Control Management Plan Development

Structural and material properties, rock geometry, excavation geometry, and mining strategy play a role in outlining the requirements for ground reinforcement techniques. Ground improvement is a specific technique that includes methods for instillation of rock bolts, surface support (such a shotcrete or wire mesh), and grout injection processes. The primary objective is to improve the rock mass characteristics in the UMEC.

The UMEC shall conduct risk assessments to support the development of the GCMP and all related activities. Risk assessments will include but are not limited to the following considerations:

- Geotechnical assessment and monitoring,
- Ground stability, surface subsidence and potential fluid in-rush (i.e. air, mud, and bodies of water),
- Material and ground control equipment selection criteria,
- Significant changes in operating plans or ground conditions, and
- Ground condition monitoring methods focusing on earliest possible detection.

Support and reinforcement are essential components for excavation safety and stability. The UMEC and World Museum of Mining facilities are unique because the facilities are also designed with longevity in mind; therefore, ground control techniques must consider the longevity and the safety of the facilities. Ground control aspects that should be considered in the development and implementation of the GCMP are:

- Visual inspections of headings ,
- Installing ground support and reinforcement where necessary,
- Survey mark-up, and geotechnical mapping, and
- Blast hole drilling and blasting activities.

3.1 Application and Standards

The areas covered in this GCMP apply to all active underground working areas operated by Montana Tech and the World Museum of Mining facilities. Although the UMEC and the World Museum of Mining facilities are non-operational mines and are not covered under the regulations outlined by the Mine Safety and Health Administration (MSHA) it is important to state that guidelines provided in the Code of Federal Regulations CFR 30 – Part 57 Metal and Non Metal Underground Mines: 57.3200 – 3203 and 57.3360 are applicable to these facilities. Additionally, rock bolts and their accessories used for ground control management conform to the American Standards for Testing Materials (ASTM) standard ASTM F432-13.

4.0 Geology and Geotechnical Considerations in Field and Laboratory Analyses

4.1 Mine Geology

The primary geologic unit at the UMEC is the Butte Quartz Monzonite (BQM), a granitic body consisting of plagioclase, orthoclase, quartz, biotite, hornblende, magnetite, ilmenite, and apatite (Rose, 2017). The BQM hosts aplite and quartz-porphyry dikes that are responsible for much of the copper mineralization of the Butte District. The UMEC and World Museum of Mining facilities are located slightly northwest of a rhyolitic dike that intruded the BQM in the Butte District. This rhyolitic complex contained veins of rhodochrosite, galena, and small amounts of silver. A full geologic description is available in Section 2.0: Geologic Setting by Rose (2017).

The granite at the UMEC is subdivided by weathering grade. Based on current mapping results, three distinct weathering grades are present in the UMEC: Grade I, Grade II, and Grade III. Grade I granite is classified as fresh rock and possesses an average Unconfined Compressive Strength (UCS) of 5,730 pounds per square inch (psi). Grade II is classified as slightly weathered granite and possesses an average UCS of 3,690 psi. Grade III is classified as moderately weathered granite and possesses an average UCS of 2,740 psi. Weathering

grade mapping indicates that the most prominent weathering grade present in the UMEC is Grade II (Rose, 2017).

4.2 Geotechnical Considerations

Alteration processes that can affect granite strength in the UMEC are hydrothermal alteration, metamorphic alteration due to the intrusive rhyolitic dike, and clay alteration due to shearing of the granitic material.

Geotechnical analysis conducted by (Rose, 2017) indicates that there are four distinct joint sets responsible for wedge formation in the UMEC (Table 2).

Table 2. Average strike and dip measurements from SLS conducted by Rose (2017).

| Joint Set | Strike | Dip (°) |
|-----------|--------|---------|
| 1 | 259 | 60 |
| 2 | 070 | 80 |
| 3 | 108 | 62 |
| 4 | 003 | 52 |

4.2.1 Stress Conditions

Due to the weak and highly structured ground, general in situ stress conditions are assumed. Since the UMEC is approximately 100 feet below the surface, the approximate vertical stress 106 psi and horizontal stress is approximately 30 psi.

4.3 Data Collection

Assigned students will collect the rock mass data pertinent to maintain an updated GCMP. Field data collection for the GCMP will consist of weathering grade mapping, SLS conducted in new excavations, and sample collection for laboratory analysis. If it became feasible to conduct core drilling at the UMEC, core samples should be gathered from areas that best represent Grade I, Grade II, and Grade III granite in the ribs of an excavation.

4.3.1 Weathering Grade Mapping

Weathering grade mapping will be conducted based on the weathering grade profile outlined by the International Society of Rock Mechanics (ISRM) (Barton, 1978). The simplified version of the profile is shown in Table 3.

Table 3. ISRM classification system (Modified from Barton, 1978).

| Zone | Term | Description |
|------|----------------------|---|
| I | Fresh | Fully intact; no fractures present. |
| II | Slightly Weathered | Discolored and stained; weathered micas are present; small fractures are present. |
| III | Moderately Weathered | More rock than soil; Potassium feldspar and plagioclase feldspar crystals have begun to weather. Material must still be broken with tools, cannot break with hand. |
| IV | Highly Weathered | Essentially soil; potassium feldspar and plagioclase feldspar crystals are decomposed. Material is highly fissured but will not disintegrate in water. |
| V | Completely Weathered | Similar to saprolite. Completely weathered into soil with relict rock structure intact because material has not been disturbed. Can break without the use of tools. Will disintegrate in water. |
| VI | Residual Soil | Original crystal structure is not present. Disintegrated into soil with no relict rock structure present. |

4.3.1.1 Mapping Guidelines

Recognized ground control concerns should be addressed immediately if noticed during field data collection. Record features of the rock mass that may influence the stability of an excavation. Factors that could influence the stability of a new excavation include:

- Intact strength of the rock (weathering grade, fracture/fissure zone, alteration),

- Orientation, spacing, persistence, roughness, aperture, infill, and shearing surface of the joints, and
- Effects of water.

4.3.2 Scanline Survey (SLS)

A SLS will be conducted along the ribs of new excavations. Each joint surface along the measuring tape used for the SLS will be documented. The distance from the closest survey point to the beginning of the SLS will be documented in order to properly georeference the joint surfaces in the Maptek Vulcan database after field data collection is complete.

4.4 UMEC Analysis Methods

Structural modeling for the UMEC should be conducted using the RocScience DIPS program. Stress modeling should be conducted using the RocScience Unwedge program. Previous models for the UMEC can be found in the following directory:

\\mtsmemg\Mining\02. Department Info\05. Research\2016_Rose_UMEC_GCMP\Modeling

The rock mass has been characterized as blocky, with low stresses; therefore, structural driven wedge failures are the likely issues mitigated by supports. At the time of this GCMP (March 2017), Unwedge analyses indicate that there is one stable wedge that can be stabilized using a 3-foot horizontal, 3-foot vertical spacing (Figure 1).

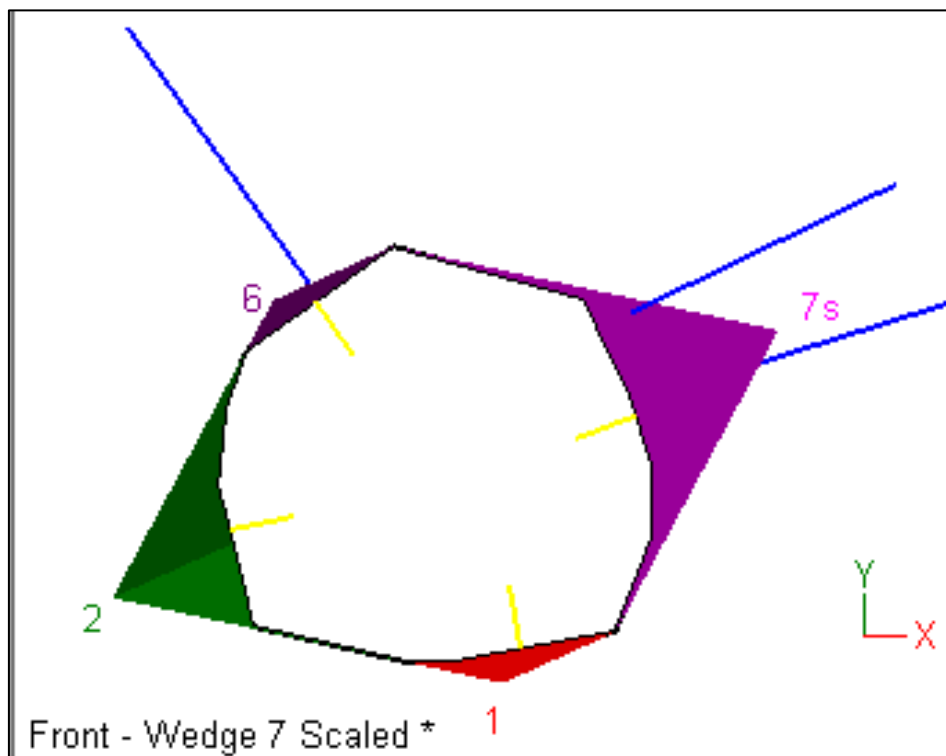


Figure 1. Unwedge model at tunnel orientation 0°.

It is important to note that Unwedge models should be conducted at tunnel orientations of 0°, 45°, 90°, and 135° to ensure that a representative sample of potential wedge failures are obtained. Orientation should always be evaluated to identify the best working orientation for the UMEC. At the time of this GCMP (March 2017) the recommended orientation for future excavations is 90°.

4.5 Rock Mass Classification for Rock Support and Reinforcement

The granitic rock mass at the UMEC is structurally controlled due to the distinct joint surfaces that exist within the body. These features play a role in the mechanical behavior of excavations developed in the material. Localized behavior (such as wedge size) is based on the orientation of the joint surfaces relative to the orientation of the excavation. Rock mass characterization determines the rock mass behavior at the UMEC. Rock mass classifications used for the UMEC include the Rock Quality Designation (RQD), Tunneling Quality Index (Q), and the Rock Mass Rating (RMR).

4.5.1 Tunneling Quality Index (Q)

The Q system, developed by Barton (1974) was developed as a system to qualify a rock mass based on a numerical assessment of the rock quality using six different parameters:

- Rock Quality Designation (RQD)
- Joint Set Number (J_n)
- Joint Roughness Number (J_r)
- Joint Alteration Number (J_a)
- Joint Water Reduction Factor (J_w)
- Stress Reduction Factor (SRF)

The Q index is obtained from the relationship:

$$Q = \left(\frac{RQD}{J_n} \right) * \left(\frac{J_r}{J_a} \right) * \left(\frac{J_w}{SRF} \right) \quad (3)$$

At the time of this report (March 2017), the Q for the UMEC ranges from 5.6 to 8.5. Since this value falls within the range of $0.1 < Q < 10$, the Q_{wall} for the UMEC is equal to $2.5Q$, according to Hoek (2007). Figure 2 shows the Q system chart for the UMEC. The Q falls within Zone 1: Bolt spacing outside areas with shotcrete, requiring a 1.5 meter (5 feet) to 2.0 meter (7 feet) bolt spacing. Q_{wall} falls within Zone 1, requiring a bolt spacing of approximately 2.25 meters (7.5 feet). The Q system classification chart is available in the following directory:

\\mtsmemg\Mining\02. Department Info\05. Research\2016_Rose_UMEC_GCMP\Modeling

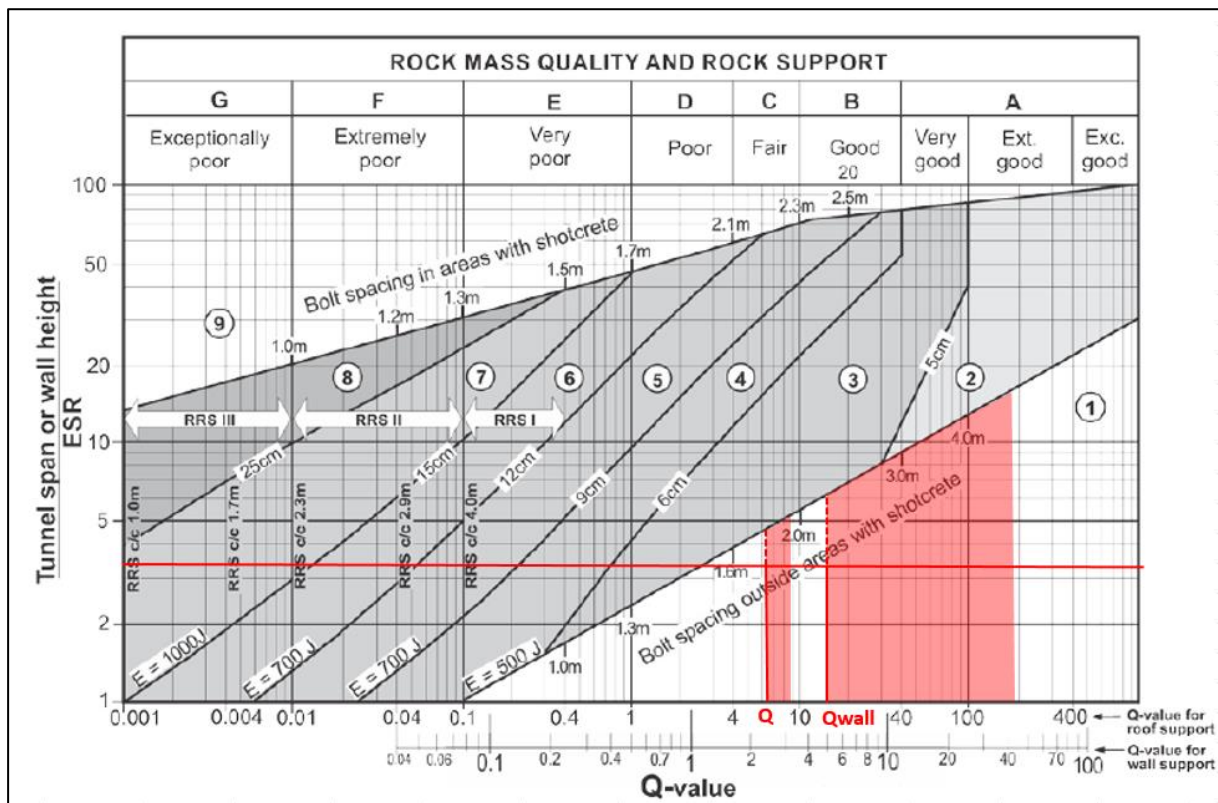


Figure 2. Q system chart for UMEC (Modified from Hoek, 2007).

5.0 GROUND CONTROL PROGRAM

Ground support design, ground conditions, ground behavior, ground support standards, operating practices, the Geotechnical database and the GCMP should be updated every other year to keep information up-to-date. Different types of ground support and reinforcement have different load-deformation characteristics. Soft ground support, such as wire mesh and rock bolts, will allow more deformation around the excavation rather than a hard ground support option. Jointed material, like the UMEC granite, generally requires more roof-surface maintenance and support to prevent unsafe wedges from falling. The key to determine the correct support is determining the load-deformation behavior of the material and finding a suitable option to mitigate risk with respect to timing of support installation. For the UMEC, ground control concerns relate to:

- Jointing of material,
- Soft ground and subsequent deformation, and
- Wedge orientation based on excavation orientation.

The Unwedge analysis method was determined to be the most appropriate support evaluation method for the UMEC; therefore, the following support criterion is to be employed at the UMEC:

- Split-set friction bolts are installed in all mining and infrastructure areas. Additional cable bolts and Swellex bolts could be used in addition to the split-set bolts given the availability of the bolts on hand.
- Drifts are bolted and meshed from back to rib to ensure stable excavations and control surface deterioration for the longevity of the facility.

5.1 Ground Support Material Definitions

Throughout this document the following definitions are used:

Standard Bolt Types: 6-foot split-set bolts.

It is possible that additional types of rock bolts could be donated to the Montana Tech Mining Engineering Department. Specialty coated bolts that could be used include polymer or plastic coated bolts. Additional bolts that could be used at the UMEC include:

- 8-foot standard and 12-foot standard Swellex,
 - Standard Swellex bolt refers to any type of bolt with 11-ton minimum of breaking strength.
 - If Super Swellex are donated, the bolt would hold a 24-ton minimum
- Cable bolts.
 - Bolts with 0.6—inch, seven strand cable with ultimate strength of 58,600 pounds. The primary use is in intersections and wide excavations. If cable bolts are used, a competent person should ensure that the bolt is fully grouted.
- Dywidag bolts
 - Standard Dywidag bolts ranging from 6-foot length to 8-foot length with 10-ton minimum breaking strength.

Plates:

6 inch square x 3/16” thick plates to be used in conjunction with split-set friction bolts.

6 inch square x 3/16” thick plates to be used in conjunction with standard Swellex bolts.

6 inch square x 3/16” thick plates to be used in conjunction with Super Swellex bolts.

6-inch square x 3/16” thick plates to be used in conjunction with Dywidag bolts.

Mesh:

9 gauge Galvanized chain link fencing with 2” square openings.

Hole Diameter:

- 1-3/8” Split-set friction bolt installation under normal conditions.
- 1-1/2” Standard Swellex
- 1-7/8” Super Swellex
- 2” Cable bolts

Shotcrete:

General application will be 2-4 inch thickness.

5.2 Specialized Ground Support Recommendations

The following section outlines a quick reference for additional ground support standards at the UMEC. Standards should always be met, and exceeded if ground conditions warrant additional support. Always notify a teaching assistant or the practical underground mining professor if adverse ground conditions are encountered or if ground conditions change.

In localized areas of poor ground (such as hydrothermally altered ground):

- Blast shorter rounds (6’),
- After blasting, muck and bolt the heading without any delays,
- Bolt and mesh as designed,
- And apply shotcrete if absolutely necessary or if available.

5.3 Standard Operating Procedure for Ground Support in UMEC Drifts

- 1) Headings will be mucked clean of material. Face, ribs, and back scraped down with loader or barred down manually if equipment is unavailable.
- 2) Heading will be bolted with wire mesh. Split-sets will be employed on a **maximum**

3H: 3V-foot pattern to ensure no wedges will fail out of the back. Wire mesh should be overlapped with previous support. Ribs will be supported to mid-height to ensure the longevity of the excavation.

- 3) Above is the minimum amount of ground support needed. Additional ground support can be added at the discretion of the student, teaching assistant, and practical underground professor.

5.4 Standard Operating Procedure for bolting

- 1) Bolts should be installed on a **maximum** 3H: 3V –foot interval to ensure safety. Though the Q-value indicates the excavation is stable with a 5H: 5V –foot spacing, the 3x3 is recommended for stability and longevity of the facility. If a competent person recommends a smaller bolt spacing due to weak ground, always add additional bolts for support.
- 2) Bolt Pull Testing

Bolts are spot checked for suitability by pull testing periodically by the Geomechanics class. Pull test should be conducted at least once per year. For new ground conditions, pull tests are required.

5.5 Installation Guidelines

Split Sets

- No further than three feet between bolts; use tighter spacing in weaker ground conditions (higher weathering grades).
- 6-foot split sets installed in the back and in the ribs
- Installed using hole spacing guidelines in Section 5.1.
- If split-sets are not enough support in the excavation, shotcrete is recommended to mitigate any potential rock fall hazard.
- Report any and all machine or support material defects to practical underground mining professor so that s/he may notify necessary stakeholders³.

5.6 Reminders

- **Never** go out under unsupported ground.
- Have a work plan prior to entering the UMEC.
- Scale from supported ground and have a clear path of retreat.
- Bolt to the brow of the face.
- Trim damaged ends of wire mesh to prevent injuries for on-foot personnel.
- Pay attention to the support installed behind you. The workplace inspection begins on the way to the workplace.
- Advance all support from supported ground. Never skip ahead and spot bolt the middle of the rows.
- Maintain housekeeping in work area.

³ Stakeholder: any individual with interest or concern in the UMEC and its use of products, services, and materials.

6.0 Future Recommendations

The following list outlines future recommendations or protocols that should be considered during each update the GCMP incurs after March 2017:

- Consider the use of pocket penetrometer and Schmidt hammer testing for granitic weathering characterization,
- In order to provide definitive weathering grade characterizations, supply a Geology graduate student with a project outlining the mineralogical characterization in thin-section for the existing weathering grades in the UMEC,
- Consider the application of field Ultrasonic velocity testing if the equipment becomes available for use,
- Future GCMPs for the UMEC should contain a SOP for a simple quality control guidelines for rock bolts,
- Consider “drive-time” testing for split-set bolts in new ground conditions in addition to pull testing,
- A crown pillar analysis should be conducted for the UMEC to determine the stability of the opening given the shallow depth of the operation, and
- Future excavations should be driven at an orientation of 90°.

7.0 REFERENCES

ASTM Standard F432 - 13 (2013). Standard Specification for Roof and Rock Bolt and Accessories. ASTM International, West Conshohocken, PA.

Barton, N. (1978). Suggested methods for the quantitative description of discontinuities in rock masses. *International Journal of Rock Mechanics and Mining Sciences & Geomechanics Abstracts*, 15(6), 319-368.

Hoek, E. (2007). *Practical Rock Engineering*. Retrieved from <https://www.rocscience.com/learning/hoek-s-corner/books>

Palmström, A. and Broch, E. 2006. Use and misuse of rock mass classification systems with particular reference to the Q-system. *Tunnels and Underground Space Technology*, 21, 575-593.

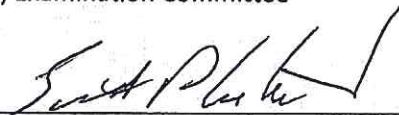
Rose, E. (2017). Characterization of granite and subsequent ground control management plan at Orphan Boy Mine – Butte, Montana.

SIGNATURE PAGE

This is to certify that the thesis prepared by Emily Rose entitled "Characterization of Granite and Subsequent Ground Control Management Plan at Orphan Boy Mine – Butte, Montana" has been examined and approved for acceptance by the Department of Mining Engineering, Montana Tech of The University of Montana, on this 28th day of March, 2017.



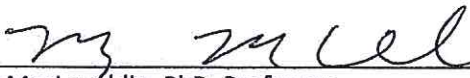
Scott Rosenthal, P.E, Assistant Professor and Department Head
Department of Mining Engineering
Chair, Examination Committee



Scott Carlisle, P.E.
Newmont Mining Corporation
Member, Examination Committee



Jeff Johnson, PhD, Associate Professor
University of Utah Department of Mining Engineering
Member, Examination Committee



Mary MacLaughlin, PhD, Professor
Department of Geological Engineering
Member, Examination Committee